

JOÃO PAULO ARAGÃO PEREIRA

**A hybrid model for long-term prediction of glycemic
oscillation in individuals with type 1 diabetes and
suggesting personalized recommendations**

(Versão Corrigida)

São Paulo
2023

JOÃO PAULO ARAGÃO PEREIRA

**A hybrid model for long-term prediction of glycemic
oscillation in individuals with type 1 diabetes and
suggesting personalized recommendations**

Ph. D. Thesis presented to the Graduate
Program at the Escola Politécnica da
Universidade de São Paulo to obtain the
degree of Doctor of Science.

São Paulo
2023

JOÃO PAULO ARAGÃO PEREIRA

**A HYBRID MODEL FOR LONG-TERM
PREDICTION OF GLYCEMIC OSCILLATION IN
INDIVIDUALS WITH TYPE 1 DIABETES AND
SUGGESTING PERSONALIZED
RECOMMENDATIONS**

Ph. D. Thesis presented to the Graduate Program at the Escola Politécnica da Universidade de São Paulo to obtain the degree of Doctor of Science.

Concentration Area:


Computer Engineering


Advisor:

Anarosa Alves Franco Brandão

São Paulo
2023

Autorizo a reprodução e divulgação total ou parcial deste trabalho, por qualquer meio convencional ou eletrônico, para fins de estudo e pesquisa, desde que citada a fonte.

Este exemplar foi revisado e alterado em relação à versão original, sob responsabilidade única do autor e com a anuência de seu orientador.	
São Paulo, 27 de janeiro de 2023	
Assinatura do autor	
Assinatura do orientador	

Documento assinado digitalmente
 ANAROSA ALVES FRANCO BRANDAO
Data: 27/01/2023 12:58:56-0300
Verifique em <https://verificador.itib.br>

Catálogo-na-publicação

Pereira, João Paulo Aragão

A hybrid model for long-term prediction of glycemic oscillation in individuals with type 1 diabetes and suggesting personalized recommendations / J. P. A. Pereira -- versão corr. -- São Paulo, 2023.
169 p.

Tese (Doutorado) - Escola Politécnica da Universidade de São Paulo.
Departamento de Engenharia de Computação e Sistemas Digitais.

1.AGENTES INTELIGENTES 2.SISTEMAS DE RECOMENDAÇÃO
3.SISTEMAS HÍBRIDOS I.Universidade de São Paulo. Escola Politécnica.
Departamento de Engenharia de Computação e Sistemas Digitais II.t.

ACKNOWLEDGMENTS

Even before finishing this work, I thank God first, and the women in my life, ... mother, wife and two daughters, besides my dear brother. I am grateful for the unconditional support of my teacher, advisor and friend PhD Anarosa Alves Franco Brandão (POLI-USP), and my other teachers and friends for their extra official joint supervision, PhD Joyce da Silva Bevilacqua (IME-USP) and PhD Maria Lúcia Corrêa-Giannella (FM-USP).

"Even discredited and ignored by everyone, I can't give up, because for me, winning is never giving up."

-- Albert Einstein

RESUMO

O sistema regulador glicose-insulina e suas oscilações glicêmicas é um tema recorrente na literatura devido ao seu impacto na vida humana, principalmente dos acometidos pelo diabetes mellitus. Diversas abordagens foram propostas, desde modelos matemáticos até modelos baseados em dados, com o objetivo de modelar a curva de oscilação da glicose. De posse desta curva, é possível prever quando e quanto injetar de insulina, a quantidade ideal de carboidratos e possíveis estados hiper- ou hipoglicêmicos em indivíduos com diabetes tipo 1 (DM1). No entanto, a literatura apresenta horizontes de previsão não superiores a seis horas, o que pode ser um problema considerando o tempo de sono. Além disso, a modelagem existente não pode ser personalizada para cada indivíduo, considerando seu estilo de vida. Este trabalho apresenta o Tesseractus, um modelo que adota um sistema multiagentes para combinar aprendizado de máquina e modelagem matemática para prever a oscilação da glicose em até oito horas. O Tesseractus também utiliza a farmacocinética das insulinas, além dos dados coletados dos indivíduos com DM1. A captura periódica de dados pode melhorar o processo de aprendizado dos agentes. Seu resultado principal é, essencialmente, valores de predição de glicose durante horizontes que variam de 15 a 480 minutos. Tais valores podem ser visualizados em gráficos para auxiliar os endocrinologistas na prescrição de tratamentos diários para indivíduos com DM1. Além disso, também podem ser usados para fornecer recomendações personalizadas para esses indivíduos, a fim de manter sua concentração glicêmica na faixa ideal. Em um experimento envolvendo 15 indivíduos com DM1 e nove indivíduos virtuais com DM1, Tesseractus apresentou resultados pioneiros para horizontes de previsão de oito horas para o período noturno. Utilizando Parkes Error Grid como métrica de avaliação, pode-se observar que 95,53% das medições, em média, caem nas zonas A e B, durante o período diurno, e 95,1% no período noturno, sendo o Erro Absoluto Médio igual a 26.75 e 27.16 mg/dL, respectivamente. Consideramos que o Tesseractus será uma referência para a classificação do modelo de predição glicêmico, apoiando a mitigação de complicações de curto e longo prazo nos indivíduos com DM1. Dessa forma, o modelo preditivo proposto tende a retardar as complicações agudas e crônicas de uma população com projeção de 78 milhões de adultos com diabetes tipo 1, em todo o mundo, em 2045.

Palavras-Chave – Sistema Regulatório Glicose-Insulina, Diabetes Tipo 1, Sistemas Multiagentes, Aprendizado de Máquina, Equações Diferenciais Ordinárias, Predição, Personalização.

ABSTRACT

The glucose-insulin regulatory system and its glycemic oscillations is a recurring theme in the literature due to its impact on human life, especially those affected by diabetes mellitus. Several approaches have been proposed, from mathematical models to data-based ones, in order to model the glucose oscillation curve. With this curve, it is possible to predict when and how much to inject insulin, the ideal amount of carbohydrates and possible hyper- or hypoglycemic states in individuals with type 1 diabetes (T1D). However, the literature presents prediction horizons not exceeding six hours, which can be a problem considering the sleeping time. Also, existing models cannot be customized for each individual considering their lifestyle. This work presents Tesseratus, a model that adopts a multi-agent system to combine machine learning and mathematical modeling to predict glucose oscillation in up to eight hours. Tesseratus also uses the pharmacokinetics of insulins, in addition to data collected from individuals with DM1. Periodic data capture can improve the learning process of agents. Its result is essentially glucose prediction values over horizons ranging from 15 to 480 minutes. Therefore, it can assist endocrinologists in prescribing daily treatments for individuals with T1D and providing personalized recommendations for these individuals in order to maintain their blood glucose concentration in the optimal range. Tesseratus brings pioneering results for prediction horizons of eight hours for the night period, in an experiment with 15 real individuals with DM1 and 9 virtual ones. Using the Parkes Error Grid as an evaluation metric, it can be observed that 95.53% of measurements, on average, fall into zones A and B, during the daytime period, while at night it reached 95.1%, with the Mean Absolute Error equal to 26.75 and 27.16 mg/dL, respectively. It is our assertion that Tesseratus will be a reference for the classification of the glycemic prediction model, supporting the mitigation of short and long-term complications in individuals with T1D. In this way, the proposed predictive model tends to delay the acute and chronic complications of a population with a projection of 78 million adults with type 1 diabetes, worldwide, in 2045.

Keywords – Glucose-Insulin Regulatory System, Type 1 Diabetes, Multi-agent System, Machine Learning, Ordinary Differential Equations, Prediction, Personalization.

LIST OF FIGURES

1	Nominal sequence of Design Science Research Methodology.	22
2	Simplified Glucose-Insulin Regulatory System (T1D).	36
3	Typical Structure of a Multi-Agent System (BORDINI; HÜBNER; WOOLDRIDGE, 2007).	43
4	Explanatory learning.	45
5	Simple pool-based active learning cycle.	50
6	Classification for glucose prediction techniques (WOLDAREGAY et al., 2019).	51
7	Taxonomy of blood glucose monitors.	58
8	Example architecture for data collection/transmission and remote monitoring.	61
9	Structure of a learning agent adapted from (RUSSELL; NORVIG, 2016).	65
10	Tesseract architecture.	69
11	Example of the action flow of Tesseract model in real life.	69
12	Approximate curves of insulin glargine concentrations (24h).	79
13	Approximate curves of insulin aspart concentrations (5h).	81
14	Phase one of learning (supervised process to learn).	82
15	Phase two of learning (by reinforcement).	83
16	Sliding window approach for timeseries data: carb., exercise and insulin.	92
17	Tesseract model implementation architecture in the cloud.	96
18	Glycemic oscillation pattern of participant R-BRA07 (every 30min of 00h-8h).	100
19	Glycemic oscillation pattern of participant R-BRA05 (every 30min of 00h-8h).	101
20	Parameters used - agent Math (60 min. exercise).	101
21	Generated graphs of glycemic oscillation and insulin concentration for 60 min. of exercise.	102

22	Parameters used - agent Math (120 min. exercise).	102
23	Generated graphs of glycemic oscillation and insulin concentration for 120 min. of exercise.	103
24	Parkes Error Grid linked with 7 Brazilian volunteers (daytime).	104
25	Parkes Error Grid linked with 7 Brazilian volunteers (night time).	105
26	Parkes Error Grid linked with 8 volunteers from OHIO (day time).	108
27	Parkes Error Grid linked with 8 volunteers from OHIO (night time).	109
28	Parkes Error Grid linked with nine virtual individuals (day time).	112
29	Parkes Error Grid linked with nine virtual individuals (night time).	113
30	FreeStyle Libre [®] sensor graph related to 24 hours with recommendations (5pm).	118
31	Embodied Opinion of the Ethics Committee.	141
32	Proof of approval on 05/20/2020.	141
33	Proof of authorization for recommendation with one individual.	142
34	Curr-Gluco agent action flowchart.	143
35	Exercise agent action flowchart.	144
36	Inbolus agent action flowchart.	145
37	Inbasal agent action flowchart.	146
38	Carb-in agent action flowchart.	147
39	Prot-in agent action flowchart.	148
40	Fat-in agent action flowchart.	149
41	Alcohol-in agent action flowchart.	150
42	Capillar-in agent action flowchart.	151
43	Tesseractus model: phase 1 of learning.	152
44	Tesseractus model: phase 2 of learning.	153
45	Recommender agent action flowchart.	154
46	Monitor error agent action flowchart.	155

47	ODE parameters actions flowchart.	156
48	Anomaly detector action flowchart.	157
49	Flowchart of the bibliographic research methodology.	168

LIST OF TABLES

1	Devices (glucometers) used in this research.	29
2	Summary of glycemic oscillations – information from the Brazilian Society of Diabetes (SBD, 2019).	30
3	Detailed information about the types of insulin used in this work.	31
4	Parameters of the glucose and insulin compartment models.	39
5	Functional and non-functional requirements of the Tesseractus model.	64
6	Tesseractus model reward policy (fasting period).	72
7	Tesseractus model reward policy (postprandial period).	72
8	Parameters, variables and initial conditions.	75
9	Reference parameters of the Glucose-Insulin Regulatory System.	76
10	Insulin glargine concentration approximation (pmol/L) - 24h.	78
11	Insulin glargine: polynomial functions and R^2	78
12	Aspart insulin concentration approximation (pmol/L) - 5h.	80
13	Aspart insulin: polynomial functions and R^2	80
14	Characteristics of <i>in vivo</i> volunteers of Brazil.	87
15	Characteristics of <i>in vivo</i> volunteers from Ohio.	88
16	Information to calculate eGDR for Brazilian volunteers.	88
17	Characteristics of <i>in silico</i> individuals.	89
18	Results of Parkes Error Grid for Tesseractus (zones) - daytime (Brazil).	105
19	Results of Parkes Error Grid for Tesseractus (zones) - nighttime (Brazil).	106
20	MAE (mg/dL) - daytime (Brazil).	106
21	MAE (mg/dL) - nighttime (Brazil).	106
22	MAPE (%) - daytime (Brazil).	107
23	MAPE (%) - nighttime (Brazil).	107

24	Results of Parkes Error Grid for Tesseractus (zones) - daytime (Ohio). . . .	109
25	Results of Parkes Error Grid for Tesseractus (zones) - nighttime (Ohio). . .	110
26	MAE (mg/dL) - daytime (Ohio).	110
27	MAE (mg/dL) - nighttime (Ohio).	110
28	MAPE (%) - daytime (Ohio).	111
29	MAPE (%) - nighttime (Ohio).	111
30	Results of Parkes Error Grid for Tesseractus (zones) - daytime (Virtual). . .	111
31	Results of Parkes Error Grid for Tesseractus (zones) - nighttime (Virtual). .	112
32	MAE (mg/dL) - daytime (Virtual).	113
33	MAE (mg/dL) - nighttime (Virtual).	114
34	MAPE (%) - daytime (Virtual).	114
35	MAPE (%) - nighttime (Virtual).	114
36	Results through metrics after recommendations at daytime (R-BRA05). . .	117
37	Results through metrics after recommendations at nighttime(R-BRA05). . .	117
38	Actions and conditions of reactive agents (AgR).	159
39	ODE Parameter agents actions and conditions (AgR).	160
40	Actions and conditions of Monitor Error agent.	160
41	Actions and conditions of Anomaly Detector agent.	161
42	Actions and conditions of the smart Recommender agent.	162
43	Actions and conditions of the smart Predictor agent.	163
44	Actions and conditions of the smart Mathematical agent.	164
45	Actions and conditions of the smart ML agent.	165
46	Results after first filter.	167
47	Articles related to hybrid models.	169

LIST OF ABBREVIATIONS

- ABM** agent-based model. 166
- AP** artificial pancreas. 19, 59–61
- CGM** continuous glucose monitoring. 20, 28, 61, 63, 75
- CNS** Central Nervous System. 74
- DM** diabetes mellitus. 18, 27–30, 33, 35, 38
- DSRM** Design Science Research Methodology. 22
- eGDR** estimated glucose disposal rate. 33
- GIRS** glucose-insulin regulatory system. 19, 35–38, 70, 76, 120, 121
- IGR** ideal glycemic range. 23, 27, 34
- ISF** insulin sensitivity factor. 32
- IT1D** individuals with T1D. 23, 24, 28–31, 33, 34, 36, 37, 51, 52, 55, 56, 59–61, 70, 75, 76, 85–87, 99, 120, 121, 123, 167
- MAE** Mean Absolute Error. 20
- MAS** Multi-agent System. 19, 120
- PH** prediction horizon. 38
- T1D** type 1 diabetes mellitus. 18, 23, 25, 27, 28, 31–35, 37, 38, 41, 46, 49, 56, 57, 63, 65, 81, 84, 85, 120, 121

CONTENTS

List of Abbreviations

Part I: FOUNDATION	17
1 Introduction	18
1.1 Objective	19
1.2 Expected contributions	20
1.3 Document Structure	20
2 Method	22
2.1 Applying DSRM to this work	22
2.1.1 Problem confirmation	23
2.1.2 Definition of goals	24
2.1.3 Design and development	24
2.1.4 Demonstration	24
2.1.5 Evaluation	25
2.1.6 Communication	25
3 Theoretical Foundation	27
3.1 Type 1 Diabetes Mellitus	27
3.1.1 Glycemic monitoring	28
3.1.2 Insulin	30
3.1.3 Insulin Resistance	32
3.1.4 Macronutrients	33
3.1.5 Glucose-Insulin Regulatory System (GIRS)	34

3.2	Mathematical modeling of the GIRS	37
3.2.1	Numerical Methods for Ordinary Differential Equation	39
3.2.2	Approximation of functions by polynomials	40
3.3	Agents and Multi-Agent System (MAS)	41
3.3.1	Interaction and coordination between agents	45
3.3.2	Agents that learn	46
3.3.2.1	Supervised learning	47
3.3.2.2	Reinforcement learning	49
4	State of the Art in Prediction of Glycemic Oscillation	51
4.1	Mathematical approaches	52
4.2	AI approaches	53
4.3	Discussion	54
5	State of Practice in Prediction of Glycemic Oscillation	56
5.1	Data-driven solutions	56
5.2	Blood glucose monitors, flash sensors and apps	57
5.3	Automatic insulin delivery	59
5.4	Discussion	60
	Part II: PROPOSAL	62
6	Tesseractus model	63
6.1	Overview	63
6.2	Tesseractus multiagent system	64
6.3	Discussion	70
7	Tesseractus Instantiation	71
7.1	The rewarding policy	71

7.2	The Math agent	73
7.2.1	The glucose compartment equation	73
7.2.2	The exogenous insulin equation	77
7.3	The first learning phase	80
7.4	The second learning phase	83
7.5	Discussion	84
8	Tesseractus Implementation	86
8.1	Dataset	86
8.2	Algorithms and numerical libraries	88
8.3	Multiagent platform and agents implementation	92
8.4	Cloud reference architecture	95
8.5	Testing	96
	Part III: RESULTS AND CONCLUSION	98
9	Results	99
9.1	Applying Tesseractus to data from Brazilian Volunteers	103
9.2	Applying Tesseractus to data from Ohio University	107
9.3	Applying Tesseractus to data from virtual individuals	109
9.4	Using Tesseractus as a Recommender to one Brazilian Volunteer	113
9.5	Discussion	117
10	Conclusion and Future Work	120
10.1	Final remarks	120
10.1.1	Main contributions of Tesseractus Model	122
10.2	Future Work	123
10.3	Publications	124

References	126
Appendix A – Ethics Committee	141
Appendix B – Authorization from the Ethics Committee of the University Hospital of USP	142
Appendix C – Flowchart of actions	143
Appendix D – Tables of agent actions and conditions	158
Appendix E – Bibliographic research methodology	166

PART I

FOUNDATION

1 INTRODUCTION

Diabetes mellitus (DM) is a syndrome characterized by hyperglycemia resulting from defects in insulin secretion associated or not with resistance to the action of this hormone (KEEN; BARNES, 1997). People of all ages, from all continents and communities are affected by DM, which is one of the fastest growing health challenges of the 21st century. The number of adults living with DM has more than tripled in the last 20 years. More specifically in Brazil, in 2021, approximately 16 million adults (20–79 years old) were reported to have DM (IDF, 2022). Another consequence of the increase in the number of diagnosed cases is hospital admissions, with a total diabetes-related health expenditure of around 42 billion, only in Brazil, in 2021 (IDF-ATLAS, 2021).

World Health Organization (WHO, 2022) estimates that high blood glucose is the third most important cause of premature mortality, surpassed only by increased blood pressure and tobacco use. About 90% of all premature deaths and 87% of all deaths related to DM occur in low- and middle-income countries. This can be attributed to the lower rates of diagnosis and difficulties in accessing treatment for DM when compared to high-income countries (IDF, 2022). In addition, the prevalence of type 1 diabetes (T1D) is increasing, and there is a projection for 2045 of 78 million adults with T1D (IDF, 2022). Therefore, public policies aimed at adults, children and adolescents, associated with a model that can facilitate the routine of a 24-hours (circadian) cycle of individuals with DM are needed to reduce the complications associated with this condition (DANEMAN, 2006).

Some of the challenges that researchers and health professionals face are the following: (1) the need for improving the prediction model for individuals with T1D, especially in high-risk populations, and to support the development of effective and safe interventions that avoid hypoglycemia or hyperglycemia; (2) the need for developing treatment approaches that bring better results in terms of glycemic control and reduction of the risks of developing complications; (3) the possibility of having mechanisms to provide personalized recommendations. From the perspective of individuals with T1D, the challenges are

more incipient, from lack of access to trained professionals to even continuous treatment.

Current literature is composed of non-customizable methods and models, and most of them are state-of-the-art built for specific scenarios of T1D control, for example, focused only on nocturnal hypoglycemia or for the treatment of adolescents (HOBBS et al., 2019), and there is no path to combine them. Furthermore, no results were found with prediction horizons longer than 6 hours (FOSS-FREITAS et al., 2020), or with continuous learning (SCHINDELBOECK; PRAUS; GALL, 2016).

The prediction horizon of pharmaceutical devices already available on the market, such as insulin pumps, does not exceed 30 minutes (FDA-CONTROLIQ, 2019), (MINIMED-670G, 2020) and, consequently, does not have a desirable predictability, in the post-prandial state ($>$ two hours). Another point to be highlighted is the non-socially egalitarian access to an artificial pancreas (CONTROL-IQ, 2020) (hybrid closed-loop systems). In addition, the dynamic nature of the human organism, more specifically of glucose-insulin regulatory system (GIRS) makes it complex to create a model that mimics the dynamic exchange of information between its components (KISSLER et al., 2014).

Thus, we propose Tesseractus, a model that uses a Multi-agent System (MAS) approach (RUSSELL; NORVIG, 2016) to overcome challenges (1) and (3), as well as supporting physicians to overcoming challenge (2). The model is characterized as hybrid as it combines ordinary differential equation (ODE) (SMITH, 2011), mathematical modeling of insulin pharmacokinetics data and machine learning techniques to mimic the glucose-insulin dynamics, monitor and correct the input parameters, and customize the profile of each individual with T1D.

This process of information gathering and continuous learning can facilitate daily decision-making (TACK et al., 2018), such as the correct amount of carbohydrates in addition to the duration of physical exercises. The Tesseractus model is embedded in the concept of precision medicine (ELEMENTO, 2020), and can be used as a tool for the Precision Medicine in Diabetes Initiative (NOLAN et al., 2022). The name Tesseractus is related to the 4-dimensional hypercube – *tesseract* (RAMÍREZ; PÉREZ-AGUILA, 2002), as the model has four main agents with pre-established responsibilities.

1.1 Objective

The main objective of the research is to build a hybrid model to predict glycemic oscillation and suggest personalized recommendations for individuals with T1D. This

prediction must combine concepts of artificial intelligence and applied mathematics, in order to cover a minimum period of four hours, during daytime, and up to eight hours in the nighttime.

1.2 Expected contributions

The main scientific contribution is the definition of a hybrid model that can predict, in an interval between four to eight hours, the glucose level of an individual with T1D, with a Mean Absolute Error (MAE) ranging from 0 to 30 mg/dL, according to the prediction horizon. In addition to an accuracy above 95% in Parkes Error Grid's zones A + B according to (PFÜTZNER et al., 2013), representing less risk for individuals with T1D who use the predictions as a guide to exercise, eat, etc.

Other contributions are an extension of the compartmentalized glucose model proposed via: (1) dynamic correction of ODE glucose parameter values; (2) the use of insulin pharmacokinetics (basal and rapid effects) to replace the insulin compartment; (3) in addition to the side effect, with social and economic impact, through the improvement of DM control and consequently the reduction of diabetes-related health expenditure; (4) creation of a dataset with seven real and nine virtual individuals with T1D.

As a technological contribution, is an artifact that implements Tesseratus, and could be coupled to an artificial pancreas (OPENAPS, 2021), or to continuous glucose monitoring (CGM) devices. Thus, it will be possible to automate the learning of each T1D individual's GIRS and make personalized recommendations, such as insulin dosage, amount of macronutrients, in addition to the time and intensity of physical exercises.

1.3 Document Structure

The document is organized into three parts: Foundations, Proposal, Results and Conclusion. In the first part, we have more four Chapters: Chapter 2 describes the research method. Chapter 3 describes the basic concepts for a good understanding of the text. Chapter 4 discusses the works related to the present research, involving prediction of glycemic oscillation in individuals with T1D, using Machine Learning, Multi-agent System, Polynomial Equations and Ordinary Differential Equation. Chapter 5 summarizes the state of practice and the main application scenarios of this model. In the second part, we have three Chapters: Chapter 6 contains the architecture and details of the Tesseratus

model, Chapter 7 with details about initial instantiation of agents and model, and the implementation of the model is detailed in the Chapter 8. In the last part, we have two Chapters: Chapter 9 describes the experimental results and the test approach adopted to verify the accuracy of the proposed model. Finally, Chapter 10 presents associated publications and future works that may derive from this research.

2 METHOD

The research method adopted to support this work is the Design Science Research Methodology (DSRM) (PEFFERS et al., 2007) in its nominal sequence. This method includes six steps: (1) problem identification and motivation; (2) definition of the objectives of a solution; (3) design and development; (4) demonstration; (5) evaluation; and (6) communication, as we can see in Figure 1. The method allows the search to start at any of steps (1), (2), (3) or (4), and therefore the nominal sequence of the process may not be followed. For this research, the solution sought is centered on motivation and, therefore, its first nominal activity was number one.

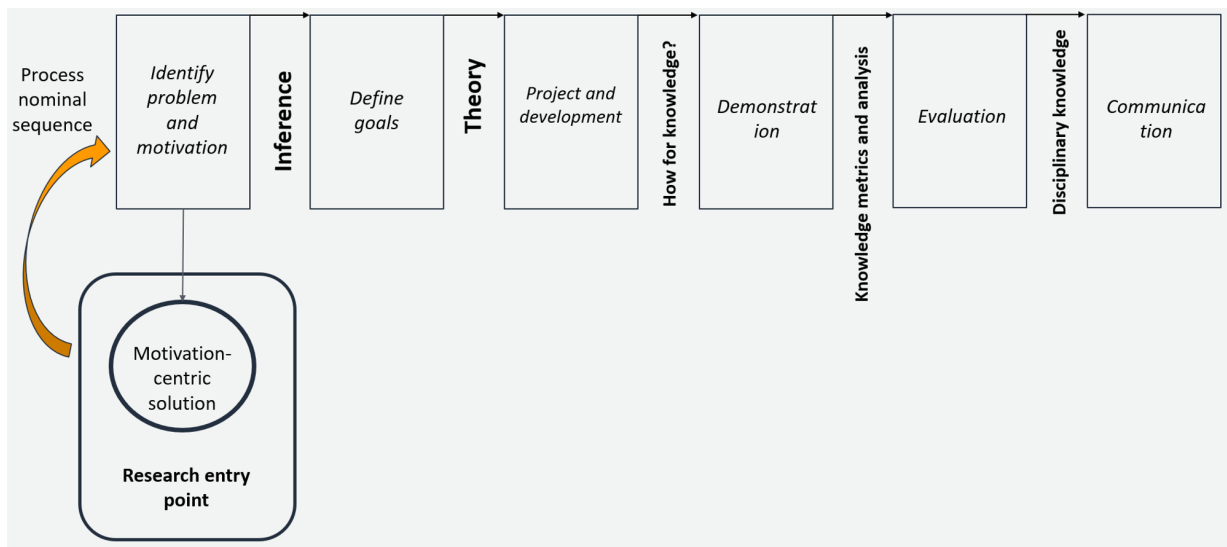


Figure 1: Nominal sequence of Design Science Research Methodology.

2.1 Applying DSRM to this work

This section describes the applicability of DSRM to this job, from problem confirmation to communication.

2.1.1 Problem confirmation

T1D is a condition characterized by persistent hyperglycemia resulting from defects in insulin secretion. It is a disease known since antiquity (before Christ) (KARAMANOU et al., 2016) and, to this day, there is no cure (ADA, 2023). T1D can affect people of any age, but it usually develops in children or young adults (IDF, 2022). The increased prevalence of T1D results in higher rates of hospitalization and use of health services, impacting, in most cases, the Public Health System (SBD, 2022a). Thus, without proper treatment, individuals with T1D can suffer serious complications such as diabetic nephropathy, neuropathies, among others (BROWNLEE et al., 2011).

Thus, T1D is a real public health problem and, in many cases, there is no technology to allow continuous glucose control, nor a personalized recommendation system. A system like the proposed model could infer about the time and appropriate amount of insulin to be injected, or amount of carbohydrates to be ingested, for example, in a continuous recommendation process. It is observed that, if this calculation is performed incorrectly, the individual with T1D may experience hypoglycemia (glucose levels lower than 80 mg/dL), if they exceed exogenous insulin, or hyperglycemia (elevated blood glucose levels, in general greater than 120 mg/dL in fasting period and greater than 180 mg/dL two hours after a meal [postprandial]), if they inject less insulin than necessary (SBD, 2022a). It is important to emphasize that in clinical practice, we consider hypoglycemia < 70 mg/dL, which is considered the lower limit of normality. The American Diabetes Association (ADA) working group considers ≤ 70 mg/dL the alert value (SEAQUIST et al., 2013).

Therefore, the continuous task of maintaining balance close to ideal glycemetic range (80–120 mg/dL in the fasting period and up to 180 mg/dL in the postprandial period) (SBD, 2022a) is a problem to be addressed since it requires frequent follow-up by endocrinologists. And, according to recent research, there is an estimate that an individual with T1D makes extra 180 health-related decisions daily, compared to an individual without T1D (TACK et al., 2018).

From the literature review presented in Chapter 4, it was confirmed that most studies related to the prediction of glycemetic oscillation, in individuals with T1D, have a short prediction horizon, less than or equal to two hours, and are decoupled from a continuous learning and correction system. Another obstacle found was that most studies do not focus on systematic and continuous prediction (KISSLER et al., 2014) of glycemetic oscillation. Thus, the relevance and classification of the problem as a research was concluded, and the objectives that the model should achieve were established, in order to support a

technological solution more adequate to the context of individuals with T1D, starting the activity two of the research method adopted.

2.1.2 Definition of goals

Considering that the main problems associated with the existing models are short prediction horizons and the impossibility of personalized recommendation, it was established the goal of proposing a model that (i) predict glucose oscillation in a horizon up to eight hours, and (ii) recommend the amount of exogenous insulin (fast-acting and basal), in addition to the amount of macronutrients to be ingested, besides the time of exercise.

Possible solutions to the problem were analyzed, deciding on the combination of existing solutions, namely the use of mathematical modeling (ordinary differential equation) (section 3.2) and MAS (section 3.3).

2.1.3 Design and development

The Motivation-Centered Solution was triggered by a real problem, and can be treated with the development of a prototype, which allows the validation of hypotheses that serve as a basis for the solution design.

The definition of the model started with the architectural design of the MAS, and how the mathematical model would provide information to the agents and, at the same time, be fed by them, as described in Chapter 6. The MAS is composed of agents, which can be reactive and learning agents (RUSSELL; NORVIG, 2016). Part of this model is described in a book chapter (PEREIRA et al., 2019).

As the model depends on data from individuals with T1D, authorization was requested from the Ethics Committee (appendix A), granted on 05/20/2020. Data was collected from seven volunteers between the months of June and August, 2020. A dataset (eight individuals), from an external source (OHIO-UNIV-T1D, 2020), was also used to evaluate the model. Another dataset was created with nine virtual individuals to complement and compare with real individuals. All results with this data are detailed in Chapter 9.

2.1.4 Demonstration

This activity consisted of training and testing the proposed model from the data collected. After the development of the model, at a proof-of-concept level, the artifact was

adapted to receive as input the dataset of each individual with T1D. A mobile app is used to present the agent’s predicted value with the final value suggested by the recommender agent in addition to its recommendations. These results are compared with the values received from the continuous glucose monitor (CGM). The performance measures that are used are detailed in subsection 2.1.5.

2.1.5 Evaluation

The evaluation of the results obtained in the demonstration is carried out using performance measures. The quality of the response of the hybrid model is controlled through the absolute error between the measured and calculated values. Thus, the proposed hybrid model is extensively tested with the real dataset of the seven Brazilian volunteers with T1D to evaluate these measures, in addition to the data of eight individuals from the University of Ohio (OHIO-UNIV-T1D, 2020), and nine virtual ones created from the University of Virginia simulator (UNIV-VIRGINIA, 2020).

The first performance measure is **(1)** check feasibility to predict for long prediction horizons; **(2)** most of the percentage of predictions versus measurements should fall within Parkes Error Grid (zones A and B) (PARKES et al., 2000), determining to be a clinically accurate predictor (PFÜTZNER et al., 2013), regardless of the prediction horizon (PH); **(3)** the MAE to check the quality (GINSBERG, 2009) of each predicted glucose value for each individual; **(4)** the prediction, as well as the correction suggestions, and the recommendations must be carried out in near-real time.

For comparison purposes only, the established standard for real-time measurements is ISO15197 (KATZ, 2020), which dictates that **95%** of the values must fall within the range of ± 15 mg/dL to < 100 mg/dL, while the values must be within the range of $\pm 15\%$ in blood glucose ≥ 100 mg/dL. An award model facilitates the evaluation of the performance measure (5), according to the guidelines of the Brazilian Society of Diabetes (SBD, 2022a).

2.1.6 Communication

The manuscript related to the proposed model was discussed in a *Doctoral Consortium*, at the **31st International Symposium IEEE CBMS** (Computer Based Medical Systems) (CBMS, 2018). As reported in activity three, the dissemination of preliminary results has already been carried out (PEREIRA et al., 2019), in an academic conference

on **Intelligent Systems - 2019**. The predictive model was also recently published in the journal Applied Sciences (PEREIRA et al., 2022) with analysis of data from seven individuals from Brazil.

The final results will be compiled in another article to be submitted to the journal **Engineering Applications of Artificial Intelligence** (EAAI, 2022). For EAAI, the focus will be on the description of the technological artifact and on the comparison of personalized recommendations generated for Ohio University and virtual individuals.

The software based on Tesseractus was registered in the Brazilian National Institute of Intellectual Property (INPI) in 2022, under the process BR5112022000522-0 (INPI, 2022).

3 THEORETICAL FOUNDATION

In this Chapter, some of the most relevant and pertinent topics for this multidisciplinary research are detailed.

3.1 Type 1 Diabetes Mellitus

Glucose is vital for health because it is a source of energy for the cells, and the main source of energy for the brain. Regardless of the type of diabetes mellitus (DM), it is related to hyperglycemia (high blood glucose concentrations) (IDF, 2022). The pancreas is a human organ that makes up the digestive and endocrine systems, and produces important hormones for our digestive system. It carries out glycemic regulation, mainly by producing and releasing insulin, through β cells, and glucagon, through α cells (KATSAROU et al., 2017). Normally, in an individual without DM β cells produce insulin when blood glucose rises. Thus, according to the body's needs at the moment, it is possible to determine whether this glucose will be used as fuel for the body's activities or will be stored as a reserve, in the form of glycogen or fat. This makes the blood glucose return to ideal glycemic range (SBD, 2020).

Type 1 diabetes (T1D) has two subtypes: 1A in which insulin deficiency is due to autoimmune destruction of β cells; and 1B in which insulin deficiency is of an idiopathic nature (which manifests itself spontaneously). As a result, the body produces little or no insulin (ROEP, 2013). For both types of T1D, the therapeutic recommendations are the same, and there is no evidence of distinct risks for chronic complications between the subtypes (SBD, 2022a). T1D has no cure, and no effective and safe intervention currently exists to prevent it.

Constant hyperglycemia can lead to long-term complications such as macrovascular and microvascular disorders, as well as cerebrovascular diseases (KATSAROU et al., 2017), that are responsible for the increased morbidity and mortality associated with T1D (DANEMAN, 2006). To avoid these long-term complications, the first therapeutic

step is ongoing education about diabetes mellitus, in addition to treatment of T1D with a multidisciplinary healthcare team is recommended, and requires ongoing attention to many aspects, including administration of exogenous insulin, continuous glucose monitoring, meal planning, screening of comorbidities and complications related to T1D (DANEMAN, 2006).

3.1.1 Glycemic monitoring

Hyperglycemia, measured in mg/dL or mmol/L, has been used for many years as a defining criterion for DM. To avoid both hyperglycemic and hypoglycemic states, the blood glucose monitoring task is mandatory and must be continuous for individuals with T1D (SHLOMO et al., 2019). Individuals with T1D can collect glycemic values in some ways, either through the continuous glucose monitoring devices (CGM) or blood glucose monitors.

Blood glucose monitors are devices capable of determining the blood glucose concentration (ACCU-CHECK, 2020). The sample (1-2 μ L) of capillary blood, which is found in capillary blood vessels (GROSSI et al., 2009), is usually obtained by puncturing one of the fingers of the hand (GLUCOMETER, 2020). The Accu-Check Active[®] model, for example, has a minimum accuracy of 95% on most measured values that must be within: (1) 10% of blood glucose values above 100 mg/dL; and (2) 10 mg of blood glucose levels below 100 mg/dL (Table 1).

However, in recent years, continuous glucose monitoring is performed by individuals with T1D more frequently, and the devices that perform it are in constant technological evolution. These new devices have a sensor positioned in the interstitium (MOSER; YARDLEY; BRACKEN, 2018), which contains the interstitial fluid between the skin and the human circulatory system, and reads the interstitial glucose concentration each five minutes, in addition to communicating with remote applications via Bluetooth (RODRÍGUEZ, 2020). There are models (DEXCOM-G6, 2020) that are coupled to insulin pumps (MINIMED-670G, 2020), forming a closed system better known as an artificial pancreas (CONTROL-IQ, 2020).

There are also standalone devices, such as FreeStyle Libre[®] (FREESTYLE, 2020), which use NFC (Near Field Communication) (RODRÍGUEZ, 2020), but there is a delay, in average of 10 minutes, between the measurement of capillary blood glucose and the interstitial glucose concentration (SBD, 2022a). In addition, FreeStyle Libre[®] has a minimum accuracy of 94.2% on most measured values which must be within: (1) $\pm 20\%$ of

blood glucose values above 100 mg/dL and (2) ± 20 mg of blood glucose levels below 100 mg/dL (Table 1). The accuracy of FreeStyle Libre[®] is adequate throughout its lifetime (14 days), but is less accurate during the first and last days (FREESTYLE-LIBRE, 2020). The error in the accuracy of these glucometers can cause confusion in the calculation of proportion of insulin to be administered by individuals with T1D.

According to the US Food and Drug Administration (FDA) (FDA, 2021), for all integrated CGM measurements, in the range from 70 to 180 mg/dL, the percentage of measurements within $\pm 15\%$ of the corresponding glycemic value must be calculated, and the lower one-sided confidence limit of 95%, must exceed 70%. Table 1 details the accuracy and drawbacks of the three devices used by the all volunteers in this research.

Glucose meter devices			
Model	Capture	Accuracy	Inconvenience
Accu-Check Active [®]	capillary blood	within 95% for ± 10 mg/dL or 10% of value measured	Painful finger puncture, manual
FreeStyle Libre [®]	interstitial fluid	within 94.2% for ± 20 mg/dL or 20% of value measured	Sensor must be changed every 14 days, need to check with a glucometer
Medtronic Enlite [®]	interstitial fluid	within 94.9% for ± 15 mg/dL or 15% of value measured	Sensor must be changed every six days, need to check with a glucometer

Table 1: Devices (glucometers) used in this research.

The Brazilian Diabetes Society (SBD) adopted blood glucose and glycated hemoglobin (HbA1c) values used to diagnose DM: fasting blood glucose for values greater or equal to 126 mg/dL; postprandial glycemia (two hours) after overload with 75g of glucose for values greater or equal to 200 mg/dL; glycemia at random for values greater or equal to 200 mg/dL with unmistakable symptom; HbA1c of 6,5% (SBD, 2022b). In this way, in individuals with T1D, the continuous permanence of blood glucose in the recommended range between 70 and 180 mg/dL can be facilitated by the use of CGM devices.

To define a state of hyper- or hypoglycemia, the metabolic control goals are based on the scientific societies (SBD, 2022a), with glycemic values between 70 and 180 mg/dL. Glycated hemoglobin (HbA1c) is considered the standard test to assess the metabolic control of individuals with DM, and there is a well-established relationship between increased values of HbA1c and chronic complications (SBD, 2022a). Glycemic goals can also be different in each period of the day (24 hours), in accordance with the targets defined in (SBD, 2022b).

Glycemic values are pre-defined as goals by scientific societies, but the symptoms of hypoglycemia, such as apathy or mental confusion, can occur, for example, with a blood glucose value in the suggested range (70–180 mg/dL).

There are many factors that can interfere with postprandial glycemic oscillations (SBD, 2019), some of them related to food ingestion. A summary of such factors are presented in Table 2. In this work, at least the following factors are used to predict glycemic oscillation: (1) amount of carbohydrates, proteins and fat; (2) pre-prandial blood glucose; (3) insulin sensitivity; (4) physical activity.

Food related	Non-food related
Amount and type of carbohydrate	Pre-prandial glycemia
Consumption associated with Protein and fat	Gastric emptying time
Consumption associated with proteins and lipids	Exogenous insulin
Food cooking process	Insulin Resistance
Time spent at meal	Physical activity
Intake of dietary fiber	Stress
Alcohol consumption	Puberty and menstrual period

Table 2: Summary of glycemic oscillations – information from the Brazilian Society of Diabetes (SBD, 2019).

The glycemic oscillation of individuals with T1D is very peculiar, and in addition to the factors mentioned in Table 2, it can be affected by some morning and evening hyperglycemic phenomena. The dawn phenomenon (FURUTANI, 2019) and the twilight phenomenon (DU et al., 2018) are some of them.

3.1.2 Insulin

In the early 1920s, Frederick Banting and Charles Best discovered insulin under the supervision of John Macleod at the University of Toronto. With the help of James Collip, the insulin was purified, making it available for successful treatment of DM. Banting and Macleod won the Nobel Prize for their work in 1923 (SHI, 2020).

All individuals with T1D need to inject insulin to control blood glucose, and there are different therapeutic that can be used to treat them. Normally, exogenous insulin replacement is performed with a combination of basal insulin (effect during circadian cycle), an insulin during meals (meal bolus to control blood glucose between meals and sleep), and and bolus insulin doses to cover mealtime insulin needs (prandial bolus) and to correct hyperglycemia (correction bolus) (SBD, 2022a).

There are different types of insulin, related to pharmacokinetics characteristics (start, peak and duration of action). Types of insulin include ultrafast, fast, intermediate, long-acting, ultralong acting and premixed. In this work are considered the fast acting insulin analogs *lispro* and *aspart*, and the basal insulin analogs *glargine* and *degludec* (long and ultra-long acting analogs, respectively), due to their use by individuals with T1D. The pharmacokinetics features of these insulins are described in the subsection 7.2.2, and details related to the time they must be taken, how long they last and the time needed for the start of their action are described at Table 3.

Type	Start of Action (minutes)	Peak (hours)	Duration (hours)	Moment of injection
BOLUS - applied before or at mealtime				
Ultra-fast analogues				
Lispro	10 to 15	1 to 2	3 to 5	15 min. before meals
Aspart	10 to 15	1 to 2	3 to 5	15 min. before meals
BASAL - not specific for meals				
Slow analog				
Glargine	90	NA	up to 24	Once a day, before bed or at dawn
Degludec	90	NA	24 to 42	Once a day, before bed or at dawn

Table 3: Detailed information about the types of insulin used in this work.

For each individual with T1D, the daily insulin dosage is calculated based on fasting blood glucose, and interstitial or capillary blood glucose results throughout the day, pre- and postprandial. For example, the basal insulin dose at bedtime, for example, is adjusted according to the fasting blood glucose, while the other doses are according to the previous preprandial blood glucose levels or glycemic values measured during sleep (SBD, 2022a). Dose adjustments of basal analogues should be performed based on the fasting blood glucose result, and at least every six days. The adjustment of fast-acting or ultra-fast-acting insulin analogues is also performed based on the result of capillary or interstitial blood glucose, two hours postprandial, considering insulin sensitivity factor (ISF) (SBD, 2022a).

Thus, there is no general treatment that covers all individuals with T1D, due to individual characteristics, such as body mass, age, risk factors and daily activities. Therefore, each insulin therapy must be personalized.

3.1.3 Insulin Resistance

Insulin resistance is defined as the difficulty of insulin exerting its effects on muscle, liver and fat cells after binding to its receptor (PRIYA; KALRA, 2018). It is known that sensitivity to insulin action varies from one individual to another, and even at different times of the day in the same individual. Insulin sensitivity factor (ISF) is defined as how much a unit of insulin lowers blood glucose (SBD, 2022a).

In some commercial insulin pumps, ISF is used as the ratio of 1700 divided by the total daily of insulin administered, the result being on the scale of mg/dL of glucose per unit (U) of insulin. The ISF is used, by educated individuals with T1D, in insulin pumps to deliver the correct amount of insulin, and correct the glycemic value to reach the ideal (MINIMED-640G, 2020). ISF can be calculated for regular insulin according to equation 3.1, while for fast-acting analogue insulin, equation 3.2 is used. Manually, some calculations can also be performed to find the ISF according to the type of insulin (SBD, 2022a):

$$ISF = \frac{1500}{\text{total daily insulin dose}} \quad (3.1)$$

$$ISF = \frac{2000 \text{ [or 1700 or 1800 or 2100]}}{\text{total daily insulin dose}} \quad (3.2)$$

Carbohydrate counting is also used to adjust the doses of fast-acting or ultra-fast-acting insulin analogues, and it is common to use the insulin:carbohydrate ratio (SBD, 2021), which is obtained by the formula 3.3 (SBD, 2022a).

$$ratio = \frac{400 \text{ or } 500}{\text{total daily insulin dose}} \quad (3.3)$$

Another alternative is to start carbohydrate counting, in adults, considering the individual's body mass (SBD, 2021).

Kissler and colleagues (2014) demonstrated that the ISF can be defined as a scale factor γ . The γ factor can take values from **zero** to **one**, with **zero** corresponding to no ability of muscle and fat cells to take up glucose, and **one** corresponding to the glucose uptake capacity of an individual without DM. In this case, the individual with T1D would have a value of γ close to **one** with adequate insulin doses and close to **zero** without insulin administration.

In 2001, Rabasa-Lhoret and colleagues (2001) evaluated the need to reduce the pre-meal insulin dose, prescribing postprandial exercises of different intensities and durations for individuals with T1D. Thus, an additional factor, $f_{ex} = 1 + s * (t_{ex} - t_{ex}Avg)$, is responsible for the positive effect of exercise on insulin sensitivity, as physical exercise increases insulin sensitivity, providing better glycemic control (NELSON et al., 2013). Thus, t_{ex} (exercise practice time) corresponds to minutes of moderate to vigorous physical activity per day, with 60 min being the daily average ($t_{ex}Avg$). This value is interpreted as the percentage increase in glucose tolerance for each additional minute of exercise, and provides the reason behind multiplying by $s = 0.0072$ (NELSON et al., 2013).

The eGDR (Estimated Glucose Disposal Rate) is another validated clinical tool to estimate insulin sensitivity in individuals with T1D. The eGDR can be calculated using routine clinical measurements, such as HbA1c, presence of hypertension (HYP = 0 no and HYP = 1 yes), and waist circumference (WaCirc) (EPSTEIN et al., 2013). The individuals with T1D with the lowest eGDR compared to the highest value (1.2 to $8.1 \frac{mg}{kg.min}$) had a significantly higher risk of any complication of DM (micro - or macrovascular) compared to less insulin resistant patients. Here is the equation to calculate the estimated glucose disposal rate (EPSTEIN et al., 2013):

$$eGDR = (21.158 - 0.09 * WaCirc - 3.407 * HYP - 0.551 * HbA1c) \frac{mg}{Kg.min}$$

There is also the insulin dose for correction in the case of hyperglycemia (SBD, 2022a), which should be added to the prandial dose, according to the preprandial glycemia, in order to adapt the individual to the glycemic goal pre-established.

3.1.4 Macronutrients

Nutritional therapy is the treatment of a disease or condition by changing nutrient intake or an entire food stream (SBD, 2022a). The relevance of nutritional therapy in the treatment of T1D has been emphasized since its discovery, as well as its challenging role in managing and preventing the development of the resulting complications (SBD, 2022a). Dietary assessment techniques represented by apps (ZHU et al., 2010), for example, are used to assess macronutrient intake (carbohydrates, proteins and lipids) including a 24-hour food record, and are essential to maintain optimal glycemic control in individuals with T1D.

Carbohydrates are important source of energy for the brain and other metabolic processes (SBD, 2022a). However, they are considered the predominant macronutrients that

raise postprandial blood glucose, as 100% of them are converted into glucose (MANUAL1-CC, 2020) in a time ranging from 15 to 120 minutes. Both the quantity and quality of carbohydrate play a crucial role in the glycemic control of T1D. In addition, several studies have shown that lipids and proteins added to the diet can also significantly affect the postprandial glycemic profile, especially when ingested in excessive amounts (SBD, 2019).

The glycemic index (IG-CG, 2016) represents the effect of carbohydrates on blood glucose, and is obtained after analyzing the glycemic oscillation produced by 50g of carbohydrate of the evaluated food, in relation to the curve of 50 grams of carbohydrate of the standard food (white bread). The glycemic index of each food can be found in manuals (MANUAL-CC, 2020) (MANUAL1-CC, 2020), in order to assess the rise and speed of rise in blood glucose caused by food.

The carbohydrate/insulin ratio is used by individuals with T1D to calculate fast-acting (bolus) insulin doses before meals (GUPTA; LAL; KHANDELWAL, 2018). Carbohydrate counting is a known method to establish the prandial insulin bolus dose, when analyzed with pre- and postprandial blood glucose. However, each individual with T1D has its own individualized insulin:carbohydrate ratio, even differentiated throughout the day. For example, an insulin:carbohydrate ratio of 1:12, that is, one unit of rapid or ultra-rapid insulin administered for every 12 grams of carbohydrates, may be acceptable in the morning, but may cause hypoglycemia in the afternoon, or hyperglycemia at night.

The correct carbohydrate/insulin ratio can improve glycemic control in individuals with T1D, as a result of stabilizing the glycemic oscillation, in addition to making food choices more flexible and simplifying meal planning. Thus, the individualization of the dietary assessment and the food plan aims to identify the characteristics of this consumption, and adapt them to the proposed glycemic targets, such as ideal glycemic range. Mixed meals with carbohydrates, proteins, lipids and fiber tend to make it difficult for the individual with T1D to count total carbohydrates. Scientific evidence has shown that nutritional intervention has a significant impact on the reduction of HbA1c in individuals with T1D. The nutritional management must be subjective, with a behavioral and personalized approach, focusing on improving the lifestyle of the individuals with T1D (SBD, 2022a).

3.1.5 Glucose-Insulin Regulatory System (GIRS)

The human body must be able to maintain the balance of the internal environment, through various physiological processes, such as the production of insulin or glucagon,

to balance blood glucose. In this case, the internal medium is the interstitial fluid, and any phenomenon that interferes with the feedback mechanism, can disturb homeostasis (DAVIES, 2016). In the continuous human homeostatic process, two types of oscillation in the human glucose-insulin interaction were observed, with two different periods: one fast (10-15 min.) (PØRKSEN et al., 2002) and the other slow (100-150 min.) (STURIS et al., 1991). The slow oscillation may originate from the dynamic regulatory negative feedback interaction of the glucose-insulin system. This oscillation is detected in the human body, for example, in different physiological situations, such as after the ingestion of macronutrients (AL-HUSSEIN; TAHIR, 2020).

Thus, normally in an individual without DM, in the postprandial period, the insulin concentration increases in eight to ten minutes, reaches a peak concentration in 30 to 45 minutes, and then rapidly decreases to initial values in 90 to 120 minutes (GARDNER; SHOBACK, 2018). The endocrine pancreas secretes about 30 units (U) of insulin per day into the circulation of adults without DM, and insulin concentration rarely rises above 100 $\mu\text{U}/\text{mL}$ after meals (SHLOMO et al., 2019).

Glucose is the most potent stimulant of insulin release, however, blood glucose levels below 80 to 100 mg/dL do not stimulate insulin release. The endocrine pancreas releases insulin in two phases in response to glucose stimulation. When blood glucose rises suddenly, there is a short-lived initial release of insulin (the first phase), and if the glycemic elevation persists, the insulin release gradually decreases and then begins to rise again to a stable level (the second phase) (GARDNER; SHOBACK, 2018).

In addition to insulin, another hormone that should be considered is glucagon, because physiologically, glucagon secretion increases in hypoglycemia and is suppressed in hyperglycemia. Insulin released during hyperglycemia inhibits glucagon secretion, whereas insulin reduction in the presence of hypoglycemia allows glucagon to be secreted (KAWAMORI; KULKARNI, 2009).

The glucose-insulin regulatory system (GIRS) is part of the human endocrine system (SHLOMO et al., 2019), and is responsible for maintaining the homeostasis of hormones such as insulin and glucagon (endogenous) and, consequently, in the regulation of glycemia. In this case, insulin plays a dominant role in the regulation of glucagon secretion compared to blood glucose (KAWAMORI; KULKARNI, 2009).

In the case of T1D, the destruction of β (beta) cells prevents the endocrine pancreas from producing insulin, and consequently from maintaining blood glucose in the normal range (80–120 mg/dL - *status quo*). Figure 2 represents the glucose-insulin regulatory

system of individuals with T1D. Some components were added and removed, such as exogenous insulin infusion and β cells, respectively (PEREIRA et al., 2019). The glucose-insulin regulatory system in Figure 2 cannot be considered a physiological system, as there is an exogenous component (synthetic insulin), which mimics endogenous insulin.

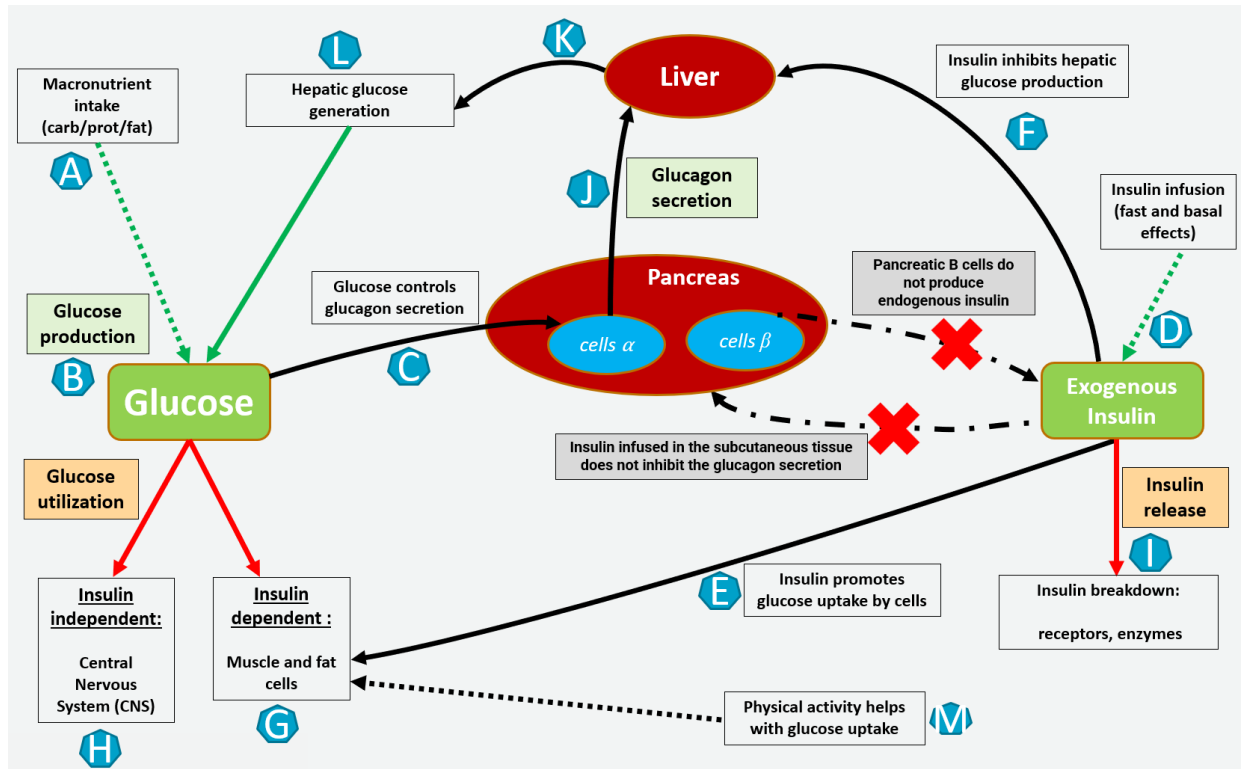


Figure 2: Simplified Glucose-Insulin Regulatory System (T1D).

Each point of the system described in Figure 2 can generate a different flow depending on external stimuli, such as time and the amount of macronutrients ingested, and intensity of physical exercises, influencing the amount of hormones secreted, such as insulin and glucagon. In Figure 2 (PEREIRA et al., 2019), dotted arrows indicate external stimuli, being the ones labeled A and D (the green ones) related to insulin production. The solid arrow from L to B (the green one) indicates endogenous insulin production, while the ones from D to I and B to G and H (the red ones) indicate endogenous insulin consumption. Dash-dot arrows highlight the gap that exists in individuals with T1D. A brief description of possible flows within the system is presented in the following:

- A - Glucose-insulin regulatory system is stimulated by the intake of macronutrients.
- B - Glucose is produced from the metabolism of macronutrients (GARDNER; SHOBACK, 2018).
- C - Glucose controls glucagon secretion by α cells.

- D - The individual with T1D must inject exogenous insulin. There is a delay in action and exogenous insulin injected into the subcutaneous tissue does not inhibit glucagon secretion by α cells.
- E - Insulin promotes glucose uptake by muscle and fat cells (SHLOMO et al., 2019).
- F - Insulin inhibits hepatic glucose production.
- G - Insulin-dependent fat and muscle cells, stimulated by insulin and physical exercise, capture glucose.
- H - The components of the Central Nervous System (CNS), such as the brain, independently of insulin, capture glucose.
- I - Insulin is eliminated by all insulin-sensitive tissues, as well as by the liver and kidney.
- J - The α cells secrete the hormone glucagon.
- K - Delay time in hepatic glucose generation.
- L - The liver, if not inhibited by insulin, is stimulated by glucagon to produce glucose (gluconeogenesis and glycogenolysis) (SHLOMO et al., 2019).
- M - Physical activity, as an external stimulus, helps in the uptake of glucose by muscle and adipose cells.

In summary, T1D blood glucose should be kept within a relatively narrow range in preprandial period (70–120 mg/dL) or up to 180 mg/dL in postprandial period, despite wide variations in glycemic flow. This remarkable homeostatic feat is accomplished by a series of hormonal, neural and glucoregulatory factors (SHLOMO et al., 2019). The dynamic nature of glucose-insulin regulatory system, in individuals with T1D, requires a model that mimics this exchange of information between its components, in a personalized way. One of the contributions of Tesseractus is to use ordinary differential equation (ODE), in one of its agents, to mimic this behavior, and serve as a source of knowledge for the other agents in the model, as well as the ML agent.

3.2 Mathematical modeling of the GIRS

One of the goals of metabolic physiology is the development of quantitative methods, related to the specific processes involved in the regulation of macronutrient metabolism,

more specifically of carbohydrates, in the body of individuals with DM (SHLOMO et al., 2019). A simplified mathematical representation is by means of ODE compartmental models (SMITH, 2011).

Existing mathematical models to GIRS were considered to support Tesseratus. Among them, the one proposed by Ackerman and colleagues (1964) reduces the number of kinetic parameters to only the most relevant ones, and is used to predict a combination of response to an oral glucose assumption, in the characterization of glucose-insulin regulatory system. Another model is the Bergman's "Minimal" (BERGMAN; COBELLIT; TOFFOLO, 1981), which uses complex nonlinear models to represent this physiological behavior. Also, Lehmann and Deutsch (1992), adopt a concise mathematical formulation with as few parameters as possible in order to make the model simple. However, external factors that influence blood glucose, such as physical exercise, cannot be considered, and there is no correlation with the prediction horizon (PH). Still considering nonlinear models, Hovorka and colleagues (2004) and Dalla Man and colleagues (2004) are based on meal absorption and insulin sensitivity.

Another alternative modeling would be to use more recent models that are based on delayed secretion of the glucagon hormone and also accept the insertion of exogenous insulin as an input parameter, in addition to exercise as a stimulating factor in glucose uptake, in order to approach the behavior of the human glucose-insulin regulatory system, as in (KISSLER et al., 2014) and (AL-HUSSEIN; TAHIR, 2020).

Nevertheless, we adopted the modeling proposed by Kissler and colleagues ((KISSLER et al., 2014)) as basis for our model. It has two compartments modeled, which is feasible to be applied in individuals with T1D. Initially, it can be represented mathematically as input and output of the glucose G and exogenous insulin I compartments, described on equations (3.4) and (3.5), respectively.

$$G'(t) = \overbrace{(G_{in} + f_1(I(t - \tau_2)))}^{\text{glucose production}} - \underbrace{(f_2(G(t) - \gamma [1 + s.(m - m_b)]) . (f_3(G(t)) . f_4(I(t))))}_{\text{glucose consumption}} \quad (3.4)$$

$$I'(t) = \overbrace{(I_{in} + \beta f_5(G(t - \tau_1)))}^{\text{insulin infusion}} - \underbrace{\left(\frac{V_{MAX} I(t)}{K_M + I(t)} \right)}_{\text{insulin release}} \quad (3.5)$$

In the glucose compartment $G'(t)$, f_1 describes the hepatic glucose production (HGP); f_2 describes the central nervous system glucose utilization; f_3 describes the muscle/fat glucose utilization; f_4 describes the muscle/fat insulin uptake; and f_5 describes the pancreatic insulin production. The parameters semantics are given in Table 3.2.

Our model adopts their glucose compartment and substitutes the insulin compartment by a polynomial approximation of it given by data from the pharmacokinetics data of four types of insulin. To solve the ODE from the glucose compartment we adopted the Runge-Kutta numerical method for solving it (see subsection 3.2.1). Also, as a pioneering part of this work, the insulin compartment based on ODE was replaced. Thus, the oscillation of the exogenous insulin concentration is a function of time, based on the pharmacokinetics of each type of insulin (units U/Kg), such as insulin lispro (ROACH; WOODWORTH, 2002). The function approximation method used to represent the pharmacokinetics of insulins is detailed in the subsection 3.2.2.

Symbol	Description
I_{in}	Insulin infusion rate
G_{in}	Glucose intake rate
β	Relative pancreatic β -cell function
γ	Relative insulin sensitivity
s	Rate of insulin sensitivity increase per minute of exercise
m	Daily minutes of physical activity
m_b	Baseline minutes of physical activity
V_{max}	Maximum insulin clearance rate
K_M	Enzyme's half-saturation value

Table 4: Parameters of the glucose and insulin compartment models.

3.2.1 Numerical Methods for Ordinary Differential Equation

There are several numerical methods for solving Ordinary Differential Equations. Among the existing methods there are the Runge-Kutta ones. All Runge-Kutta methods are yielded from approximations of Taylor series. The higher the Runge-Kutta method order, the larger the number of terms of the Taylor approximation (BUTCHER, 2016). The most popular Runge-Kutta method is the order four, also known as RK4. Its formula is given by equation (3.6).

$$y_{n+1} = y_n + \frac{1}{6}h(k_1 + 2k_2 + 2k_3 + k_4), \quad (3.6)$$

where

$$\begin{aligned} k_1 &= f(x_n, y_n), \\ k_2 &= f\left(x_n + \frac{1}{2}h, y_n + \frac{1}{2}hk_1\right), \\ k_3 &= f\left(x_n + \frac{1}{2}h, y_n + \frac{1}{2}hk_2\right), \\ k_4 &= f(x_n + h, y_n + hk_3). \end{aligned}$$

The integration step h was chosen by recursive adjustments from an initial guess h_0 . The results from the simulations must be within the proposed mean absolute error (MAE) of prediction model being smaller than 30 mg/dL, and within the specified numerically determined margin for insulin error (0.025 units), normally used in insulin pumps.

The quality of your numerical solution depends exclusively on controlling the error made at each integration step and the global error, that is, the error accumulated in the total time interval. To solve ODEs linked with glucose compartment, the Runge-Kutta RK4 method was chosen because it is of order 4 ($O(h^4)$), robust and easy to implement.

Specifically in this work, an error smaller than 0.025 should be considered, due to the smaller increment units of the participants' insulin pumps: (1) Medtronic Minimed 670G[®] - 0.025 units (U)/hour (MINIMED-670G, 2020); (2) Medtronic Minimed 640G[®] - 0.025 units (U)/hour (MINIMED-640G, 2020); (3) Medtronic Paradigm Veo 754[®] - 0.025 units (U)/hour (MINIMED-754, 2020) ; (4) Medtronic Paradigm 715[®] - 0.05 units (U)/hour (PARADIGM-715, 2020). Traditional pens and injection consider 1 and 0.5 unit (U) of increment.

3.2.2 Approximation of functions by polynomials

The polynomial trendline works well for datasets with fluctuating values with multiple range points, such as the ones from pharmacokinetics of insulins, where we want to have a good approximation over the entire range of the function $f(\cdot)$ (OMANA; MOORTHI, 2022). In an analytical approach, we adopted the regression equation, with the least squares method to analyze errors. Another motivator for using polynomials to approximate functions is that their derivatives and integrals are easy to determine (EULER, 1988).

Data from the pharmacokinetics of insulins, with their respective concentrations, were obtained from publications by the pharmaceutical industry and from scientific articles,

detailed in the section 7.2. Thus, each point means the insulin concentration prescribed at a given time (t), considering the parameters of the individual with T1D. Thus, given $n+1$ pairs $(t_i, f(t_i))$, $i = 0, 1, 2, \dots, n$, there is one and only one polynomial $p_n(t)$ of degree $\leq n$, in which

$$f(t_i) = p_n(t_i), i = 0, 1, 2, \dots, n. \quad (3.7)$$

We can express the polynomial p (3.8):

$$p_n(t) = \sum_{i=0}^n c_i t^i \quad (3.8)$$

where the coefficients c_i are the solutions of the equations' system below (3.9):

$$\begin{cases} c_0 + c_1 t_0 + c_2 t_0^2 + \dots + c_n t_0^n = f(t_0) \\ c_0 + c_1 t_1 + c_2 t_1^2 + \dots + c_n t_1^n = f(t_1) \\ \vdots \\ c_0 + c_1 t_n + c_2 t_n^2 + \dots + c_n t_n^n = f(t_n) \end{cases} \quad (3.9)$$

The idea of the the Tesseratus model is to mitigate the complexity of the simplified GIRS with the insertion of insulin pharmacokinetic curves. The model is minimal, regarding the number of parameters. It is mainly used to quantify the characteristic parameters related to glucose and insulin metabolism, which can be identified from the transient response of these variables in the system.

3.3 Agents and Multi-Agent System (MAS)

Agents are entities (computer programs) situated in an environment that have the ability to perceive it through their sensors and act on it through their actuators. A Multi-Agent System (MAS) (RUSSELL; NORVIG, 2016) is a collection of several autonomous agents, each acting towards its goals while all interacting in a shared environment, being able to communicate and possibly coordinate their actions.

In the view of the agent(s), there is a continuous flow of perception, through sensors, decision making based on perceptions and action through the execution of actions/tasks via actuators. On the other hand, the environment reacts to the actions and returns with feedback to the agent. The spectrum of autonomy is intrinsic to agents, which is

adjustable, and decisions can often be handled over to an agent with higher authority, if it is beneficial to achieve the goals of the MAS (RUSSELL; NORVIG, 2016).

In complex domains, such as physiological processes and their influencing external factors, the agent may have, at best, partial control of the environment. In the agent's view, the same action performed twice, under apparently identical circumstances, may have totally different effects. Thus, agents in complex environments must be prepared for possible failures (RUSSELL; NORVIG, 2016).

Normally, an agent has a base with available actions, along with its preconditions, which enable it to modify the environment in which it is situated. The key point is for the agent to select the best action to take in order to achieve the common goal (RUSSELL; NORVIG, 2016). Intelligent agents have at least 3 skills that can facilitate the feedback process in the environment involved (WOOLDRIDGE, 2009):

- Reactivity - perceive the environment and respond in a timely manner to changes;
- Proactivity - able to deliberately exhibit goal-directed behavior;
- Social Skill - able to interact with other agents or humans.

Other interesting properties of intelligent agents that learn (RUSSELL; NORVIG, 2016), and must be inherent to a MAS, when modeling human physiological systems, are:

- Truthfulness - they must decide which of the actions prior to the reinforcement (reward or punishment for the action) was most responsible for it, in order to avoid false communications and maximize the reward;
- Learning and Adaptation - should be able to improve performance over time.

Whenever we consider a MAS in physiological processes, an environment tends to be (RUSSELL; NORVIG, 2016): (1) **partially observable**, where the agent does not obtain complete, updated and accurate information; (2) **stochastic**, in which any action does not have a single guaranteed effect; (3) **dynamic**, where there are other processes operating in parallel, and therefore, the environment can change without the agent's control; (4) **continuous**, where there is no fixed number of actions and perceptions; and finally (5) **sequential**, in which the current decision can affect future decisions. The agent complexity is related to these characteristics of the environment. Thus, the interaction

and cooperation between agents, inserted in a complex environment, help to achieve the overall MAS goal.

The prerequisite for building a MAS is the ability to build at least two agents, but the most common case is to have multiple agents interacting with each other to achieve a common goal. In Figure 3, the agents are in a shared environment, but each one has full or partial control over a portion of the environment (sphere of influence) (BORDINI; HÜBNER; WOOLDRIDGE, 2007). For example, in real life, insulin and glucose are components that need to be in constant homeostasis to maintain the glycemic value in the ideal range. Thus, spheres of influence can overlap in a jointly controlled environment. In this case, to achieve a result focused on the MAS goal, the agent has to consider how the other agents act (RUSSELL; NORVIG, 2016). Agents may also maintain organizational relationships with each other, and may be aware of each other or not fully aware of other agents in the MAS (WOOLDRIDGE, 2009).

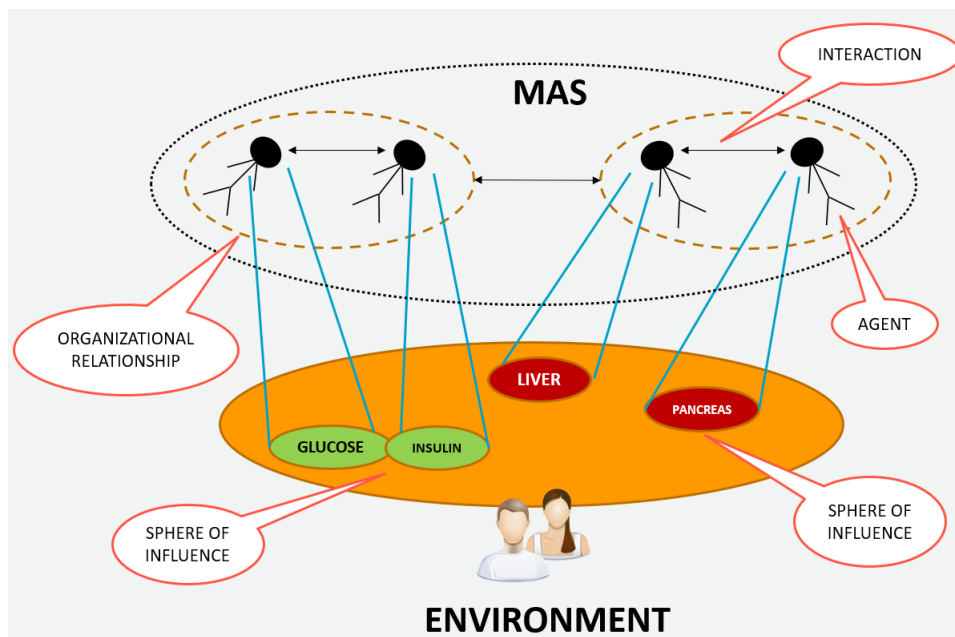


Figure 3: Typical Structure of a Multi-Agent System (BORDINI; HÜBNER; WOOLDRIDGE, 2007).

A pertinent classification for the Tesseract model is on its average heterogeneity, as its intelligent agents differ by problem solving methods, and are not identical agents (BORDINI; HÜBNER; WOOLDRIDGE, 2007). These agents may differ in the method of resolution, through continuous learning, ML models or the use of math equations, or even the way they react to environment changes.

In a complex environment such as physiological environments, it is necessary to combine one or more characteristics of each type of agent to optimize the model, making

it more efficient over time. Reactive agents can react to messages from other agents or to changes in the environment. They have no ability to reason about their actions, just taking them by reacting to events previously described. In the proposed model, one of the main abilities of these agents is to send messages to humans, or to other agents in the environment. The architecture of reactive agents support some advantages of the model, such as simplicity, robustness to failures, in addition to computational savings, in situations where time is essential (WOOLDRIDGE, 2009).

However, only a purely reactive MAS would not be able to support the complexity of a physiological system. Thus, in the Tesseract model, other agents are needed that can build new representations of this environment, through inferences, and these new representations are used to discern actions. The idea is to use the reasoning process that operates on internal representations of knowledge, and this approach to intelligence is embodied in knowledge-based agents (RUSSELL; NORVIG, 2016).

The learning characteristic associated with an agent that can create a knowledge base brings advantages in a complex environment. Knowledge-based deliberation allows the agent to plan hypothetical actions in advance. Learning has another advantage, as it allows the agent to operate in initially unfamiliar environments and become more competent than its initial knowledge (RUSSELL; NORVIG, 2016).

A learning agent has four basic components (RUSSELL; NORVIG, 2016): (1) **learning element**, which is responsible for making improvements, (2) the **performance element**, which is responsible for selecting external actions. The learning element uses feedback from (3) **critical** on how the agent scores, and the last component is (4) **problem generator**, which is responsible for suggesting actions that lead to new and informative experiences.

Tesseract model uses Active Learning (THORVE et al., 2020), detailed in the subsection 3.3.2, to define the action taken to request knowledge from other agents. In this case, the idea of Active Learning is to reduce the number of learning simulations, using knowledge from the mathematical and ML agents, which has more knowledge about the context. Explanatory learning, as shown in Figure 4 (RUSSELL; NORVIG, 2016), is an example of cooperation between agents, as agents deliberately, from their knowledge base, can compile actions in an automated way. Thus, reflective agents can execute them efficiently with lower computational cost.

In summary, our MAS must be able to use the beneficial characteristics of each agent, in a hybrid architecture. An important property of hybrid architectures is that the bound-

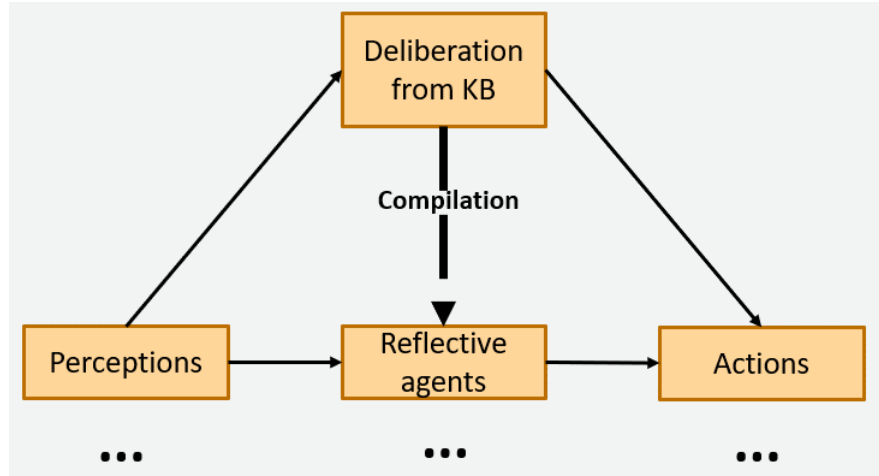


Figure 4: Explanatory learning.

aries between different decision components are not fixed. Thus, as the requirement of agents is to be both reactive and proactive, a decomposition into separate subsystems approach is adequate (WOOLDRIDGE, 2009). Interactions between agents and their respective coordination are detailed in sub-section 3.3.1.

3.3.1 Interaction and coordination between agents

The human physiological system (environment) is in the context of a data-driven problem, as the agents' knowledge base (KB) has facts about the environment, a set of rules, and the generation of new facts is continuous. Thus, to maximize the global results of the model, cooperation between agents must take advantage of the combination of sharing tasks and results. The performance of agents can be improved, with the sharing of results related to accuracy, for example. Regarding task sharing, the problem can be decomposed into sub-problems, and allocated to agents with different and specific skills to solve that particular sub-problem (WOOLDRIDGE, 2009).

In the same environment, when more than one autonomous agent is situated, interactions may occur, depending on their defined capabilities and goals, whether individual or global. These interactions can be simple, like sending messages, or complex, like coordinating to achieve common goals. Joint plans can be built, but they must be conducted with coordination if two agents want to reach an agreement on which joint plan to execute (RUSSELL; NORVIG, 2016).

Thus, when agents are engaged in a cooperative activity, they must have a defined joint commitment. The joint commitment shares the persistence properties of each agent, and social conventions must identify when the joint commitment should be canceled or

maintained. Thus, coordination is achieved when agents have a goal and motivation established, according to the mental map of a team of agents, in a cooperative reasoning cycle (WOOLDRIDGE, 2009), as described next:

- Initially, every agent does not believe that the objective is satisfied, but believes that it is possible;
- Every agent has a goal, until the termination condition is satisfied;
- While the termination condition is not satisfied:
 - If the agent believes that the goal has been achieved, then it will have a goal and this becomes a mutual belief;
 - If the agent believes the goal is impossible, then it will have a goal that becomes a mutual belief;
 - If the agent believes that the goal motivation is no longer present, then this becomes a mutual belief.
- Termination condition is when it is mutually believed that:
 - Goal achieved;
 - The goal is impossible to achieve;
 - The motivation for the goal is no longer present.

Cooperation in Tesseractus is essential, since planning is centralized and plans are partially distributed to specific agents, each one responsible for some executing some tasks that yield important outputs to serve as inputs to other agents' subplans. Tesseractus model is completely cooperative, being its agents in relationships of mutual dependence, since they depend on each other to achieve the overall MAS goal (RUSSELL; NORVIG, 2016). The interaction and coordination between agents facilitates the learning process, which will be described in sub-section 3.3.2.

3.3.2 Agents that learn

The main capability required of a MAS is to follow the state of the environment, in a continuous flow of perception and updating of the internal representations. In the context of personalization and precision related to circadian rhythms, the importance of having a schedule and a routine to control T1D are well known. Although circadian rhythms are

endogenous, they are adjusted to the local environment by external causes, for example, the time. Often, several tasks are routinely performed at the same time, such as eating, exercising, or injecting insulin. Furthermore, the effectiveness of insulin, as measured by the insulin correction factor, can change over time, following a pattern throughout the day (RODRÍGUEZ-RODRÍGUEZ et al., 2019). Therefore, an important characteristic of some agents in our MAS is the ability to learn.

There are several learning approaches that can be adopted, such as supervised learning, unsupervised learning and reinforcement learning. In this work we adopt supervised learning and reinforcement learning as approaches to make our agents to learn.

3.3.2.1 Supervised learning

Supervised learning is a learning task that, given a (training) set of n examples for (input, output) pairs of an unknown function $f(x)$, $\{(x_1, y_1), (x_2, y_2), \dots, (x_n, y_n)\}$, find a function h , that better approximates $f(x) = y$ (RUSSELL; NORVIG, 2016). The function h is called *hypothesis* and finding it is essentially search h along the space of all possible hypothesis, one that performs well when compared other set of (input, output) pairs of examples. Whenever the output is one of a finite set, this learning problem is called a *classification* problem, otherwise it is called a *regression* problem. Finding solutions to regression problems is finding a conditional expectation or an average value for y .

In our MAS, the learning problem is a regression one, where agents observe examples of input and output from the environment, that is, data provided by the individual with T1D (for instance, $\langle \text{glucose, insulin, exercises} \rangle$), and learns a function that maps from input to output. If the dataset does not have labels, it is necessary to include them with the transfer of knowledge from another agent (SILVA, 2020), for example.

There are several classical supervised learning methods, such as Decision Trees, Linear and Logistic Regression, and Support Vector Machines (SVM). Nevertheless, there is also the ensemble learning methods, where the idea is to select a collection (ensemble) of hypotheses from the hypothesis space and combine their predictions. Boosting methods are the most popular ensemble learning methods.

Gradient boosting (XGBOOST, 2019) is a supervised learning algorithm that attempts to accurately predict a target variable by combining an ensemble of estimates from a set of simpler and weaker models. The XGBoost (eXtreme Gradient Boosting) is a popular and efficient open-source implementation of the gradient boosted trees algorithm, and is constantly used in ML algorithms, due to its robust handling of a variety of

data types, relationships, distributions and tunable hyperparameters (XGBOOST, 2019). We can also use XGBoost for linear regression and forecasting. The linear regression algorithm based on decision trees minimizes a regularized objective function (L1 and L2) that combines a convex loss function (based on the difference between predicted and target outputs) and a penalty term for the regression tree functions. The training proceeds iteratively, adding new trees that predict the residuals or errors of the previous trees which are then combined with the previous trees to make the final prediction (ALFIAN et al., 2020).

Hyperparameters are used for tuning the supervised algorithm as, for example, (HASAN et al., 2020), : (1) **eta**: step size shrinkage used in updates to prevent overfitting. After each boosting step, you can directly get the weights of new features; (2) **eval-metric**: evaluation metrics for validation data; (3) **max-depth**: maximum depth of a tree. Increasing this value makes the model more complex and likely to be overfit; (4) **objective**: specifies the learning task and the corresponding learning objective, for example, reg:logistic; (5) **subsample**: subsample ratio of the training instance and prevents overfitting; (6) **tree-method**: define the tree construction algorithm; (7) **lambda**: regularization term on weights; (8) **gamma**: minimum loss reduction required to make a further partition on a leaf node of the tree. The generic gradient boosting method is detailed below (FRIEDMAN, 2001):

- Input data (training set)

$$(x_i, y_i)\}_{i=1}^n \quad (3.10)$$

- A differentiable loss function

$$Loss(y, F(x)), \quad (3.11)$$

- Number of iterations M.
- Algorithm: initialize model with a constant value:

$$F_0(x) = \arg \min_{\gamma} \sum_{i=1}^n L(y_i, \gamma) \quad (3.12)$$

- For $m = 1$ to M, compute residuals:

$$r_{im} = - \left[\frac{\partial L(y_i, F(x_i))}{\partial F(x_i)} \right]_{F(x)=F_{m-1}(x)} \quad \text{for } i = 1, \dots, n \quad (3.13)$$

- Fit a weak learner (tree) closed under scaling $h_m(x)$ to pseudo-residuals, i.e. train

it using the training set

$$\{(x_i, r_{im})\}_{i=1}^n \quad (3.14)$$

- Compute multiplier γ_m by solving the following one-dimensional optimization problem:

$$\gamma_m = \arg \min_{\gamma} \sum_{i=1}^n L(y_i, F_{m-1}(x_i) + \gamma h_m(x_i)) \quad (3.15)$$

- Update the model:

$$F_m(x) = F_{m-1}(x) + \gamma_m h_m(x) \quad (3.16)$$

- Output $F_M(x)$

3.3.2.2 Reinforcement learning

Reinforcement learning is a task where observed rewards are used to learn an optimal (or near optimal) policy for the environment. For this task, no previous knowledge about the environment is considered, neither the agent knows the effects its actions may cause within it (LIM et al., 2021). In this case, the agent needs to know if its action generated a positive or negative result, through rewards or reinforcements, being reward or punishment, respectively. RL is different from supervised learning because there is no labeled training set. In addition, reinforcement learning can be passive learning or active learning (RUSSELL; NORVIG, 2016). The RL is particularly suited to problems that include a long-term versus short-term reward compensation. Active Learning allows an agent to assign labels to typical examples of performance improvement in the learning system. By using such an approach, we reduce the computational cost, through the active selection of items for labeling, selecting only specific queries.

The algorithm Q-learning (WATKINS; DAYAN, 1992) is a RL algorithm that maximizes the cumulative reward and minimize the learning time, through the responsibility assigned to the agent. The "Q" is related to the quality of an action in a certain state. From a series of reinforcements, agents can discern which of the actions prior to the reinforcement were the most accurate. More specifically in the context of T1D, the Q-learning algorithm (RUSSELL; NORVIG, 2016), can identify the different states of the individual with T1D, and recommend corrective actions in insulin doses or amount of carbohydrates to be ingested, among other actions (recommendations), based on the current glycemic state. In this way, the Q-learning algorithm is off-policy, that is, it can update estimated value functions using actions that have not yet been performed. Also, it is a time difference of the learning method that learns functions from the value of Q (Q-value), and can

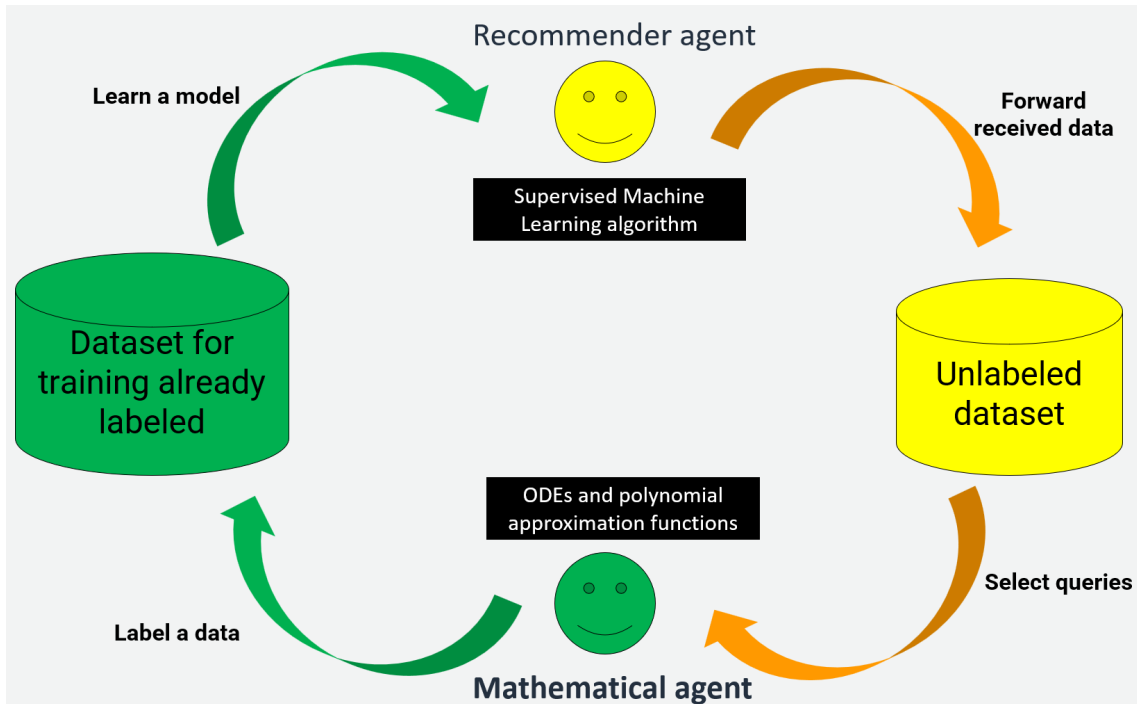


Figure 5: Simple pool-based active learning cycle.

be updated by following the below function (JAVAD et al., 2019):

$$Q(e, a) = Q(e, a) + \alpha * (reward + \gamma * \max_a Q(e', a) - Q(e, a))$$

Being that:

- e : it is the previous state;
- e' : it is the current state;
- a : it is the previous action;
- α : it is the learning rate, between zero and one;
- γ : it is the discount factor, between zero and one, that determines whether future rewards are worth less than current ones;

In the context of this work, intelligent agents use the Q-learning algorithm that selects actions based on exploration with greedy searches (exploit). These agents have a Q-table as a reference, and use it with all possible available actions for a given state.

4 STATE OF THE ART IN PREDICTION OF GLYCEMIC OSCILLATION

This Chapter discusses the main techniques for predicting glycemic oscillation, in addition to mimicking the glucose-insulin regulatory system (GIRS) based on Machine Learning (ML) and mathematical models, found in the literature. In fact, in a survey, Woldaregay and colleagues (2019) presents a taxonomy of different approaches for predicting glucose oscillation in individuals with T1D, reproduced in Figure 6.

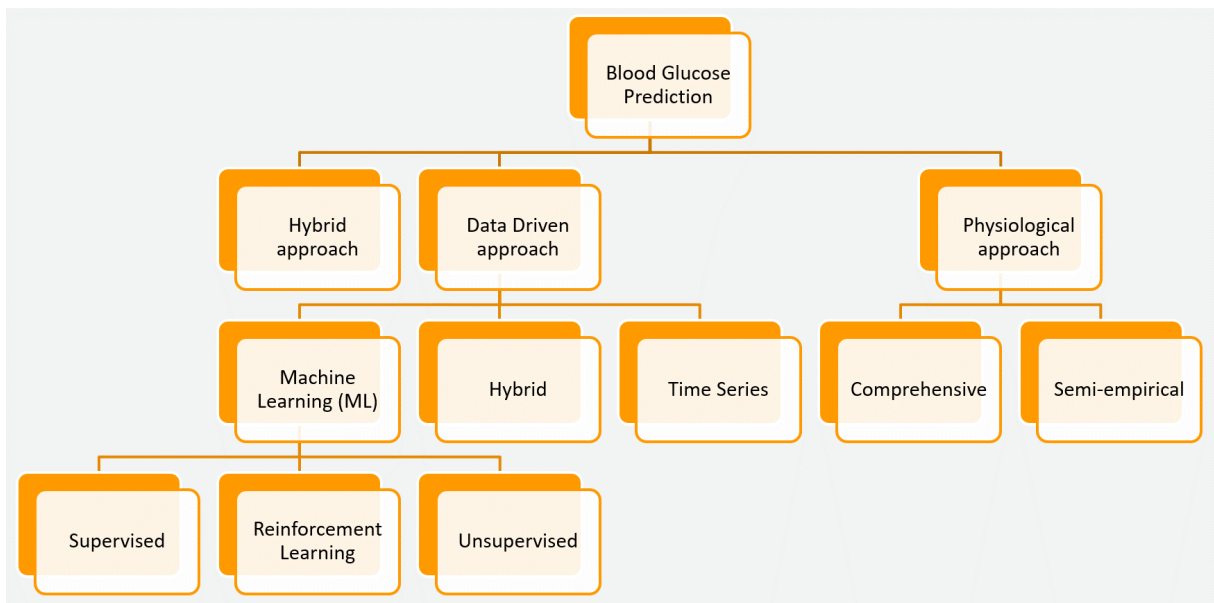


Figure 6: Classification for glucose prediction techniques (WOLDAREGAY et al., 2019).

Hybrid solutions usually combine mathematical modeling with data-driven techniques. In a literature search, (GEORGA et al., 2013),(LIU et al., 2019),(CESCON; JOHANSSON; RENARD, 2015),(CONTRERAS et al., 2018), presented hybrid predictive models with PHs from 90 to 120 minutes. Nevertheless, for (MUNOZ-ORGANERO, 2020), (ZARKOGIANNI et al., 2013),(SAITI et al., 2020),(BUNESCU et al., 2013),(BERTACHI et al., 2018), (LIU et al., 2018),(MIRSHEKARIAN et al., 2017),(WANG et al., 2020),(ISFAHANI et al., 2020),(ZECCHIN et al., 2014),(HAJIZADEH et al., 2018), the prediction horizon (PH) varies from 30 to 60 minutes.

4.1 Mathematical approaches

The literature presents some mathematical approaches to model and simulate the physiological behavior of GIRS. Some of them are described in the following.

Kissler and colleagues (2014) used ordinary differential equations (ODEs) to mimic the behavior of GIRS, using two compartments: glucose and insulin, detailed in section 3.2. However, in the proposed model, there are two inherent delays related to the action of fast-acting exogenous insulin and hepatic glucose production. Thus, it can be characterized as delayed differential equations (DDEs) which can be exemplified by a new synthetic model of the GIRS for inference of physiological parameters (CONTRERAS et al., 2020), including intestinal absorption and insulin resistance.

Makroglou and colleagues (2006) modeled glucose-insulin dynamics in IVGTT (intravenous glucose tolerance test) using integro-differential equations, that is a powerful tool to assess glucose metabolism in a single individual. Another characteristic is that both analysis and numerical simulations are performed, especially, when insulin dependent glucose tissue uptake is assumed to follow Michaelis–Menten dynamics (CAO, 2011). They also adopted partial-differential equations to build a model for the absorption of subcutaneously injected insulin.

Minimal models are nonlinear physiological and serve as references for simulators of individuals with T1D, for example (BROWN et al., 2019a), with their respective derivations including new compartments such as glucagon (NATH et al., 2018). Bergman and colleagues (1981) developed a minimal model of insulin secretion and glucose disappearance, limited to evaluate IVGTT results. Hovorka and colleagues (2004) presented a minimal model that is based on meal and subcutaneous insulin absorption, but with a maximum prediction horizon (PH) of 60 minutes, and a squared error of 8.48 mg/dL when related to PH of 30 minutes. Dalla Man and colleagues (2004) do not consider other external factors that influence blood glucose, such as physical exercise, and Panunzi and colleagues (2020) included meal disturbance, and parameters for uncertainty analysis in Sorensen model, resulting in a nineteenth order model wherein the glucose sub-system is divided into six more sub-systems.

In summary, isolated mathematical techniques do not have the characteristic of adaptability to automatically correct the error, and don't differentiate between insulin and food type.

4.2 AI approaches

Several ML techniques have been developed and evaluated to predict glucose oscillation including Artificial Neural Networks (ANN), Autoregressive model (AR), Support Vector Machine (SVM), Support Vector Regression (SVR), Gradient Boosting Decision Tree, Linear Regression and Genetic Programming (GP) (WADGHIRI et al., 2022). Specifically in the glucose oscillation prediction approach, this set of ML techniques (ensembles) are used, combining multiple single learners to find a better variance/bias trade-off and hence improve the prediction accuracy (WADGHIRI et al., 2022).

After a systematic mapping along related work, whose protocol and main findings are in appendix E, we adopted supervised learning with regression based on decision trees and reinforcement learning (RL) to support glucose oscillation prediction.

In fact, (MUNOZ-ORGANERO, 2020), (BERTACHI et al., 2018) and (MIRSHEKARIAN et al., 2017) adopt neural network approaches that yield a PH of 60 min when dealing with nine, six and 10 real patients, respectively; (ZARKOGIANNI et al., 2013) adopts a combination of compartment model and self-organizing map with 12 real patients, achieving a PH of 60 min; (SAITI et al., 2020) and (BUNESCU et al., 2013) adopt a support vector machine approach tested with six and five real patients, respectively, both achieving PH of 60 min. Moreover, (WANG et al., 2020), (ISFAHANI et al., 2020), (ZECCHIN et al., 2014), and (HAJIZADEH et al., 2018) achieved PH of 30 min by adopting bayesian inference, fuzzy logic & neural networks, neural networks and Kalman filter, respectively.

For long-term prediction horizon, we can state that Georga and colleagues (2013) adopted a multivariate regression approach, to derive a predictive model for subcutaneous glucose concentration prediction in T1D individuals. The method was evaluated with a dataset composed of 27 real T1D individuals and presented an average prediction mean square errors of 5.21 mg/dL for 15-min, 6.03 mg/dL for 30-min, 7.14 mg/dL for 60-min, and 7.62 mg/dL for 120-min PHs. Liu and colleagues (2019) presented a glucose forecasting algorithm suited for long-term PHs. The algorithm is based on compartmental models for the HGIRS. It was evaluated with clinical data of ten real T1D individuals. For a 120-min PH, an improvement of 18.8% on prediction accuracy measured with the root mean square error (RMSE), 17.9% A-region of error grid analysis (EGA), and 80.9% hypoglycaemia prediction calculated by the Matthews correlation coefficient. Cescon, Johansson and Renard (2015) presented a subspace-based linear multi-step predictor as a predictive model for short-term glucose oscillation. The model was evaluated with seven real T1D individuals and had obtained the prediction error standard deviation of 58.06

mg/dL on 120-min. Contreras and colleagues (2018) combine physiological models for HGIRS with grammatical evolution as a search-based technique to design a predictive model for short-term glucose oscillation. Considering the CEG, they achieved more than 96% results falling inside regions A and B for 90-min.

Since there are T1D individuals that feed at intervals greater than two hours, their results are not helpful for them. The proposal of the Tesseratus model is to extract the best features of each approach (physiology, data and multi-agent) in order to reach a longer PH, at personalized intervals of four hours in the full daytime period, and eight hours in the night period, keeping the MAE below 28 mg/dL in both periods and for all PHs.

4.3 Discussion

Regarding the physiological model inputs, two trends have been identified according to (OVIEDO et al., 2017): (1) most of the works referenced in Table 47 use meal models and insulin models to pre-process the carbohydrate estimation and insulin amount inputs. In general, hybrid glycemic prediction models use information about the amount of carbohydrates, and 78.5% of the studies surveyed used an insulin kinetics model to incorporate this input into the data-driven model (OVIEDO et al., 2017). In most of the works studied, the intake of insulin and food is continuous, and this is not the reality of an individual with T1D. In addition, there is also no differentiation on the amount of protein and fat ingested, which can change the glycemic curve at different times after meal.

However, the hybrid model developed by (GEORGA et al., 2013) has a lower quadratic error (7.62 mg/dL) among the others with the longest PH (120 minutes). One of the positive factors of this work is the use of insulin kinetics modeling. In fact, they adopt a mechanical approach, which is able to describe the absorption of different insulin formulations and their analogues, including fast-acting (lispro, aspart), short-acting (regular), intermediate action (NPH - Neutral Protamine Hagedorn) and long action (glargine). However, it has no long-term prediction and does not present continuous learning. Based on the values achieved by Georga and colleagues, this was one of the trends of our work to be hybrid, in order to achieve smaller error values between the measured and predicted values.

According to Wadghiri and colleagues 2022: (1) regression trees, ANN and AR models were the most used to construct the ensembles; (2) ensembles in general outperformed

their single techniques. Nonetheless, other recent works, (FOSS-FREITAS et al., 2019) and (FOSS-FREITAS et al., 2020), based on Recurrent Neural Networks (deep learning architecture), do not use hybrid techniques such as ML and physiological models, but they serve as a comparison and should be in the state of the art in glucose prediction, as they also aims for long PH, such as 6 hours.

About the 16 hybrid models discovered, the proposed PH does not exceed 120 minutes, due to the time correlated with the metabolism of carbohydrates in the human body and also the increase in error in terms of predicted glycemic value. For details about each model, see Table 47 in appendix E. Nevertheless, naturally there are individuals with T1D that feed between intervals longer than 120 minutes, for example, four hours in daytime (morning and afternoon) or from six up to eight hours in nighttime.

In summary, this Chapter describes relevant techniques applied to combine data-based and physiological modeling for dynamics of glycemic prediction, exclusively in individuals with T1D. Tesseractus model extracts the best features of each approach (physiology, data and MAS), where physiological dynamics is represented by differential equations for glucose compartment and polynomial equations for insulin, described in section 3.2. The second category uses historical data recorded by the individual, for example, through machine learning described in the subsection 3.3. In the third category, the agents consolidate the combination of the physiological model and also based on data, the last being the Tesseractus model approach.

5 STATE OF PRACTICE IN PREDICTION OF GLYCEMIC OSCILLATION

In this chapter, some devices such as glucometer, insulin pump and artificial pancreas are presented. They can benefit from the Tesseract Model, feeding it with data and receiving recommendations, creating a positive loop of interaction with the individual.

5.1 Data-driven solutions

To improve the accuracy of the prediction of glucose oscillation, it is necessary to obtain details about the individuals with T1D's lifestyle. The possibility of incorporating software into devices with low computational capacity can facilitate the integration of individuals with T1D with applications, in a model capable of collecting and receiving basic information from each individual and then predicting glucose oscillation (PEREIRA et al., 2019).

The use of IoT (Internet of Things) devices and sensors has become increasingly common for this real-time data collection function (RODRÍGUEZ, 2020). In fact, individuals with specific diseases, as T1D, are encouraged to perform most of their checks through an app and receive data through a device (COBELLI; RENARD; KOVATCHEV, 2011). Remote monitoring and self-management of T1D has been one of the application areas of mHealth (mobile health). This proliferation was reflected in the numerous pilot studies and hundreds of commercial applications for individuals with T1D, in addition to mobile self-management systems created since 2007 (ISTEPANIAN; AL-ANZI, 2018).

Using technology to implement remote management is essential for proper control of T1D. Nowadays, an app, installed on a cell phone, and continuous glucose monitoring (CGM) devices are designed to collect data, monitor and adjust the results in real time. In addition, studies show that the glycemic control of the individual with T1D can be improved, if there is access to the following individual data (RODRÍGUEZ-RODRÍGUEZ; ZAMORA-IZQUIERDO; RODRÍGUEZ, 2018): (i) feeding profile and ingested macronu-

trients; (ii) duration and intensity of physical exercises; (iii) age; (iv) body mass; (v) medications such as basal and bolus insulins; (vi) stress information; (vii) quality of sleep; (viii) heartbeat; (ix) current and historical blood glucose.

All stakeholders across the healthcare industry, including the individual with T1D themselves, need to have access to this data, in full, anywhere, whether locally on mobile or remotely on cloud service providers (AZURE, 2022). The insights generated by the data need to be considered in managing the evolution of the individual with T1D (CHAKI et al., 2020). Individuals with T1D, together with their endocrinologist, must access and process them subjectively, in order to discern about adjustments in routines and medication. The main objective of this analysis is to control the course of blood glucose, changing the profile dynamically. Obviously, the entire data sharing process must have consent and respect data privacy laws with 13709 (LGPD - Brazil) (LGPD, 2023).

Subjective interpretation by the individual with T1D or even incorrect correlation of these data can sometimes lead to treatment errors, which can also occur due to partial data evaluation. The quality of data organization and the increase in the amount of data requires an adequate format for extracting and processing data, efficiently and effectively (RODRÍGUEZ-RODRÍGUEZ; ZAMORA-IZQUIERDO; RODRÍGUEZ, 2018).

5.2 Blood glucose monitors, flash sensors and apps

In (SIDDIQUI et al., 2018), a taxonomy of glucose monitors is proposed, as described in Figure 7. Devices are of three types: non invasive, minimally invasive and invasive. In the last decade, technology supports the development of non-invasive glucose monitors, and some are already commercialized, such as the glucose meter through photometric techniques (CNOGA, 2020), and there are others in the research phase with the use of contact lenses (KEUM et al., 2020). These new devices are designed to provide more options for managing T1D. However, the most common monitors are invasive or minimally invasive.

Minimally invasive monitors, which use glucose strips (ACCU-CHECK, 2020), are the most common, with few copies that can be integrated into applications via bluetooth. They are characterized by the manual process of capillary blood collection, and further analysis on the device. However, the introduction of the CGM brought about a revolution in the control of T1D. CGM devices allow continuous measurement of the glucose present in the subcutaneous interstitial fluid, with sampling frequency normally every five minutes.

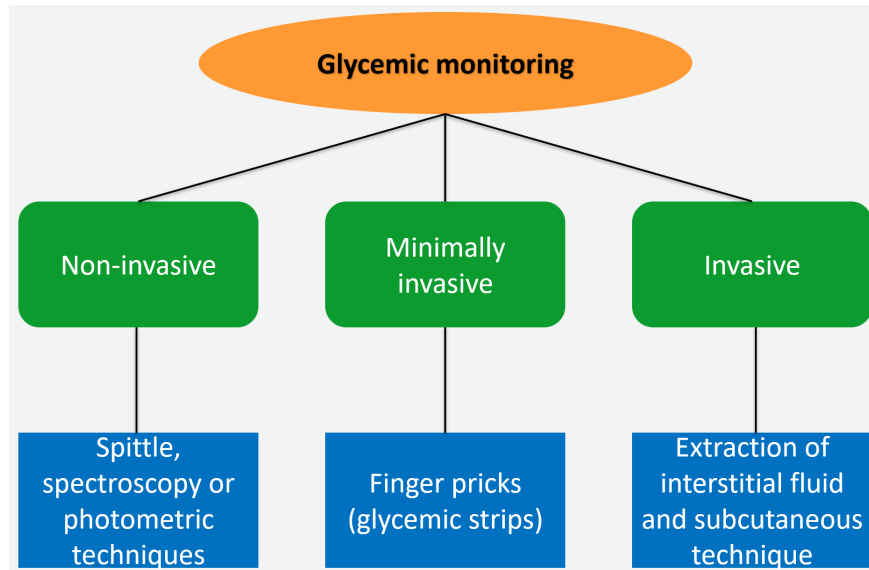


Figure 7: Taxonomy of blood glucose monitors.

This average duration varies from six (DEXCOM-G6, 2020) up to 14 days (FREESTYLE, 2020), so that, through correction algorithms, they present the glucose values in the interstitial fluid to the user. Research on new methods of CGM and possible improvements is frequent. One of the research examples is about evaluating a new algorithm for an invasive device (FREESTYLE, 2020), as in (KARINKA et al., 2019).

However, these monitors and glucometers must follow accuracy requirements already established by Health Organizations or Federations. For the prediction horizon (PH), in real time, the ISO1597 of 2015 (JENDRIKE et al., 2017) established that if the glucose is greater or equal to 100 mg/dL, the results should be within $\pm 15\%$ of the reference standard. If glucose is less than 100 mg/dL, results should be within ± 15 mg/dL of reference comparator. In total, 95% of all results must meet the following criteria:

- 95% of values in the range ± 15 mg/dL to < 100 mg/dL (characteristic of hypothetical hypoglycemia);
- 15% for values ≥ 100 mg/dL, and above 180 mg/dL is characterized as hyperglycemia.

However, in FDA guidelines (KATZ et al., 2020), 95% of all blood glucose results must be within $\pm 15\%$ and 99% within $\pm 20\%$ of the baseline comparator, regardless of where in the glucose range the results are:

- 95% of all values must be in the $\pm 15\%$ range;

- 99% of all values must be in the $\pm 20\%$ range.

Clinical accuracy is focusing on the clinical relevance of the meter results in comparison with analytical accuracy, which gives detailed information about agreement of the home glucose meters, in comparison with a reference method. Two metrics can be used to assess clinical accuracy of glucose meters: (1) Clarke Error Grid (CEG) (CLARKE et al., 1987); (2) Parkes Error Grid (PEG) (PFÜTZNER et al., 2013). The PEG has been intended for use in assessing clinical accuracy of glucose meters for patient self-measurement, and was proposed to be an alternative to the CEG that had been criticized for the placement of its risk boundaries.

Other devices are portable monitors that range from wristbands to track health indicators, to devices for insulin delivery, such as insulin pumps, and are valuable items for individuals with T1D. In recent years, there has been an increase in the number of remote management systems for individuals with T1D, which receive information shared by applications installed, for example, on mobile phones. Smartphones increased their connection capacity and computing power, in addition to the potential use of IoT devices. Through these devices, individuals with T1D have real-time access to data with their own glycemic controls, heart rate. Thus, they can directly create or interact with their own treatment plans, through a mobile health application that brings new functionalities, such as glycemic prediction, for example, the Tesseract model.

5.3 Automatic insulin delivery

Another advanced device in glycemic prediction and insulin infusion is the artificial pancreas (AP). The AP is a system of devices that mimics the glucose regulatory function of a healthy pancreas. An AP is sometimes referred to as a closed-loop system, an automated insulin delivery system, or a stand-alone system for glycemic control (FDA-PA, 2020).

Most AP systems consist of a combination of three types of devices known to the medical community and individuals with T1D: (1) a CGM system; (2) an insulin infusion pump; and (3) a glucose meter that is used to calibrate the CGM (FDA-PA, 2020). Control algorithms for predicting glycemic oscillation and managing individuals with T1D (MEHMOOD et al., 2020) can also be used, as well as Tesseract. The prediction strategy, inserted into an AP system, can avoid hypoglycemia or hyperglycemia states, helping in the correct administration of fast acting insulin.

In 2016, the Food and Drug Administration (FDA) (FDA, 2016) of the United States of America (USA) approved the first hybrid closed-loop system. Such system monitors glucose and automatically adjusts the delivery of basal-effect insulin, based on the individual's glucose reading. The system measures the user's glucose for up to seven days, and the pump can automatically adjust the dose of insulin applied, using a mathematical equation or algorithm that incorporates information from the CGM. However, this version has some associated limitations: (i) even in automatic mode, the user must still administer insulin manually during meals; (ii) continuous monitoring for only seven days; (iii) not available in emerging countries such as Brazil; (iv) PH of up to 30 minutes; (v) it cannot be used in people who require less than a total insulin dose of eight units per day; (vi) capillary blood glucose tests are still needed.

In 2019, the FDA (FDA-CONTROLIQ, 2019) approved the second automated and interoperable insulin dosage controller designed for individuals with T1D looking to customize their diabetes management system. The AP system, called Control-IQ®, was derived from research conducted, with 168 patients, at the University of Virginia Diabetes Technology Center (UNIV-VIRGINIA, 2020),(BROWN et al., 2019a). Such a research has shown that Control-IQ® can improve glycemic outcomes in individuals with T1D (BROWN et al., 2019a). In fact, they report that individuals with T1D experienced an average increase of an additional 2.5 hours per day, within the optimal glycemic range. Another advantage is that capillary blood glucose tests are no longer necessary. However, this AP system has some limitations (UNIV-VIRGINIA, 2020): (i) although the system has been evaluated for reliability, incorrect calculations and commands can still occur, causing delays in insulin delivery; (ii) it cannot be used on individuals with T1D that require less than 10 units of insulin per day; (iii) it works only with two types of insulin: aspart and lispro (CONTROL-IQ, 2022); (iv) possibility of incorrect insulin administration as a result of loss of communication between connected devices; (v) it is not available in emerging countries such as Brazil; (vi) its PH is short (30 minutes).

5.4 Discussion

Glucometers, and their respective applications, do not have the feature of predicting, only of collecting and displaying the glycemic value. Therefore, telemedicine applications only have the glycemic point in a specific period, losing the patient's history, without the ability to predict glycemic values. Figure 8 represents a common flow of data collection, but without the prediction feature. It would be necessary a system to assist in the trans-

mission, storage and organization of this data. In addition, specific organization software, storing glycemic data, of macronutrients, such as Glic (GLIC, 2022) and (MONTANARI, 2022), does not have the ability to use them to predict glycemic oscillations.

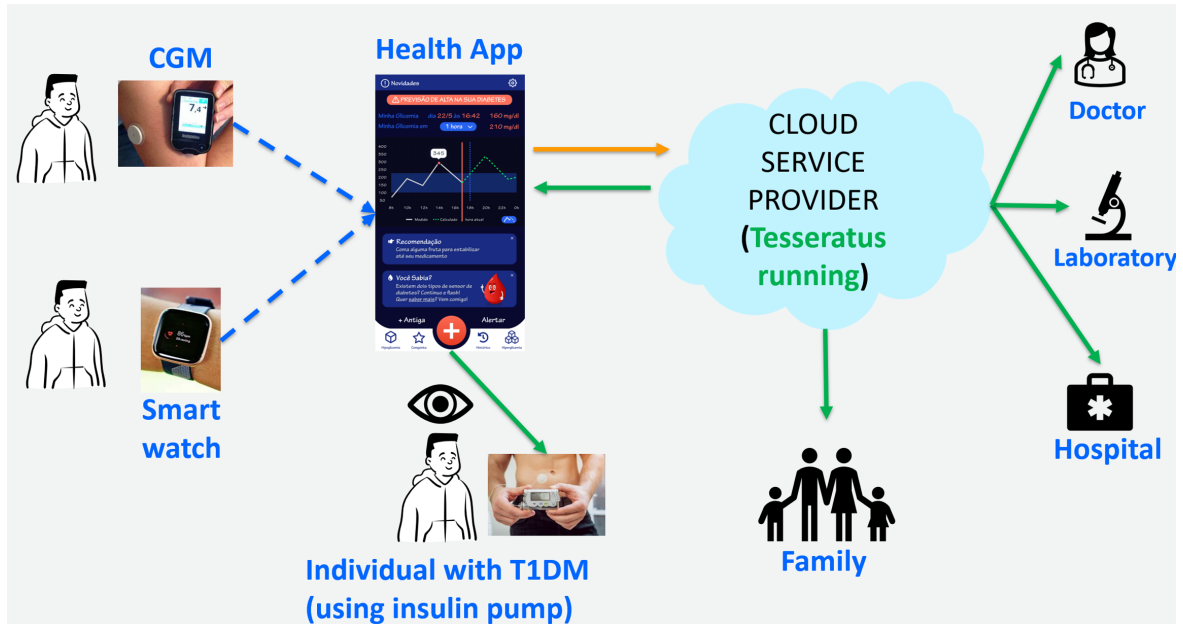


Figure 8: Example architecture for data collection/transmission and remote monitoring.

Normally, the aforementioned commercial AP systems, support only short-term prediction horizons with personalized suggestion, but they don't have the possibility to use different techniques to predict glycemic oscillations. And the most part of commercial AP systems don't have a secondary storage and management of the collected data, in order to consolidate them in a knowledge base, indexing and making them remotely accessible, for example in a public cloud of services (AZURE, 2022).

There is also an open AP system project, such as OpenAPS (OPENAPS, 2021), for individuals with T1D, but with a short prediction horizon (30 minutes). The general idea of OpenAPS is to make AP system technology basic and accessible. OpenAPS is closed-loop and uses glucose estimation from CGM to automatically adjust the insulin doses to be delivered. It performs this task by communicating with an insulin pump to get details of all recent insulin doses, and also with a continuous glucose monitoring device to get estimates of current glucose levels, and issues commands to the insulin pump. However, they cannot improve the accuracy of responses to changes in glucose values and reduce HbA1c values. Open AP system can't be massively used because they don't have a continuous learning process built in, to reduce error and improve accuracy. Tesseractus is proposed to overcome these limitations. It is presented in Chapter 6.

PART II

PROPOSAL

6 TESSERATUS MODEL

This Chapter describes the Tesseractus model, in an architecture overview (section 6.1, detailing its agents and functionalities (section 6.2).

6.1 Overview

Tesseractus adopts a multi-agent approach to define a hybrid model to predict the glucose oscillation up to four hours during daytime and up to eight hours at night period, from the moment the individual requests the prediction. The proposed model is supported by the concepts of Machine Learning (ML - discrete) and Mathematics (ODE - continuous). The models that combine discrete and continuous aspects are commonly referred to as hybrid models (CILFONE; KIRSCHNER; LINDERMAN, 2014). The main objective of Tesseractus is to improve the accuracy of the predicted value in periods longer than six hours, in a continuous learning process. Nevertheless, to achieve this objective we had established several requirements that must be fulfilled. They are described at Table 5.

Another function of Tesseractus model is to support the analysis of past behavior, learning and prediction of glycemic oscillation, with subsequent recommendations of diet modification for each individual with T1D. The model aims to understand the need for individual macronutrients and their impact on glycemic oscillation, as well as the adjustment of the dose of rapid and basal insulin. As a consequence of continuous glucose monitoring (CGM), the individual with T1D can apply it in the context of nutritional recommendations, pre- and post-prandial, and in the planning of physical exercises, influencing lifestyle in the short, medium and long-term.

The reactive and reflective behavior of some agents occurs even in complex environments as the mimicked GIRS (RUSSELL; NORVIG, 2016), and they are used in Tesseractus model to reduce the computational cost. In addition, Tesseractus integrates smart agents with the ability to learn into the model, complementing the actions and behaviors of reactive agents, as shown in Figure 9. The input data are: **a)** current glycemic level

Functional requirements	Non-functional requirements
allow predicting the glycemic value in a horizon of four hours in the full daytime period	minimize the exchange of messages among agents
allow to predict the glycemic value in a horizon of eight hours in the night period	minimize the processing of the system that executes it
allow keeping the MAE, of the predicted X measured glycemic value, less than 30 mg/dL	allow the integration with remote management systems
allow continuous learning of each individual's glycemic behavior	allow integration with open source artificial pancreas
allow dynamic correction of system input parameters, according to Table 9	—
allow the use of proteins and fats, in addition to carbohydrates, as input data	—
allow using the pharmacokinetics of each type of insulin as input	—
allow the use of exercise time as input data	—
allow you to create personalized recommendations on feed	—
allow you to create personalized bolus and basal insulin dose recommendations	—
allow you to create personalized recommendations on time and intensity of physical activity	—
allow the execution of recommendations in less than 1 minute	—
allow 90% of measurements to be in zone A of the Parkes Error Grid	—

Table 5: Functional and non-functional requirements of the Tesseract model.

(mg/dL) - source: CGMs, for example flash sensors; **b**) type and duration (minutes) of physical activities - origin: smart watches; **c**) amount of carbohydrates (grams) - origin: manual insertion after counting carbohydrates; **d**) type of insulin (slow or fast effect) and injected units (U) - origin: manual insertion; **e**) date and time - origin: from the device itself, for example from the cell phone. The details about each agent and learning process are in section 6.2.

6.2 Tesseract multiagent system

As previously stated in Chapter 1, we adopted a multiagent approach for developing Tesseract. This section describes all the agents that compose the Tesseract MAS, with their respective responsibilities.

The agents of Tesseract are situated in a partially observable, stochastic, dynamic,

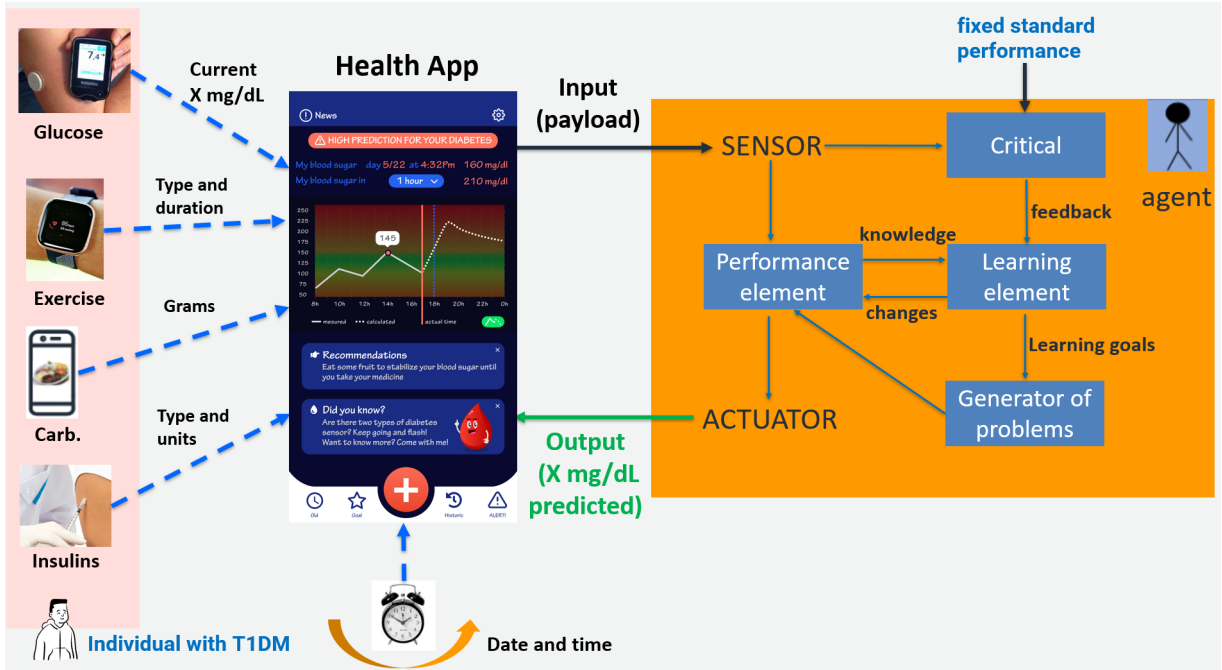


Figure 9: Structure of a learning agent adapted from (RUSSELL; NORVIG, 2016).

continuous and sequential environment (RUSSELL; NORVIG, 2016), in this case, representing the individual with T1D. To support this complex environment, the Tesseractus model includes three groups of agents that are used to decompose the complexity of the phenomenon in question (AMIGONI et al., 2003): (1) reactive agents (AgR) to collect data and pass it on to other agents from the system, via messages; (2) intelligent agents (AgInt) to learn, discern the best actions, and consequently predict and recommend based on prior knowledge, generated by itself or provided by other agents, inserted in its KB; (3) intelligent agent that generates knowledge individually (AgKnow), without receiving knowledge from other agents, generating it based on input data indirectly provided by the environment.

Active reinforcement learning is used among the agents of the Tesseractus model and takes advantage of the reuse of acquired knowledge (KHOLGHI et al., 2015) in previous tasks and/or from other agents. A mechanism of cooperative interaction between agents and balanced negotiation is also used to control and synchronize all communication between agents, and consequently monitor the environment in an uninterrupted way.

The AgR agents of the Tesseractus model are responsible for stimulating the system each time they receive new information and, in addition to immediately propagating the received message to the recommender AgInt. They also store simple condition-action rules. There are nine reactive agents that are always active and have the following responsibilities within the system:

- (1) **Curr-Gluc** agent: it is responsible for capturing the current glucose information (mg/dL), coming from CGM (interstitial fluid), and stimulating the system. This data can be automatically received each five minutes, via flash sensors, or manually entered. The actions of **Curr-Gluc** agent are represented by the flowchart in Figure 34.
- (2) **Exercise** agent: it is responsible for capturing the physical activity information: time in minutes, stimulating the system. The individual with T1D also can enter the information about the exercise intensity. This data can be automatically received via sensors, smart-watches or manually entered, and to be correlated through maximum blood oxygenation (VO_2) or heart beats per minute (BPM).
- (3) **Inbolus** agent: it is responsible for capturing information about the type and amount of bolus insulin ($\mu\text{U}/\text{mL}$ or pmol/L) (fast acting), and stimulating the system. This stimulus can occur few times a day, according to the frequency of feeding. This data can be automatically received via an insulin pump or be entered manually or by voice, if the feeding occurs by injections or applicator pens. In this work, the **Inbolus** agent expects the entry of only two types of fast-acting insulin: aspart and lispro, but it can be adapted to other types of fast-acting insulins, depending on the availability of the pharmacokinetic concentration curve by the pharmaceutical industry.
- (4) **Inbasal** agent: it is responsible for capturing information about the type and amount of basal insulin ($\mu\text{U}/\text{mL}$ or pmol/L) (slow action), and stimulating the system. Usually this stimulus happens once or twice a day. Until now, this data can only be entered manually, as insulin pumps only support bolus insulins, even when creating the basal effect with bolus insulin (by injecting these insulins continuously). In this work, the **Inbasal** agent expects the entry of only two types of long-acting insulin: glargine and degludec, but it can be adapted to other types of long-acting insulin, depending on the availability of the pharmacokinetic concentration curve by the pharmaceutical industry.
- (5) **Carb-in** agent: it is responsible for capturing information about the type and amount of carbohydrates (grams), and stimulating the system. This data is usually entered manually, but it also can be obtained through an application that calculates the nutritional content of a food photo, such as (TADA) (FANG et al., 2019), as well as the **Prot-in** and **Fat-in** agents, which includes percentages of carbohydrates, through a photo of the food. The other option would be by scanning the barcode

of the product to be ingested.

- (6) **Prot-in agent**: it is responsible for capturing information about the type and amount of proteins (grams), and stimulating the system. The **Prot-in** agent maintains in its base the rules referring to the association with carbohydrates, according to the subsection 3.1.4.
- (7) **Fat-in agent**: it is responsible for capturing information about the type and amount of lipids or fats (grams), and stimulating the system. The separate calculation or measurement of the amount of fat is more complex compared to carbohydrates and proteins, but it can be mitigated by automating the recognition process. The macronutrient fat should not be encouraged in the diet, but it is included in the mixed food menu. Therefore, the **Fat-in agent** maintains in its base the rules referring to the association with carbohydrates, according to the subsection 3.1.4.
- (8) **Alcohol-in agent**: it is responsible for capturing information about the type and volume of alcohol (ml), and stimulating the system. The data is usually entered manually. The other option would be by scanning the barcode of the product to be ingested.
- (9) **Capillar-in agent**: it is responsible for capturing the current blood glucose information (mg/dL), coming from blood glucose device (capillary blood), and stimulating the system by correcting the **Curr-Gluco agent**. This data can only be entered manually.

All AgR agents could also be integrated into a system that converts voice to text facilitating visual accessibility, such as (VOICE-AZURE, 2022), or even a typing-friendly mobile app, in order to facilitate data entry and sharing.

In addition to the nine aforementioned AgR, there are other ones that we called satellite agents in the system: (1) **(ODE parameters agent)**, each responsible for its specific parameter, which monitor all the ODE parameters; (2) **monitor error agent**. It is responsible for evaluating the mean absolute error (MAE) between the measured and predicted value, creating its own KB of errors; (3) **anomaly detector agent**, in order to avoid false alarms in terms of possible hypo- or hyperglycemia peaks.

The four main agents of Tesseractus are hybrid agents (AgInt and AgKnow). They are stimulated by reactive agents each time they receive new data. Their individual responsibilities are detailed below:

- (1) **Recommender agent**: it is an AgInt agent and one of the main agents in the model, as it also accumulates the recommendation and learning functions. It is responsible for making all recommendations based on knowledge (time, label and prediction) acquired previously, through supervised learning, from that individual who stimulated the system or from other individuals. The actions of **Recommender agent** are represented by the flowchart in Figure 45. The following actions of Predictor, ML and **Math** agents are related to phases 1 and 2 of learning: Figures 43 and 44, respectively;
- (2) **Predictor agent**: it is an AgInt agent with the responsibility of analyzing the content of the message from **Recommender agent**, verifying the values entered and asking the **Math** and ML agents, the prediction related to those values, and other values in broader intervals ($\pm 20\%$), that should reach the optimal predicted curve;
- (3) ML agent: it is an AgInt agent with responsibility divided into two phases of learning the Tesseract system: in the first one, it manages supervised learning and transfer learning, and in the second phase predict and participate in RL cycle;
- (4) **Math agent**: it is an AgKnow agent with responsibility divided into two phases of learning of Tesseract model. The **Math** agent uses ODE for the glucose compartment and polynomial approximation for the insulin compartment, detailed in the section 7.2, and is responsible for storing, and recalculating if necessary the approximation curves of the insulin pharmacokinetics (U/Kg) for fasting and prolonged action. All generated calculations are stored in your KB.

An example of actions flow is represented in Figure 11, and all steps are below:

- (1) individual X reports the following values at 8 am: current glucose level = 180 mg/dL, insulin aspart = 5U, insulin glargine = 26U, carbohydrate = 70g, exercise = 0 minutes, and request a 4-hour prediction horizon (PH);
- (2) AgR agents collect this information and propagate it to the **Recommender agent**;
- (3) **Recommender agent** checks if it has this dataset and timestamp associated with an output (action), in its KB;
- (4) if the **Recommender agent** has this action and the predicted value, it can evaluate which is the best recommendation, if the value is not in the optimal range;

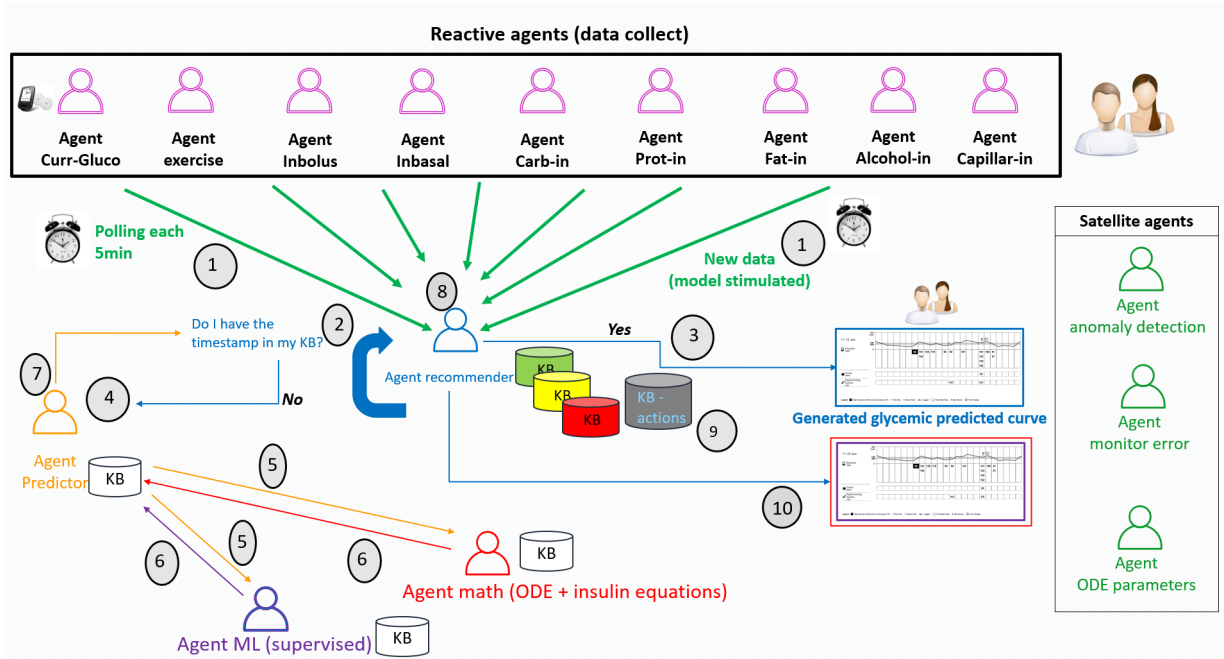


Figure 10: Tesseract architecture.

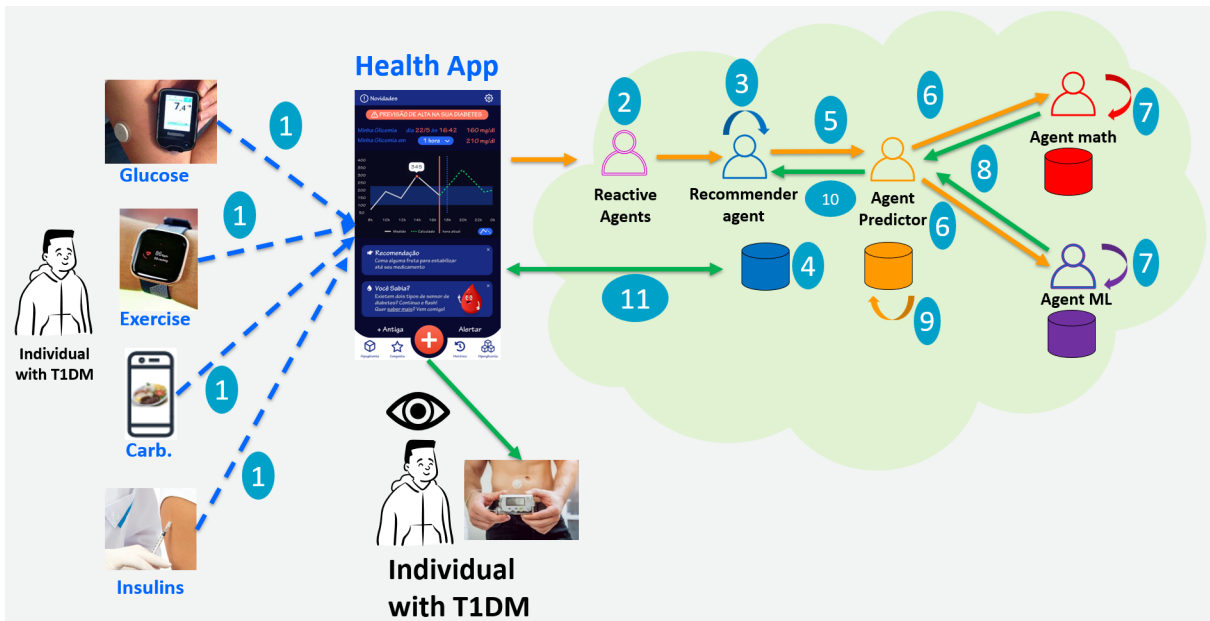


Figure 11: Example of the action flow of Tesseract model in real life.

- (5) if the Recommender agent does not have this action and the predicted value, it sends a message to the predictor agent requesting a prediction curve for $PH = 4$ hours. At this point, the Recommender agent already has in its KB the initial carbohydrate:insulin bolus ratio, which is 12:1, but the individual informed ($70g:5U = 14g$ of carbohydrates for 1 unit of insulin), which refers to a person of 60kg, and a correction to the input data values is required;
- (6) Predictor agent must send the message to the AgKnow agents;

- (7) **ML** and **Math** agents should calculate glycemic oscillation. At this point, the agents already know the body mass of individual X (70Kg). Thus, the calculation for insulin aspart would be $(5/70 = 0.07 \text{ U/Kg})$ and for insulin glargine $(26/70 = 0.37\text{U/Kg})$;
- (8) **ML** and **Math** agents return the message with the predicted value;
- (9) if the **Predictor** agent receives a non-ideal value (neutral or negative), it should automatically request recalculation based on a wider range ($\pm 20\%$): insulin aspart = from 4U to 6U, insulin glargine = from 21U to 31U, carbohydrate = from 56g to 70g, exercise = from 60 to 120 minutes. In this case, the current glucose value cannot be changed;
- (10) after recalculation, if there are more than one option within the ideal range (green area in semaphores), send to **Recommender** agent decides;
- (11) after sending the recommendations by the **Recommender** agent, the individual must evaluate the best condition to reach the ideal glycemic value at that moment. For example, it may not be appropriate to exercise at day time, but it would be better to prioritize decreasing the amount of carbohydrates than increasing the amount of bolus insulin. This individual's decision is also stored as a future prediction of behavior associated with options.

6.3 Discussion

The Tesseractus model is embedded in a complex physiological environment to predict and offer personalized suggestions. The MAS makes use of mathematical modeling and machine learning techniques to model and regulate the glucose-insulin regulatory system of individuals with T1D. The utilization of agents as well as active learning ((VERSTRAETEN et al., 2020) and (SETTLES, 2009)) are essential for the correct functioning of the Tesseractus model. Its functioning was designed in a two-phase process of learning. Therefore, instantiation of Tesseractus must be performed in two phases. Both phases adopts a hybrid approach, in the sense that agents learn based on data provided by all the nine and satellite reactive agents, and outputs of the mathematical modeling provided by the **Math** agent. The next Chapter presents how instantiation occurs.

7 TESSERATUS INSTANTIATION

This Chapter presents the steps for instantiating Tesseractus, emphasizing the two-phase learning process. As described in Chapter 6, Tesseractus has four main intelligent agents, that receive information from reactive agents and combine them with outputs of a mathematical modeling of GIRS with the support of a rewarding policy.

7.1 The rewarding policy

In order to support the two-phase learning process for instantiating Tesseractus, we define a policy reward that is domain-dependent and varies according the individual of T1D period: fasting or postprandial. The semaphore policy was adopted to label tuples of values provided by the reactive agents whenever compared to the desirable ones.

For the fasting period, we adopt a reward of 10 whenever the glucose concentration value lies on the interval between 100 mg/dL and 120 mg/dL, or the absolute error between collected and desired values are lower than 15 mg/dL. In addition, a reward of eight is established whenever the glucose concentration is between 80 mg/dL (included) and 100 mg/dL (excluded). These values are labeled as green. Glucose concentration values lying along the open interval between 120 mg/dL and 180 mg/dL, or absolute error between collected and desired values lying along the interval between 15 mg/dL and 30 mg/dL, don't get score and are labeled as yellow.

Still for the fasting period, a punishment of -10 is established whenever the glucose concentration value is greater than 200 mg/dL or lower than 80 mg/dL, or the absolute error between collected and desired values is greater than 50 mg/dL. In addition, whenever the glucose concentration values lies on the interval between 180 mg/dL and 200 mg/dL, or the absolute error lies on the interval between 30 mg/dL (excluded) and 50 mg/dL, a punishment of -5 is established. For these values, labels are red. A summary of this policy is presented at table 6.

State	fasting period	Reward
Green	$100 \leq Gluc_0 \leq 120$	10
Green	$0 < \text{Absolute error} < 15$	10
Green	$80 \leq Gluc_0 < 100$	8
Yellow	$120 < Gluc_0 < 180$	0
Yellow	$15 \leq \text{Absolute error} \leq 30$	0
Red	$180 \leq Gluc_0 \leq 200$	-5
Red	$30 < \text{Absolute error} \leq 50$	-5
Red	$Gluc_0 > 200$	-10
Red	$Gluc_0 < 80$	-10
Red	$\text{Absolute error} > 50$	-10

Table 6: Tesseractus model reward policy (fasting period).

For the postprandial period, we adopt a reward of 10 whenever the glucose concentration value lies on the interval between 80 mg/dL and 100 mg/dL, or the absolute error between collected and desired values is lower than 15mg/dL. In addition, a reward of eight is established whenever the glucose concentration is between 100 mg/dL (inclusive) and 160mg/dL (excluded). These values are labeled as green. Glucose concentration values lying along the open interval between 160 mg/dL and 180 mg/dL, or absolute error between collected and desired values lying along the interval between 15 mg/dL and 30 mg/dL, don't get score and are labeled as yellow. Red labeling follows exactly the thresholds defined for the fasting period. A summary of this policy is presented at Table 7.

State	postprandial period	Reward
Green	$80 \leq Gluc_0 \leq 100$	10
Green	$0 < \text{Absolute error} < 15$	10
Green	$100 \leq Gluc_0 < 160$	8
Yellow	$160 < Gluc_0 < 180$	0
Yellow	$15 \leq \text{Absolute error} \leq 30$	0
Red	$180 \leq Gluc_0 \leq 200$	-5
Red	$30 < \text{Absolute error} \leq 50$	-5
Red	$Gluc_0 > 200$	-10
Red	$Gluc_0 < 80$	-10
Red	$\text{Absolute error} > 50$	-10

Table 7: Tesseractus model reward policy (postprandial period).

7.2 The Math agent

The **Math** agent implements a mathematical modeling for the Glucose-Insulin Regulation System (GIRS) that adopts the Glucose compartment defined as an ordinary differential equation by (KISSLER et al., 2014) and a polynomial approximation of the Insulin pharmacokinetic data.

The glucose equation $G'(t)$ (glycemic value as a function of time) should be calculated using the Runge-Kutta method. It is directly related to the amount and type of macronutrients ingested as well as the time (Δt_{ex} – measured in minutes) and intensity (VO_2 – maximum volume of oxygen consumed) of physical exercise (NELSON et al., 2013), (LIU et al., 2018), in accordance with (SBD, 2022c).

G_{in} and I_{in} values refer to the rate of glucose intake and insulin infusion, respectively. G_{in} is measured in $mg/(dL.min)$, varying in the interval $[0, 1.08]$. The insulin equation $I'(t)$ (insulin concentration value as a function of time) and the value of I_0 (insulin concentration at $t(0)$) come from the pharmacokinetics equations of each type of insulin (subsec 7.2.2), selected by each individual.

Thus, having these two equations modeled, we feed our **Math** agent with them in order to start the labeling of our dataset, as well as to support the continuous learning in Tesseractus.

7.2.1 The glucose compartment equation

The description of how the glucose compartment is modeled by using a similar approach of equation 3.4, extending f_1 and reusing f_2 , f_3 and f_4 . Also, we rename the physical exercise contribution to the model ($f_{ex} = [1 + s(\Delta t_{ex} - \overline{\Delta t_{ex}})]$). Therefore, it is represented by equation 7.1

$$G'(t) = \overbrace{(G_{in} + f_1(I(t - \tau_2)))}^{\text{glucose production}} - \underbrace{(f_2(G(t)) + \gamma f_{ex} \cdot (f_3(G(t)) \cdot f_4(I(t))))}_{\text{glucose consumption}} \quad (7.1)$$

Our extension in f_1 considers the fact that there are two sources of glucose production: the hepatic glucose production (HGP) (KISSLER et al., 2014), and the glucose yielding from the metabolism of ingested macronutrients.

In this case, glucagon exerts control over the liver and causes it to dispense glucose, with a slight delay (given by τ_2) of between 15 and 20 minutes (BRATUSCH-MARRAIN; KOMJATI; WALDHÄUSL, 1986). In order to allow personalization, we redefine f_1 considering or not alcohol ingestion, following the understanding of Schinifelboeck et al 2016. Both equations (7.2) and (7.3) use the reference values proposed by (LI; KUANG; MASON, 2006), (STURIS et al., 1991) and (TOLIĆ; MOSEKILDE; STURIS, 2000). Then, for HGP_{max} is $180mg/min$, α is $0.29L/mU$, V_{pla} is $3L$, and C_5 is $26\mu U/L$.

Here, HGP_{max} stands for hepatic glucose production, α for hepatic sensitivity to changes in insulin, V_{pla} for the volume of plasma in the body, C_5 for the insulin concentration at which the liver is most efficient, and $A_g(t)$ for alcohol ingestion (equation 7.2).

$$f_1(I(t - \tau_1)) = \frac{HGP_{max} \cdot (1 - A_g(t))}{(1 + \exp(\alpha(\frac{I(t)}{V_{pla}}) - C_5))} \quad (7.2)$$

or

$$f_1(I(t - \tau_1)) = \frac{HGP_{max}}{(1 + \exp(\alpha(\frac{I(t)}{V_{pla}}) - C_5))} \quad (7.3)$$

For glucose utilization, four main components are considered: (1) insulin resistance in relation to exercise time, is represented by $\gamma * f_{ex}$, but the value of γ is replaced by the value of $eGDR$ (EPSTEIN et al., 2013); (2) use of glucose by the Central Nervous System (CNS), represented by $f_2(G(t))$ as a function of glucose; (3) binding of insulin to muscle and fat cells, represented by $f_3(G(t))$ as a function of insulin concentration; and finally (4) the use of glucose by muscle and adipose cells, $f_4(I(t))$ as a function of glycemia. The values of Ub , C_2 , V_{gli} , Um , $U0$, C_4 , V_{int} , T_{pla} , T_{deg} and C_3 are in Table 9. The scale factor ζ with a value of 1.77 (KISSLER et al., 2014) is used only in the equation $f_3(I(t))$. The parameters of Table 9 are constants to be monitored and can be updated by the model agents.

There are two inherent delays that is considered in the ODE system: (1) the onset of action of exogenous insulin, after its infusion, to promote glucose uptake and inhibit hepatic glucose production; and (2) hepatic glucose production, stimulated by α cells, if not inhibited (GYLFE; GILON, 2014). Discrete delay is usually a simplification of the complex physiological process, which is most often represented by a continuous and distributed delay. Therefore, it is desirable to use continuous and distributed delay parameters rather than discrete delays when modeling these systems (CAMPBELL; NCUBE, 2017). It is worth mentioning that in addition to the delay, there is resistance in the action of insulin due to peripheral (exogenous) administration in individuals with T1D,

and not endogenously, compared to individuals who do not have DM.

A point to note is that eating and exercise behaviors have an important effect on glycemic outcomes, in individuals with T1D, although these influences are difficult to evaluate in real environments. Thus, more accurate models of eating and exercise behavior are needed to capture glycemic oscillation. In a real physiological process, delays inherent to sensors or actuators in negative feedback circuits are present in the dynamics, such as, for example, CGM devices based on interstitial fluid (flash sensors). ODEs represent these phenomena more satisfactorily and are used in this modeling.

Variables	Unit	Description	Initial Condition
Glucose: $G'(t)$	$\frac{mg}{dL}$	Blood glucose value as a function of time	NA
Insulin: $I'(t)$	$\frac{\mu U}{mL}$	Insulin value as a function of time	NA
Parameters	Unit	Description	Initial Condition
Glucose $G(0)$	$\frac{mg}{dL}$	Glycemia in $t(0)$	Reported by the glucometer, $G(0) > 0$
Insulin $I(0)$	$\frac{\mu U}{mL}$	Insulin concentration at $t(0)$	0.65 or insulin type pharmacokinetic information, $I(0) > 0$
G_{in}	$\frac{mg}{dL.min}$	Glucose intake rate	Between 0–1.08 or recursive calculation from 1.08
I_{in}	$\frac{\mu U}{mL.min}$	Exogenous insulin infusion rate	Between 0-2 with recursive calculation from 0.65 or insulin type pharmacokinetic information
t_{ex}	minute	Exercise time	Reported by the individual
γ	%	Insulin Sensitivity Factor (ISF)	1700/total amount of insulin administered
$eGDR$	$\frac{mg}{kg.min}$	Estimated Glucose Disposal Rate	Individually calculated
τ_1	minute	Delay in hepatic glucose production	$\tau_1 > 0$, between 15 to 20
τ_2	minute	Insulin action depending on its type	$\tau_2 > 0$, between 5 and 180

Table 8: Parameters, variables and initial conditions.

The parameters adopted to run the numerical method for solving $G'(t)$ are presented in Table 8. Such values are related to an individual, with a weight equal to 70Kg, according to (STURIS et al., 1991), (TOLIĆ; MOSEKILDE; STURIS, 2000) and (LI; KUANG; MASON, 2006). Thus, the values would be changed individually, according to the weight of each individual. Parameter C_5 is a scale factor that cannot be dynamically collected or

inserted into the model by the individual. However, they serve as a basis for the mimic through ODE, the simplified glucose-insulin regulatory system. All other parameters used in expressions f_1, f_2, f_3 and f_4 are presented in Table 9.

Symbol	Unit	values	Meaning
K_m	$\mu\text{U}/\text{mL}$	2300	half-saturation concentration of insulin-degrading enzyme
V_{max}	$\mu\text{U}/\text{mL} \cdot \text{min}$	150	maximum rate of insulin release
HGP_{max}	mg/min	180	maximum rate of hepatic glucose production
C_2	mg/L	144	defines the sensitivity of CNS cells to changes in glucose
C_3	mg/L	1000	defines the sensitivity of muscle cells to changes in glucose
C_4	mU/L	80	defines the sensitivity of muscle cells to changes in insulin
C_5	mU/L	26	insulin concentration at which the liver is most efficient
U_b	mg/min	72	maximum rate of glucose utilization by brain and nerve cells
U_0	mg/min	40	lowest insulin threshold rate for muscle glucose consumption
U_m	mg/min	940	highest insulin threshold rate for muscle glucose consumption
V_{glu}	L	10	body volume into which glucose can diffuse
V_{pla}	L	3	body plasma volume
V_{int}	L	11	intercellular volume
T_{pla}	L/min	0.2	insulin transport rate from plasma to cells
T_{deg}	minutes	100	exponential time constant for intercellular insulin degradation
λ	%	1700/amount of insulin	Insulin Sensitivity factor

Table 9: Reference parameters of the Glucose-Insulin Regulatory System.

Tesseractus model calibrates intelligently the parameters and errors, through the continuous data collection of individuals with T1D, recursive calculations, ML and mathematical models. This is an essential task, in which the parameter values can be adjusted so that the model behavior has better accuracy. In subsection 7.2.2 we detail the replacement of the insulin compartment by approximating the pharmacokinetics of insulins through polynomial equations.

7.2.2 The exogenous insulin equation

Our approach adopts the pharmacokinetics data of four types of insulin (glargine (FDA-GLARGINE, 2022), degludec (FDA-DEGLUDEC, 2022), lispro (FDA-LISPRO, 2022) and aspart (FDA-ASPART, 2022)) to support this modeling based on the approximation of polynomial functions. The adjustment is made specifically for the insulin analogues used by the 15 *in vivo* individuals in this study: lispro and aspart (fast-acting), and the basal-effect analogues glargine and degludec (slow-acting).

Therefore, for glargine, an insulin of prolonged action, we got values from (OWENS et al., 2019), (PORCELLATI et al., 2007), (ABE et al., 2011), (BARNETT, 2006), and (LINNEBJERG et al., 2015), as well as the FDA report (FDA-GLARGINE, 2022) and the industry representative information (SANOFI, 2020). Nevertheless, only three references of insulin glargine concentrations were found: 0.4, 0.6 and 0.8 U/Kg. Since the range between 0.4 to 0.8 U/Kg does not cover all possibilities for different T1D individuals, in terms of insulin dosage and weight, we calculate approximate values for 0.2 U/Kg and 0.1 U/Kg, as a function of the concentration of 0.4 U/Kg, dividing by two and by four, respectively. In fact, intermediate values of insulin glargine concentration will need approximate initial values. For example, an individual with a weight of 82 Kg who injects 20U of insulin glargine has a ratio of 0.24 U/Kg, and the closest polynomial curve is 0.2 U/Kg. Thus, the calculation of the initial concentration value is carried out from the concentration of 0.2 U/Kg multiplied by 1.2. In Table 10 are the concentration values related to $t(x)$ in hours are: $t = 0.5$ hours, t in the interval $[1, 24]$ hours.

Having such values, we were able to build a polynomial function $p(t)$ that provide an approximation for the exogenous insulin compartment. Each point of $p(t)$ represents the concentration of insulin prescribed at a given time (t), considering the parameters of the T1D individual.

Thus, Figure 12 represents the polynomial curves of insulin glargine in the unit (pmol/L), according to Table 11. Each row of Table 11 represents the approximate polynomial function of the concentration curve and its respective squared error. The degree of the function of each curve, in relation to the 26 points determined of Figure 12, was chosen because it has the highest squared error value (R^2), associated with the guarantee of representation of the main concavity changes suggested by data.

Regarding fast-acting insulin, insulin aspart curve points referring to concentrations 0.1, 0.2 and 0.4 U/Kg were extracted from the literature: (SLATTERY; AMIEL; CHOUDHARY, 2018), (HEISE et al., 2015a), (PLANK et al., 2002), (HEISE et al., 2015b), (HEISE

Time (hours)	0.1U/Kg (approximation)	0.2U/Kg (approximation)	0.4U/Kg (from articles)	0.6U/Kg (from articles)	0.8U/Kg (from articles)
0	19	38	76	118.96	142.02
0.5	25.75	51.5	103	162.51	213.97
1	28.12	56.25	112.5	167.02	230.99
2	32.75	65.5	131	187.51	256.47
3	34.25	68.5	137	202.03	258
4	34	68	136	205.98	281.48
5	36	72	144	210.01	266.47
6	36	72	144	218	281.48
7	34.37	68.75	137.5	198	268
8	34.12	68.25	136.5	200.01	268.97
9	33.75	67.5	135	190.98	262.52
10	33.25	66.5	133	180.98	243.49
11	31.25	62.5	125	175.01	237.51
12	29.75	59.5	119	172.02	220.98
13	26.62	53.25	106.5	152.99	187.02
14	25	50	100	150.01	190.01
15	23.5	47	94	155.98	187.02
16	23	46	92	147.02	181.47
17	22	44	88	143.96	167.99
18	21.5	43	86	137.51	155.98
19	20.37	40.75	81.5	125.98	147.02
20	18.75	37.5	75	118.48	140.98
21	17.25	34.5	69	107.99	135.98
22	15.62	31.25	62.5	106.46	130.98
23	15	30	60	87.5	112.5
24	14	28	56	75	103.96

Table 10: Insulin glargine concentration approximation (pmol/L) - 24h.

U/Kg	Polynomial function	R^2
0.8 (red)	$y = -5E - 05x^6 + 0,0038x^5 - 0,1154x^4 + 1,8302x^3 - 16,527x^2 + 72,696x + 161,99$	97.32%
0.6 (black)	$y = 0,0002x^5 - 0,0179x^4 + 0,5573x^3 - 7,8789x^2 + 44,188x + 128,8$	98.27%
0.4 (light blue)	$y = -2E - 05x^6 + 0,0015x^5 - 0,0463x^4 + 0,7651x^3 - 7,3401x^2 + 34,879x + 81,985$	98.56%
0.2 (green)	$y = -1E - 05x^6 + 0,0007x^5 - 0,0232x^4 + 0,3825x^3 - 3,67x^2 + 17,439x + 40,992$	98.56%
0.1 (purple)	$y = -5E - 06x^6 + 0,0004x^5 - 0,0116x^4 + 0,1913x^3 - 1,835x^2 + 8,7197x + 20,496$	98.56%

Table 11: Insulin glargine: polynomial functions and R^2 .

et al., 2017),(HEISE et al., 2015b),(LINDHOLM; JACOBSEN, 2001),(KAKU et al., 2000),(ØSTERBERG et al., 2003). In addition, the summary of the insulin analogue

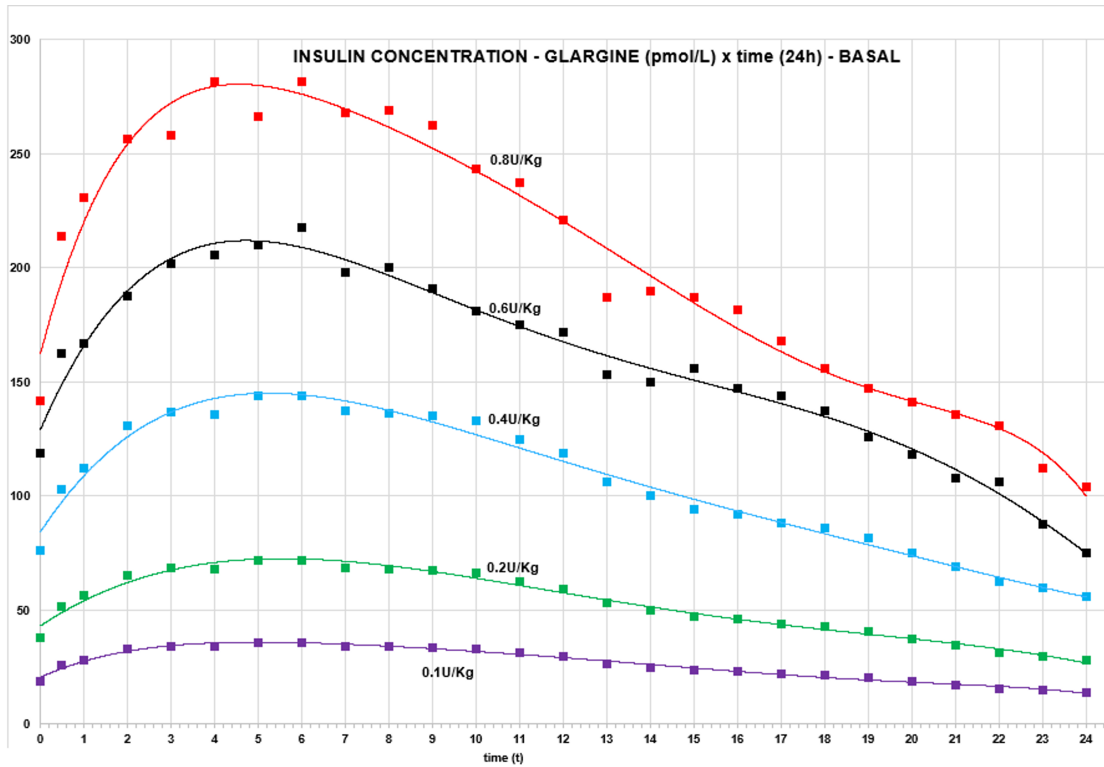


Figure 12: Approximate curves of insulin glargine concentrations (24h).

aspart produced by the FDA (FDA, 2020) was used to confirm the time-of-action and pharmacokinetic information. In the same way, we found in literature only three insulin aspart concentrations 0.1, 0.2 and 0.4 U/Kg. As the values for the concentration of the insulin aspart analogue lower than 0.1 U/Kg were not found in the literature, the values referring to 0.01 U/Kg and 0.05 U/Kg were approximated as a function of the concentration of 0.1 U/Kg, dividing exactly by 10 and by 2, respectively. The concentration values related to t in minutes are: t in the interval $[0, 60]$ at five minute intervals, $t = 90, 105, 120, 150, 180, 240, 300, 360$ minutes are in Table 12. For example, an individual with a weight of 73Kg who injects 6U of insulin aspart has a ratio of 0.08 U/Kg, and the closest polynomial curve is 0.1 U/Kg. Thus, the calculation of the initial concentration value will be performed from the concentration of 0.1 U/Kg multiplied by 0.8.

Thus, Figure 13 represents the polynomial curves of insulin aspart in the unit (pmol/L), according to Table 13. Each row of Table 13 represents the approximate polynomial function of the concentration curve and its respective squared error.

Time (minutes)	0.01U/Kg (approximation)	0.05U/Kg (approximation)	0.1U/Kg (from articles)	0.2U/Kg (from articles)	0.4U/Kg (from articles)
0	0.25	0.25	0.25	0.25	0.25
5	0.63	3.13	6.25	10.15	18.75
15	5	25	50	68.75	111
20	7.81	39.06	78.12	106.25	200
25	9.06	45.31	90.62	146.87	262.5
30	11.25	56.25	112.5	196.88	375
35	13.13	65.63	131.25	242.5	468.75
45	14.38	71.88	143.75	275	568.75
50	14.69	73.44	146.87	281.25	615.62
55	14.38	71.88	143.75	281.25	659.37
60	14.38	71.88	143.75	287.5	631.25
75	13.13	65.63	131.25	287.12	653
90	11.94	59.69	119.37	262.5	609.37
105	10	50	100	232.5	568.12
120	9.06	45.31	90.62	196	496
150	6.56	32.81	65.62	112.43	400
180	4.44	22.19	44.37	112.43	300
210	2.81	14.06	28.12	78.12	223.75
240	2.19	10.94	21.87	56.25	150
270	1.56	7.81	15.62	46.87	113.13
300	0.63	3.13	6.25	31	85.62

Table 12: Aspart insulin concentration approximation (pmol/L) - 5h.

U/Kg	Polynomial function	R^2
0.4 (rede)	$y = 1E - 10x^6 - 1E - 07x^5 + 4E - 05x^4 - 0,0054x^3 + 0,1974x^2 + 11,991x - 53,175$	98.15%
0.2 (black)	$y = 5E - 11x^6 - 5E - 08x^5 + 1E - 05x^4 - 0,0018x^3 + 0,0251x^2 + 7,5934x - 27,416$	98.21%
0.1 (light blue)	$y = 1E - 11x^6 - 7E - 09x^5 + 1E - 06x^4 + 0,0001x^3 - 0,0706x^2 + 6,2668x - 19,82$	98.19%
0.05 (green)	$y = 5E - 12x^6 - 4E - 09x^5 + 7E - 07x^4 + 7E - 05x^3 - 0,0353x^2 + 3,1334x - 9,9101$	98.19%
0.01 (purple)	$y = 1E - 12x^6 - 7E - 10x^5 + 1E - 07x^4 + 1E - 05x^3 - 0,0071x^2 + 0,6267x - 1,982$	98.19%

Table 13: Aspart insulin: polynomial functions and R^2 .

7.3 The first learning phase

Supervised learning is used in the first phase of learning, in which the agent observes examples of input and output from the environment, that is, data provided by the individual, and learns a function that maps from input to output. In this case, the dataset is

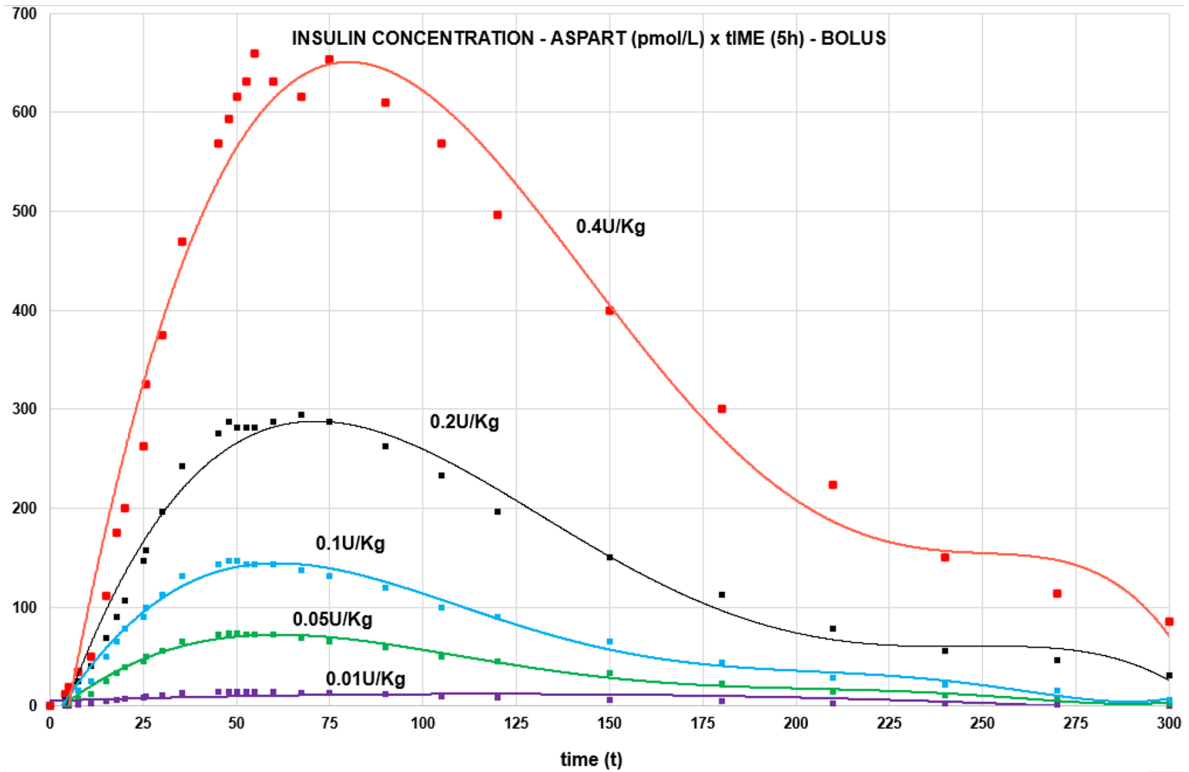


Figure 13: Approximate curves of insulin aspart concentrations (5h).

being created with labels, based on the mathematical agent. The mathematical agent uses ODE and approximation functions, and from the generated curves it can define the labels and consequently a taxonomy of proximity to the ideal glyceimic range (SBD, 2022a). It also compares with the historical data of each individual with T1D. This first learning phase can last from seven to 14 days, depending on the amount of data provided by the individual.

One of the exploited features of the supervised learning algorithm is the resolution of a multi-class classification problem. At least ten different classes are defined for the Tesseractus model, according to the proximity of the ideal glyceimic level (80–120 mg/dL), in the fasting period, represented by our rewarding policy based on traffic lights. For the postprandial period, that is, two hours after the ingestion of macronutrients, the glyceimic level can be considered up to 160 mg/dL, according to the traffic light shown in Table 9. Figure 14 presents the steps for conducting this first learning phase, detailed in the following.

1. Environmental data is collected via sensors (each five minutes from CGMs), or by voice or manually, and received by reactive agents. The payload of messages are composed by $\langle X \text{ mg/dL (glucose level), units of bolus insulin and basal (U), amount of carbohydrates, protein and fat (g) and duration of physical exercises (minutes)} \rangle$;

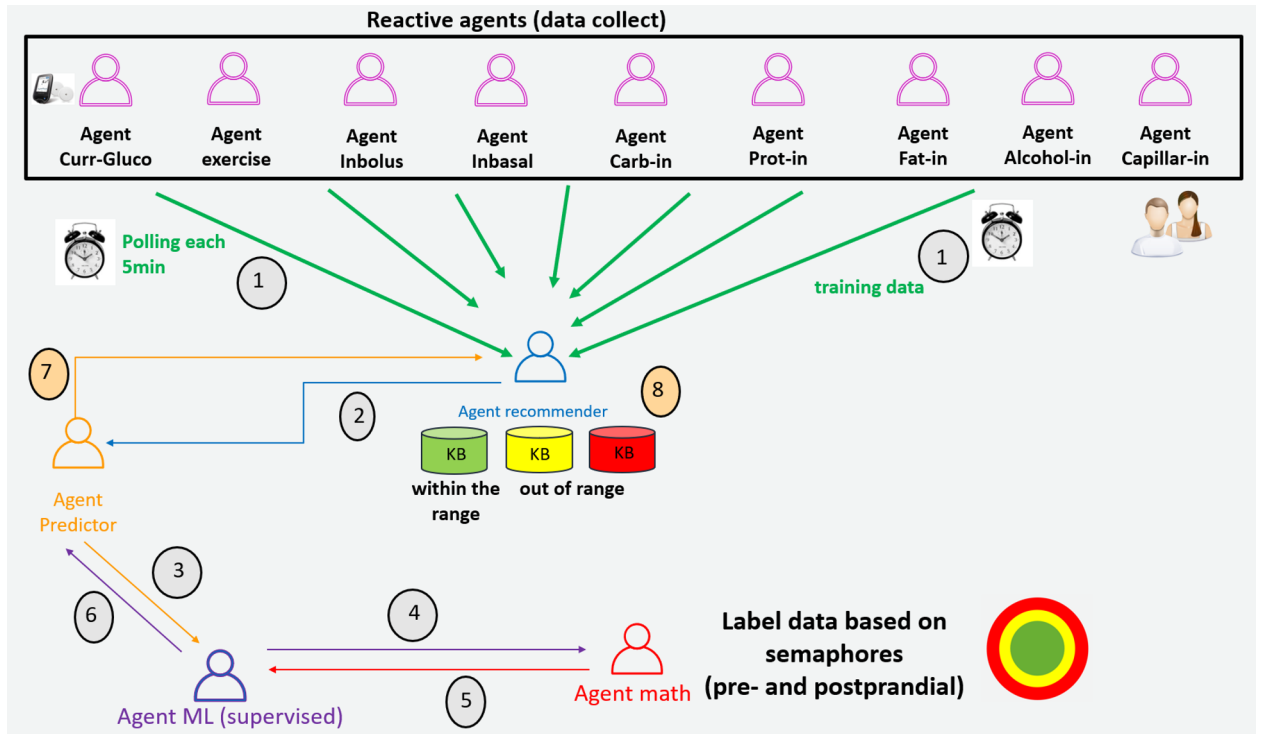


Figure 14: Phase one of learning (supervised process to learn).

2. **Recommender** agent receives the data, and sends message to the **Predictor** agent to calculate and generate the glycemc curve;
3. **Predictor** agent sends the message to the **ML** agent with time frame in order to create a tuple $\langle data, time \rangle$ and generate the glycemc curve;
4. **ML** agent asks the **math** agent for a labeling of the generated value, based on the predefined semaphores (fasting and postprandial periods);
5. **Math** agent sends the message, with the labeling payload, to the **ML** agent;
6. **ML** agent sends the message stored in **KB** to the predictor agent with $\langle time, label, curve \rangle$, based on the data received;
7. **Predictor** agent receives the message and forwards it to the **Recommender** agent;
8. **Recommender** agent receives the new information and classifies it in each knowledge base (**KB**), according to the received label, and this learning takes place for at least seven days, in order to create a personalized base for that individual.

7.4 The second learning phase

In the phase two, the Active Reinforcement Learning method (EPSHTEYN; VOGEL; DEJONG, 2008) is incorporated (EPSHTEYN; VOGEL; DEJONG, 2008) and Figure 15 presents a flow of active reinforcement learning, already considering the complete architecture of Tesseractus, where numbers are adopted to support its explanation flow. Note that there are three more groups of agents, known by the satellite characteristic, as they adjacently monitor the parameters involved and errors, which are: (a) the **anomaly detector** agent; (b) the **monitor error** agent; and (c) the **ODE parameters** agent.

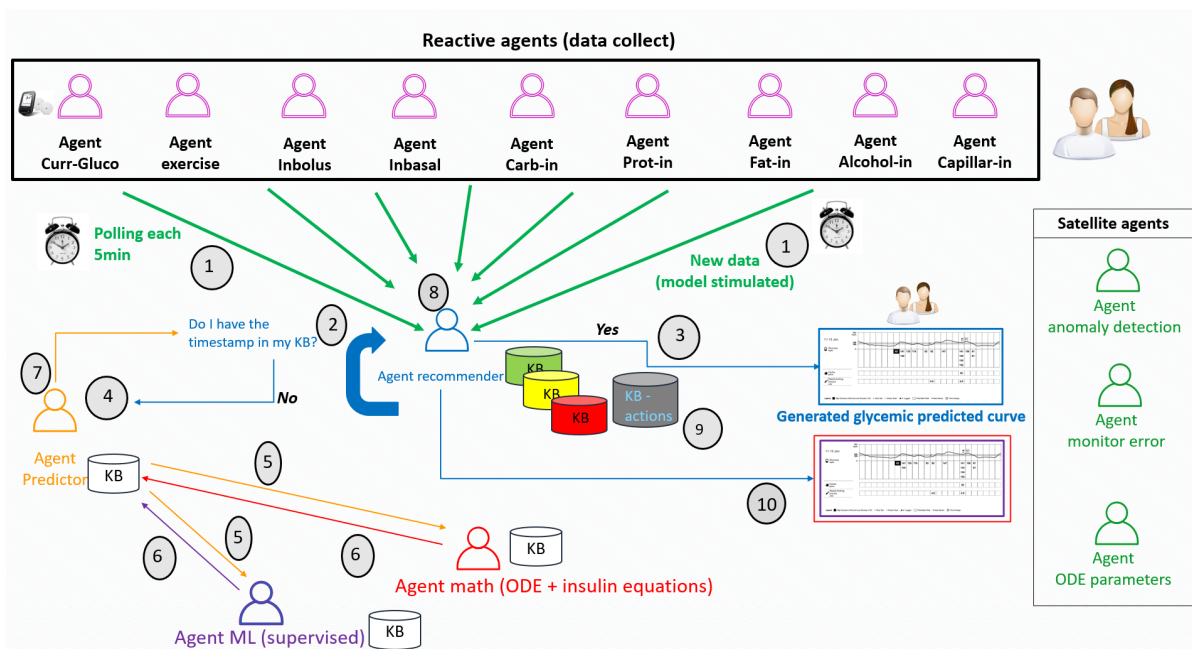


Figure 15: Phase two of learning (by reinforcement).

1. Reactive agents collect data from continuous glucose monitors (CGM), voice or manually and send them to the **Recommender** agent. The payload of messages are composed by $\langle X \text{ mg/dL (glucose level), units of bolus insulin and basal (U), amount of carbohydrates, protein and fat (g) and duration of physical exercises (minutes)} \rangle$;
2. **Recommender** agent receives data, associate it with its time frame creating a tuple $\langle data, time \rangle$ and checks its knowledge base (KB) if there are actions to be taken related to them;
3. If yes, the values of glycemic predicted curve are labeled in the ideal range, stored in the KB as $\langle time, label, curve \rangle$, and it is sent to the user;
4. If not, the **Recommender** agent requests information about prediction curves to the **Predictor** agent;

5. **Predictor agent** checks its KB to see if there is a suitable prediction curve. If don't, it propagates the request to the **ML** and **Math** agents;
6. **ML agent** and **Math agent**, at a given time frame, store the prediction values in their KB and return the value linked with prediction calculation to the **Predictor agent**;
7. **Predictor agent** analyzes the value received and, if it is a value that is in the ideal range, the **Predictor agent** sends a return message to the **Recommender agent**, otherwise it requests more options for the **ML** and **Math** agents. At this point, the **Predictor agent** stores the input and output in its KB with a specific timestamp;
8. **Recommender agent** could send recommendations to the environment, from its base of actions , or simply send the predicted oscillation curve with an ideal glucose label achieved;
9. The actions and knowledge at that specific time frame are stored in the **Recommender agent's** KB;
10. The best glucose value is sent to user, as well as their intermediate values, in the form of an oscillatory curve, as well as hypothetical complementary recommendations.

7.5 Discussion

Since Tesseractus is a model to support the simulation of personal GIRS, its instantiation is complex and requires a two-phase process to be complete.

The first phase is the supervised feature and in the second phase the focus is on reinforcement learning, that is particularly suited to problems that include a long-term versus short-term reward compensation. Initially, the algorithm Q-learning (JAVAD et al., 2019) is used to maximize the cumulative reward, minimize the learning time, through the responsibility assigned to the agent. The "Q" is related to the quality of an action in a certain state. These rewards can come frequently, whenever the environment stimulates the receptor agents, for example, with the current glucose values.

The **Math agent** is a generator of knowledge, based on the ODE and approximation functions by polynomial equations. It is well known that each individual with T1D tends to have its own physiological characteristic. For example, having different degrees of insulin sensitivity at each time point in a single day. Therefore, the use of personal data measured periodically in combination with results from mathematical models, associated

with supervised and active reinforcement learning among agents, can improve the accuracy of prediction and the provision of personalized recommendations to individuals with T1D.

Thus, the Tesseractus model suggests the amount of macronutrients to be ingested, and the delay and/or adjustment of the next infusion of rapid-acting insulin. Agents identify specific patterns of each individual with T1D, related to the time intervals of each day, for example, pre- and postprandial, after exercise, at night and dawn, and if necessary recommend correcting them, supported by MAS utilization. Furthermore, active reinforcement learning (KHOLGHI et al., 2015) is used to facilitate the learning process and knowledge transfer between agents.

Learning also consists of associating inputs with outputs (actions) of each individual. The initial dataset of the Tesseractus model consists of seven individuals with T1D volunteers, and each one can serve as a learning reference for itself and also for other individuals, with the same behavior of glycemic oscillation, or even correlation with age or gender. In addition, a dataset from the University of Ohio (OHIO-UNIV-T1D, 2020), with data from eight individuals, and from nine virtual ones generated are used to validate the active learning model embedded in the Tesseractus model. Details about how it was built is given in Chapter 8. Flow diagrams describing the functioning of each agent are provided in appendix D.

Finally, in the context of healthcare, Tesseractus model has the necessary strength to be applied to support decision making in a closed-loop system, like an artificial pancreas (FDA, 2019), or for physicians on duty in an Intensive Care Unit. It combined with an exercise monitor, e.g. bioimpedance sensor, can receive new data such as heart rate, oxygenation level, enriching it and correlating it with the measured and predicted glycemic value. Another applicability is in biotelemetry (RODRÍGUEZ, 2020), as an important tool to guide measurement parameters remotely, and also as support for pre-consultations, in addition to increasing the individual's own sense of security with T1D.

8 TESSERATUS IMPLEMENTATION

After describing the instantiation of Tesseractus, we present along this Chapter Tesseractus implementation flow.

8.1 Dataset

The items below were defined as the minimum dataset in order to determine the prediction of glycemic oscillation in individuals with T1D, as they are factors that directly interfere in the direction of the oscillatory curve:

- time frame of all stimuli;
- current glucose value (interstitial fluid);
- amount of carbohydrate, protein and lipids consumed;
- amount of alcohol ingested;
- type and intensity of physical exercises;
- type and amount of fast-acting insulin dose (bolus);
- type and amount of slow-acting dose (basal) insulin.

Other items such as heartbeat, stress level, menstrual cycle phase, infection could be added, but they are not part of the evaluation context of this work. And, no actual individuals reported alcohol consumption during the research.

Thus, the dataset formed by 15 *in vivo* individuals and nine *in silico* individuals with T1D, collected for up to 21 days, brings inherent characteristics such as precision, validity, cohesion and no manipulations, these being the standards for a Data Quality (LAYMAN, 2009) in healthcare. Through this unique and reliable dataset, it was possible to create

ML models with acceptable accuracy to predict the glycemic oscillation, in up to eight hours, detailed in the chapter 9.

The seven *in vivo* volunteers from Brazil and eight *in vivo* from the University of Ohio (USA), used in this work, are detailed in Tables 14 and 15 (OHIO-UNIV-T1D, 2020), respectively. AC refers to abdominal circumference, and the column Days refers to the number of days used for data collection.

ID	Gender	Days	Age	Body mass (Kg)	AC (cm)	Data source	Insulin type
R-BRA01	M	14	36	57	79	Flash sensor	degludec and aspart
R-BRA02	H	21	50	90	115	Insulin pump	lispro
R-BRA03	H	14	28	70	91	Flash sensor	degludec and aspart
R-BRA04	H	21	45	120	132	Insulin pump	lispro
R-BRA05	H	14	38	82	93	Flash sensor	glargine and aspart
R-BRA06	H	21	39	78.4	91	Insulin pump	lispro
R-BRA07	M	14	65	68	90	Flash sensor	degludec and lispro

Table 14: Characteristics of *in vivo* volunteers of Brazil.

With Brazilian individuals, it was possible to capture more information such as the presence of hypertension (0 or 1), calculation of eGDR, and glycated hemoglobin (HbA1c) value, as shown in Table 16. These additional data were used in the glucose compartment (ODE) for insulin sensitivity factor.

In addition to the dataset of *in vivo* individuals, data from nine *in silico* individuals with T1D were incorporated, according to Table 17, generated by a FDA-approved simulator (FDA, 2021) and (VISENTIN et al., 2018).

With the database assembled in the data mesh (AZURE-MESH, 2022) pattern, with a set of semi-structured data (.csv files) of the 24 individuals with T1D, 50% of the database was used for training in both ML models: supervised and reinforcement learning, all individuals and only the R-BRA05 individual, respectively. Mathematical modeling used the data directly, substituting the glycemic compartment parameters and polynomial

ID	Gender	Days	Age	Body mass (Kg)	AC (cm)	Data source	Insulin type
544	M	21	40-60	–	–	Insulin pump	lispro
552	M	21	20-40	–	–	Insulin pump	lispro
563	M	21	40-60	–	–	Insulin pump	lispro
570	M	21	40-60	–	–	Insulin pump	lispro
584	M	21	40-60	–	–	Insulin pump	lispro
588	F	21	40-60	–	–	Insulin pump	lispro
591	F	21	40-60	–	–	Insulin pump	lispro
596	M	21	60-80	–	–	Insulin pump	lispro

Table 15: Characteristics of *in vivo* volunteers from Ohio.

ID	Hypertensive	HbA1c	eGDR
R-BRA01	0	5	11.7
R-BRA02	1	6	4.51
R-BRA03	0	6.3	9.91
R-BRA04	1	5.6	3.2
R-BRA05	0	8	8.8
R-BRA06	0	6	10
R-BRA07	0	7.5	9.34

Table 16: Information to calculate eGDR for Brazilian volunteers.

approximation functions for the insulin component.

8.2 Algorithms and numerical libraries

In this work, the function DDE23 (DDE23, 2019) developed in Python 3.8 is used to solve the ODE. The ODE of the glucose compartment is developed according to section 3.2, and the dynamic value of the insulin concentration is entered according to the pharmacokinetics of each type of insulin, according to subsection 3.2.2.

As with all agents, `Math` agent has its KB as a NoSQL (Not Only SQL) database (MON-GODB, 2022), and uses “documents” similar to the JSON (Java Script Object Notation)

ID	Gender	Days	Age	Body mass (Kg)	AC (cm)	Data source	Insulin type
001	–	21	adult	52.6	–	Generic insulin pump	fast-acting
002	–	21	adult	75.2	–	Generic insulin pump	fast-acting
003	–	21	adult	108.4	–	Generic insulin pump	fast-acting
001	–	21	adolescent	30.4	–	Generic insulin pump	fast-acting
002	–	21	adolescent	50.8	–	Generic insulin pump	fast-acting
003	–	21	adolescent	80.3	–	Generic insulin pump	fast-acting
001	–	21	child	18.3	–	Generic insulin pump	fast-acting
002	–	21	child	30.7	–	Generic insulin pump	fast-acting
003	–	21	child	49.8	–	Generic insulin pump	fast-acting

Table 17: Characteristics of *in silico* individuals.

format to store data. The document is similar to a record, with fields and values. The database in this case was a service from a specific cloud provider. The ML models: supervised, and by reinforcement were developed in Python, using libraries (XGBOOST, 2019) and (Q-LEARNING, 2019), respectively. The design of the implementation architecture follows Figure 17.

Based on the stored dataset, after the data collection phase, the ML agent remembers the timestamps and the value of each observation, achieving a better performance in the glycemic prediction. The dataset in question, of 24 individuals with T1D, presents correlation with the previous data (backtesting), where the temporal dimension of the observations means that we cannot divide them randomly into groups. Instead, it should split the data and respect the temporal order in which the values were observed (CARTA et al., 2021), for example glycemic value and insulin dose.

In the first training phase, with data received for at least seven days, the dataset had no label, and therefore the mathematical agent was used, with code in Python developed, to add a label to the data handled by the ML agent. Algorithm 1 presents the pseudocode for the setup phase one of learning.

Algorithm 1 Supervised learning and transfer knowledge - phase 1

New data from the environment. Tesseractus model stores the label of data received along with the timestamp. Testing dataset (24 individuals with T1D).

if Receive new data **then** Check the label in the recommender's KB

if it is in the KB **then** Confirm the timestamp and increment the counter it is no in the KB Ask to predictor agent

if Predictor agent has the label in its KB **then** Send the label to Recommender agent
 Predictor agent has not the label in its KB Ask to Math agent via ML agent a label
 Math agent calculate the glycemic value based on semaphores created

for Different intervals **do**

for Values values set in traffic lights **do** Classify as green, yellow or red

while Wait **do** Check if receive new data

In the second phase of learning, Tesseractus model used the walk-forward optimization (WFO) technique (CARTA et al., 2021) and (ALFIAN et al., 2020). Thus, the model may be updated each time step new data is received from reactive agents, and this step is essential for automating the model, and would give the model the best opportunity to make good prediction at each time step. The WFO process works in loop as follows:

1. For instance, since the glucose concentration dataset is measured each five minutes, the ML agent used the last two hours of historical data about carbohydrate and five hours about bolus insulin to predict it (see green and black dashed left-right arrows of Figure 16). These time slots were chosen based on the duration of carbohydrate metabolism and the average time of fast-acting insulin action in the human body, respectively. However, this sliding window could be adapted if protein or fat consumption is associated with carbohydrates. In Figure 16 insulin values (in muU/mL), of five hours sliding window, are represented by the black dashed left-right arrow, while carbohydrate values (in grams), of two hours sliding window, are represented by the green dashed left-right arrow. They were used to predict the oscillation glucose up to eight hours (blue dashed right arrow);
2. The model was trained and fitted with the data set available in the selected windows;
3. With the model formed and the parameters established for the selected time period, it is possible to generate the model outputs for all available data during the next time step;

4. In this step, the prediction can be stored as part of a result set;
5. The sliding window can be moved forward so that all data through this window can be used for tuning and data for the next time step can be used for testing;
6. With the environment stimulated again, coming from the reactive agents, it is possible restart from step (2), adding the new predictions to the result set.

Algorithm two is the pseudocode of Tesseractus model for the reinforcement learning process (phase 2), and in the subsection 8.3 is detailed the implementation of the MAS and its rules.

Algorithm 2 Reinforcement learning - phase 2

New data from the environment after training phase. Tesseractus model sends recommendations and predict glycemic oscillation, in addition to awarding the model. New data received (individuals with T1D).

if Receive new data **then** Check the label/data in the recommender's KB

if it is in the KB **then** Confirm the timestamp, increment the counter, check the PH and the possible actions (recommendations)

for Maintain value of glycemic oscillation based on semaphores (green area) **do**

Recommend time for all recommendations, amount of macronutrients, dose of fast-acting insulin, in addition to the duration and intensity of physical exercises it is no in the KB Request help for the predictor agent

if Predictor agent has the label/data in its KB **then** Send the label/predicted glycemic curve to recommender agent Predictor agent has not the label in its KB

Ask to mathematical and ML agents a predicted glycemic curve

Mathematical and ML agents calculate the glycemic values

Mathematical and ML agents send the glycemic values, and predictor agent select the best value closest to the average value between the highest and lowest value of the range, within the green area of the traffic lights

while Wait **do** Check if receive new data and give the specific reward

for Reward verification and score creation for agents and Tesseractus model **do**

Check the reward from the Tables ?? and 7 Check the actions (possible corrections) from satellite agents (anomaly detection, monitor error and ODE parameters agents)

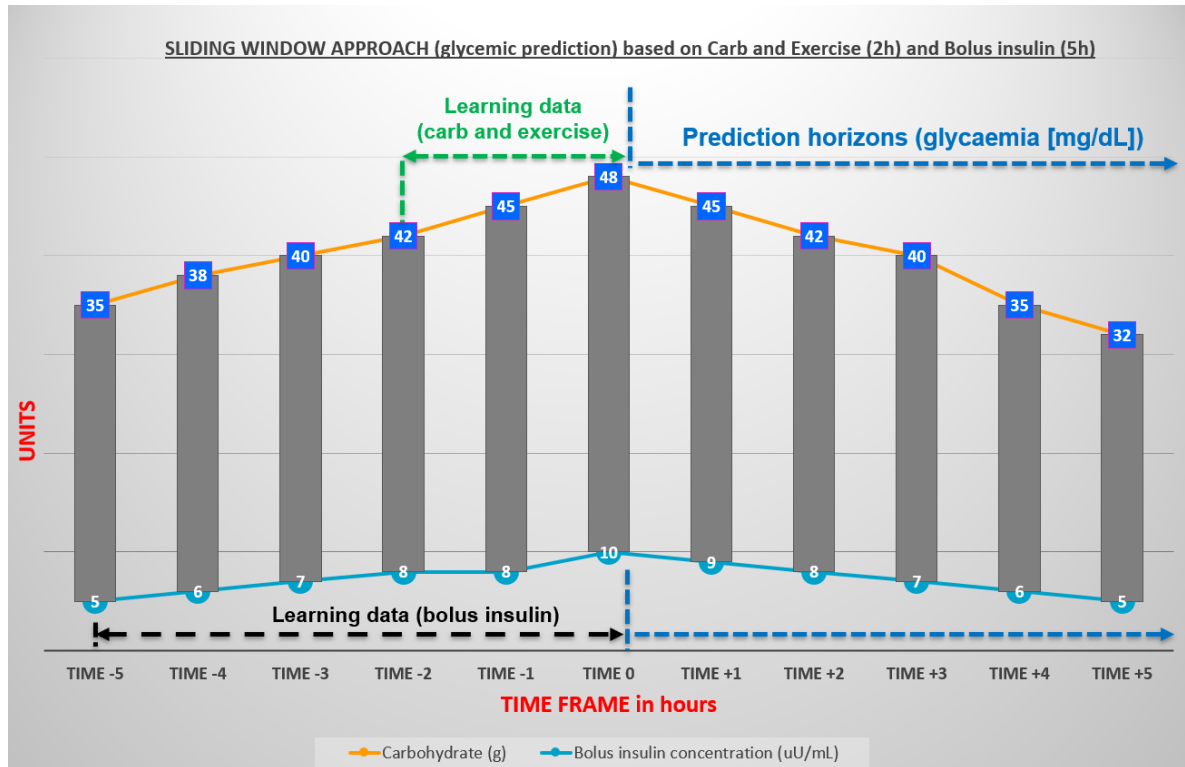


Figure 16: Sliding window approach for timeseries data: carb., exercise and insulin.

8.3 Multiagent platform and agents implementation

Some project decisions we made to implement Tesseract MAS were: adopts SPADE (Smart Python Agent Development Environment) (SPADE, 2019) to implement the agents with the use of an event driven approach, and the public cloud platform as the deployment environment (AZURE, 2022). Each agent profile and knowledge base (KB) are developed as a microservice. KB of each smart agent uses a non-relational key-value database, with flexibility for unstructured data and also for being horizontally scalable.

With the platform defined and developed, some initial rules were added to the agents, mainly to the **Recommender** agent. However, the rules are dynamically modified throughout the continuous process of learning and feedback from the environment (individual with T1D). For the **Recommender** agent, there are recommendations stored in the KB through actions and suggestive messages for the individual, always with the objective of maintaining the glycemic oscillation inside the green area of the traffic lights.

The **Recommender** agent receives the best glycemic curve values, and can request new results if a recommendation is not attractive to the individual, such as, for example, practicing 4 hours of exercise on Monday at 8:00 am. Always, the agent is based on the age of each individual and whether they are in the fasting, during the meal or postprandial

period. Furthermore, there are already *proactive messages from the Recommender* agent for the individual:

1. When taking any type of insulin, wait 10 seconds before removing the syringe from your body if you are not using an insulin pump;
2. Do not apply insulin to the same place on the body on the same day;
3. The effect of the previously applied fast- and slow-acting insulin is still active, 5h and 24h, respectively. It is recommended to wait for the full effect;
4. After eating carbohydrates, assess your capillary glycemic level after 2 hours;
5. Book at least 1 hour of physical exercise if you haven't practiced for more than 2 days (SBD, 2022a);
6. Correct your blood glucose level that is above 180 mg/dL with fast-acting insulin, and can be adjusted over time.

In the following there are the initial actions of the *Recommender* agent *for the practice of physical exercises*:

- Check glycemic level: capillary or interstitial fluid;
- Check how much time you have available to exercise;
- If glycemic level is below 90 mg/dL, consume 15–30g of carbohydrates before, if exercise duration is longer than 30min (SBD, 2022a);
- If the glycemic level is between 90 and 150 mg/dL, consume carbohydrates from physical exercise, as a rule 0.5 g/Kg/hour (SBD, 2022a);
- If the glycemic level is between 151 and 250 mg/dL, delay the consumption of carbohydrates, until it returns to the level of 150 mg/dL (SBD, 2022a);
- If the glycemic level is above 250 mg/dL, do not exercise until the insulin correction is performed, starting with 50:1 or according to the individual's input (initial action on KB) (SBD, 2022a).

Next, there are the initial actions at the *time of ingestion of macronutrients (carbohydrates, proteins and lipids)*:

- Check glycemic level: capillary or interstitial fluid;
- Check your insulin sensitivity using the rule 1700/total amount of insulin administered, which can be a fixed value over time, for periods and store the result;
- Check the amount and type of carbohydrate to be consumed, in addition to the association with protein or lipid;
- KB has the following rules regarding the amount of insulin to be applied - rate [insulin (U):carbohydrates (g)]:
 - 1:10 in the morning (06:00-12:00);
 - 1:12 on the afternoon (12:00-19:00);
 - 1:15 on the night/early period (19- 06h).
- If it is above 160 mg/dL, delay the intake of carbohydrates, correct it with fast-acting insulin, and wait 30 minutes until the next measurement;
- Bolus insulin dose adjustment of the bolus insulin dose to 75g of isolated protein, or 30g associated with carbohydrates which can result in an increase of 47 mg/dL (PANKOWSKA; BLAZIK; GROELE, 2011), (PETERS; DAVIDSON, 1993), (BELL et al., 2015) and (SMART et al., 2013);
- Bolus insulin dose adjustment for foods with a concentration greater than 35g of fat, with a possible delay of 180 minutes in the elevation of the glycemic curve (PANKOWSKA; BLAZIK; GROELE, 2011), (PETERS; DAVIDSON, 1993), (BELL et al., 2015) and (SMART et al., 2013). This elevation curve needs to be learned on a case-by-case basis.

And finally, the initial actions related to *injecting fast-acting insulin for glycemic level correction*, in the KB of the **Recommender** agent:

- Check glycemic level: capillary or interstitial fluid;
- KB has the following rules regarding the amount of insulin to be applied:
 - For 50 mg/dL, the individual injects 1U of insulin, but initially each individual uses their own, for example, the R-BRA07 uses a 30:1 correction rate.

Nevertheless, for the **Predictor** agent, the learning and decision rules are more simplified compared to the **Recommender** agent, as it passes on the new data entered in the

model, forwarded via the `Recommender` agent and sends it to the `ML` and `Math` agents. After receiving the results from both agents, it decides on the best curves to send to the `Recommender` agent, which is the closest to the glycemic level of 100 mg/dL, according to the requested prediction period. If the glycemic values fall outside the ideal range, it requests the *recalculation again with different values (macronutrients, insulin, exercise) in the range of $\pm 20\%$* .

In the same way, the `Math` and `ML` agents receive the information and calculate according to the chosen prediction horizon period. They store the predicted values and send them to the `Predictor` agent in order to resolve the dispute or forward the message. Tables containing the description of all agents' actions are presented in appendix E.

8.4 Cloud reference architecture

The architecture shown in Figure 17 has the basic components on cloud such as API Management (gateway), database (KB), serverless services for the computational part (agents), as well as viewers (dashboards) and notebooks to configure ML and mathematical models. All data collection in this case is carried out via the application, in several ways such as manual, by voice or with the use of sensors.

All access to the backend, coming from the application, is performed via APIs (Application Programming Interface), and the gateway is an API Management.

The event-driven architecture of the proposed model uses events to trigger and communicate between different microservices. An event is a state change or an update. Events can contain state or events can be identifiers. The advantage for the Tesseractus model of using an event-based architecture is the possible decoupling between the microservices, because if necessary, the agent of each microservice is only aware of the event router, not each other. This means your services are interoperable, but if one microservice fails, the rest will continue to work, maintaining the resilience of the proposed architecture.

All the input data of the Tesseractus model is collected locally, through an application that connects with the different devices or manually, in which the individual has the responsibility to enter the values in the application. To facilitate remote viewing and capture telemetry, the open source software NightScout (NIGHTSCOUT, 2020) is used, which allows connecting and transmitting glucose readings from some of the sensors used by participants, for example, (FreeStyle Libre[®] (FREESTYLE, 2020) and Minimed 640[®] (MINIMED-640G, 2020)).

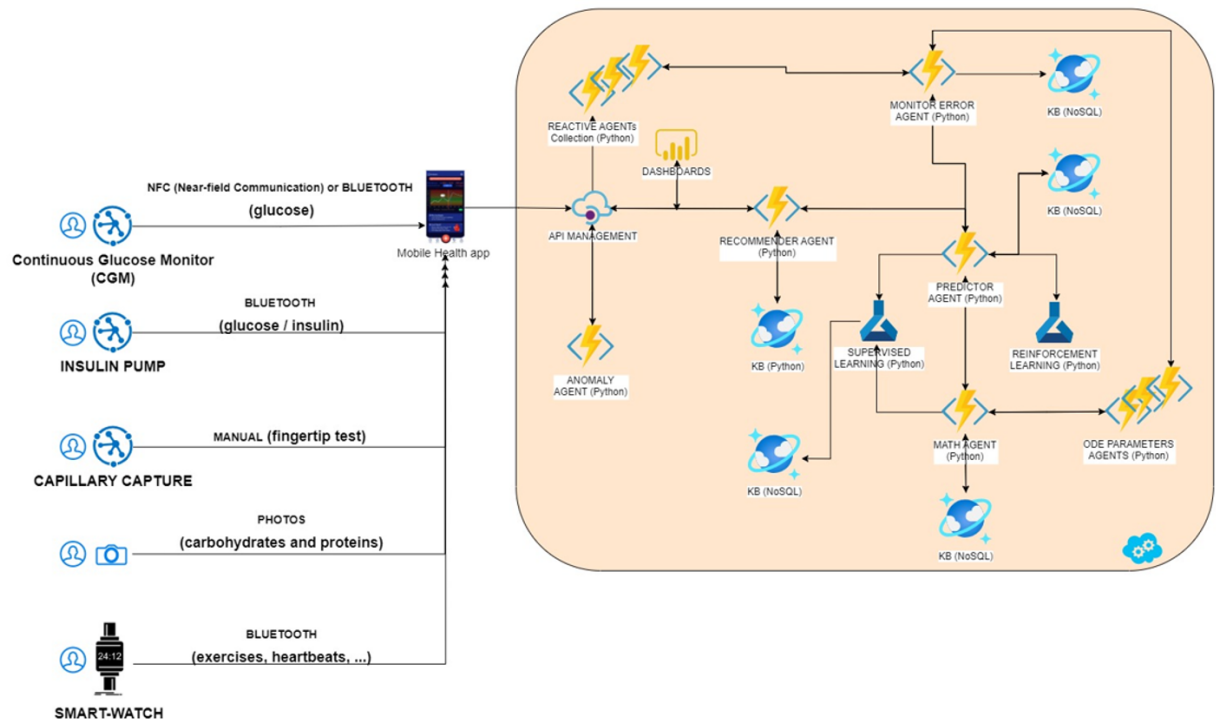


Figure 17: Tesseract model implementation architecture in the cloud.

8.5 Testing

As mentioned in subsection 8.1, all tests were performed with 50% of data from 24 individuals with T1D, 15 *in vivo* and nine *in silico*. With the data set defined, a model was created for each individual, and prediction tests were performed in the following time horizons:

- Morning and afternoon:
 - 15, 30, 60, 90, 120, 180 and 240 minutes
- Night period:
 - 15, 30, 60, 90, 120, 180, 240, 300, 360, 420 and 480 minutes

From the results obtained with the mathematical and ML models, some techniques were used to analyze the accuracy of the models and focused on the evaluation of absolute errors:

- Minor MAE (mean absolute error);
- Minor MAPE (mean absolute percentage error);

- Longer time in the ideal glycemic range defined (green area of traffic lights) - TIR (Time in Range). The TIR was collected only from one individual: R-BRA05 after authorization;
- Parkes Error Grid (PEG) (zones A + B) (PFÜTZNER et al., 2013) greater than or equal to 90%, in order to determine the deviation between predicted and measured values.

We use PEG (PARKES et al., 2000) to evaluate errors in the measurement of predicted glucose oscillation provided by Tesseractus. It was adopted because it is compliant with ISO15197 (KATZ, 2020) and it separates T1D individuals from individuals with type 2 diabetes mellitus. Moreover, PEG had its technical issues revised by Pftzner and colleagues (2013), who established exact borders for the performance zones for glucose measurements and support the accuracy definition for glucose monitors. The zones are categorized as **A**, **B**, **C**, **D** and **E**. The associate meaning for a measurement of being in a zone is:

A – clinically accurate measurements, no effect on clinical action;

B – altered clinical action, little or no effect on clinical outcome;

C – altered clinical action, likely to affect clinical outcome;

D – altered clinical action, could have significant clinical risk;

E – altered clinical action, could have dangerous consequences.

PEG was used considering the predicted **versus** measured values, and the success metric is simple: the most prediction points are within zones A and B, the better is the model.

After the model was trained and tested with historical data, only the individual R-BRA05 was used for recommendation tests, after updating the approval of the Ethics Council. All the results of tests performed are in chapter 9.

PART III

RESULTS AND CONCLUSION

9 RESULTS

At the beginning of this work, some metrics to evaluate performance were established: **(1)** the prediction horizon is up to **four hours** for daytime periods and up to **eight hours** for night periods, depending on the sleep period of each individual or feeding frequency; **(2)** the MAE value must be less than or equal to 30 mg/dL, to check the quality (GINSBERG, 2009) of each predicted blood glucose value for each individual, in relation to the prediction horizon; **(3)** from the measurements, **90%** or more must be inside the **zones A and B of the Parkes Error Grid (PEG)** (PARKES et al., 2000), determining to be a clinically accurate predictor (PFÜTZNER et al., 2013), regardless of the prediction horizon (PH); **(4)** the prediction, as well as the correction suggestions, and the recommendations must be carried out in less than **1 minute**; **(5)** performance is analyzed through the recommendations provided by the proposed model, to achieve the main goal of maintaining glycemic value within the optimal range, that is, maintaining the homeostasis of the environment.

To achieve the best results, it was established a natural competition between **Math** and **ML** agents, with their respective strategies, ODEs plus piecewise polynomial equations for approximation and, supervised learning algorithm plus sliding windows approach, respectively. Furthermore, it was possible practice a continuous flow of active Reinforcement Learning, using historical data up to 21 days. The best result is always closer to the ideal glycemic range, always considering other factors such as injecting insulin, eating carbohydrates or practicing medium or high intensity physical exercise. The exercise intensity was informed by the individuals, and according to the mathematical model, only medium and high intensity exercises are considered.

In order to be able to predict the glycemic oscillation of individuals with T1D of each one of them and in an attempt to automate the 180 extra health-related decisions (TACK et al., 2018), a personalized pattern was sought. This daily pattern exists and Figure 18 represents it, at least in the glycemic speed part. The glycemic speed in this case was calculated with interstitial glucose values (rising or falling) in relation to time each 30

min.

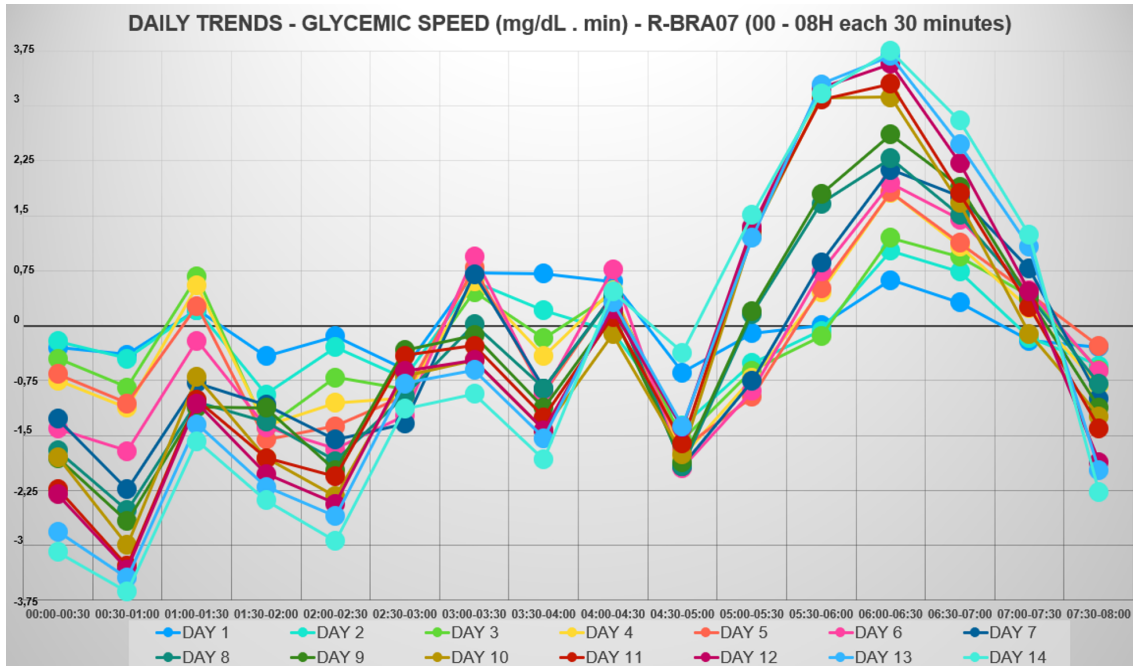


Figure 18: Glycemic oscillation pattern of participant R-BRA07 (every 30min of 00h-8h).

However, for example, the volunteer R-BRA05 presented a different pattern of glyceimic speed than the individual R-BRA07, as shown in Figure 19. It is interesting to note that the first day of measurement was discarded, as it presented a different pattern from the other 13 days, which is common to the FreeStyle Libre glucometer[®] (FREESTYLE-LIBRE, 2020), due to the period of chemical equilibrium with the fluid interstitial on the first day.

The daytime and nighttime windows were personalized for each individual, according to the new stimulus (data), with the daytime period corresponding to the period in which the individual is active. And, for some individuals with night intervals shorter than 8 hours, it was not necessary to trigger the execution of Tesseractus model for this period, and so on. The prediction triggers were performed in a personalized way, as the model is stimulated with new data, and the prediction periods were according to each individual.

Based on these premises, the first result of this work consisted in the development of the mathematical model in Python and subsequent execution. It was proved that the differential equations serve as a basis for the Tesseractus model, as a provider of labels for glyceimic levels in phase one of learning, and as a predictor, in phase two. Figure 20 illustrates the parameters used to calculate the glyceimic oscillation curve. In this case, it was simulated with a 2-hour prediction, current blood glucose value equal to 180 mg/dL and insulin sensitivity of 75%. The exercise time is equal to the minimum average time,

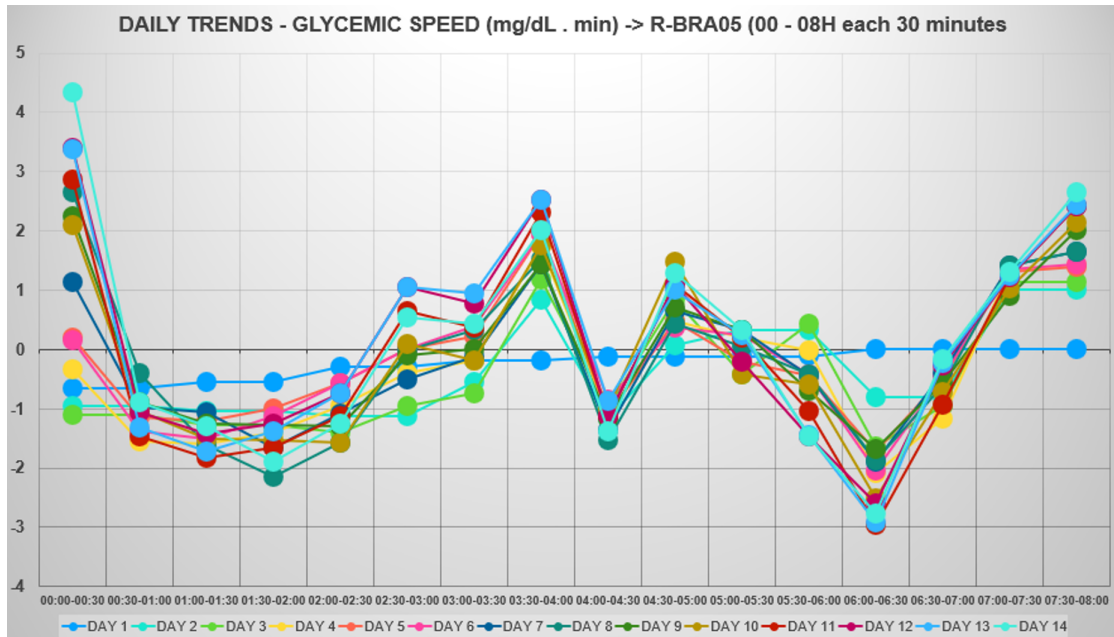


Figure 19: Glycemic oscillation pattern of participant R-BRA05 (every 30min of 00h-8h).

and in this case it does not significantly influence glucose uptake. The glucose intake rate is at a fixed rate ($1.08 \text{ mg/dL} \cdot \text{min}$), as is the insulin infusion ($20 \mu\text{U/mL} \cdot \text{min}$). Figure 21 shows that glycemia, after two hours, stabilizes around 127 mg/dL . Insulin concentration also stabilizes at $350 \mu\text{U/mL}$.

Gin (mg/dl min)	lin (uU/ml min)	G0 (mg/dl)	I0 (uU/ml)	gamma	tau2 (min)
1,08	20	180	85	0,75	15
tex (min)	texM (min)	h (Euler)	Prediction Horizon (min)	Parameters	
60	60	1	120		
Alpha	Beta	C ₂	C ₃	C ₄	C ₅
0,29	1,77	144	1000	80	26
E	Rg	ti	Uo	Ub	Um
0,2	180	100	40	72	940
Vg	Vi	Vp	Vmax	Km	s
10	11	3	150	2300	0,0072
<input type="button" value="Run"/> <input type="button" value="New"/>					

Figure 20: Parameters used - agent Math (60 min. exercise).

The first version of code developed for the physiological model, based on ODEs, was sensitive to changes in parameter values. For example, changing the exercise time from 60 minutes to 120 minutes, as shown in Figure 22, caused positive changes in glucose level, as the value was within the ideal range, that is, 100 mg/dL , as shown in Figure 23.

Specifically about the **Math** agent, the values of insulin concentration I_0 and insulin

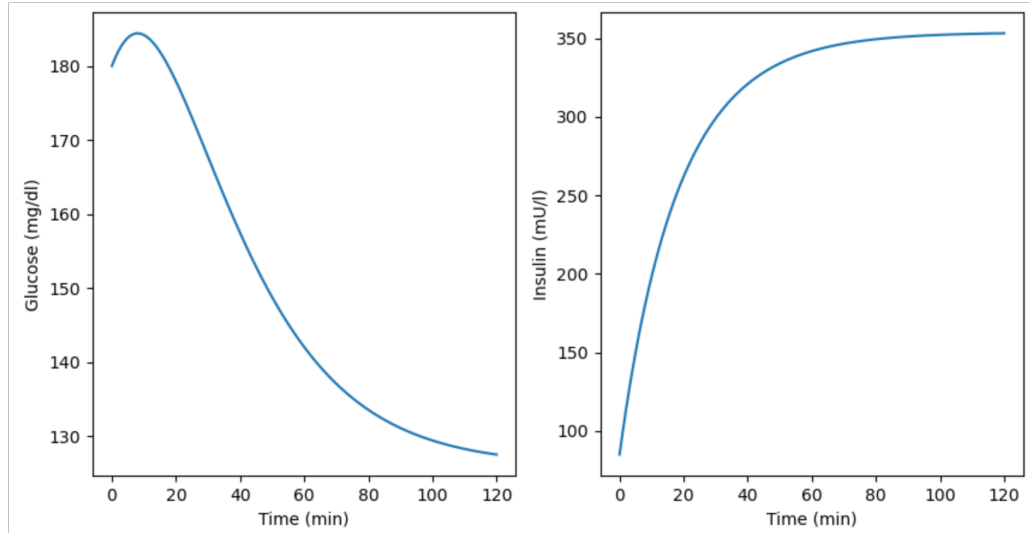


Figure 21: Generated graphs of glycemic oscillation and insulin concentration for 60 min. of exercise.

Gin (mg/dl min)	lin (uU/ml min)	G0 (mg/dl)	I0 (uU/ml)	gamma	tau2 (min)
<input type="text" value="1,08"/>	<input type="text" value="20"/>	<input type="text" value="180"/>	<input type="text" value="85"/>	<input type="text" value="0,75"/>	<input type="text" value="15"/>
tex (min)	texM (min)	h (Euler)	Prediction Horizon (min)	<input type="button" value="Parameters"/>	
<input type="text" value="120"/>	<input type="text" value="60"/>	<input type="text" value="1"/>	<input type="text" value="120"/>		
Alpha	Beta	C ₂	C ₃	C ₄	C ₅
<input type="text" value="0,29"/>	<input type="text" value="1,77"/>	<input type="text" value="144"/>	<input type="text" value="1000"/>	<input type="text" value="80"/>	<input type="text" value="26"/>
E	Rg	ti	Uo	Ub	Um
<input type="text" value="0,2"/>	<input type="text" value="180"/>	<input type="text" value="100"/>	<input type="text" value="40"/>	<input type="text" value="72"/>	<input type="text" value="940"/>
Vg	Vi	Vp	Vmax	Km	s
<input type="text" value="10"/>	<input type="text" value="11"/>	<input type="text" value="3"/>	<input type="text" value="150"/>	<input type="text" value="2300"/>	<input type="text" value="0,0072"/>

Figure 22: Parameters used - agent Math (120 min. exercise).

intake $I_i n$ were replaced by the approximate value of the pharmacokinetics $I(t)$ ($\mu U/mL$), as a function of time. The value of insulin resistance (IR) (γ) or insulin sensitivity factor (ISF), specifically for the 7 volunteers from Brazil, was replaced by eGDR (EPSTEIN et al., 2013). It is very important to point out that the scaling factor γ can take values from 0 to 1, with 0 corresponding to no ability for muscle and fat cells to take up glucose, and the closer to 1, the individual with T1D has the ability to uptake glucose through exogenous insulin, satisfactorily.

In this case, eGDR equal to 12 mg/kg/min equals 50% IR, 6 mg/kg/min equals 75% and eGDR equals 0 mg/kg/min equals 100% IR or γ equal to 1. In our research, no individual had a value of γ equal to 1, according to Table 16. However, the best 2-hour prediction results with ODEs were achieved using the rule of 1700/amount of insulin used

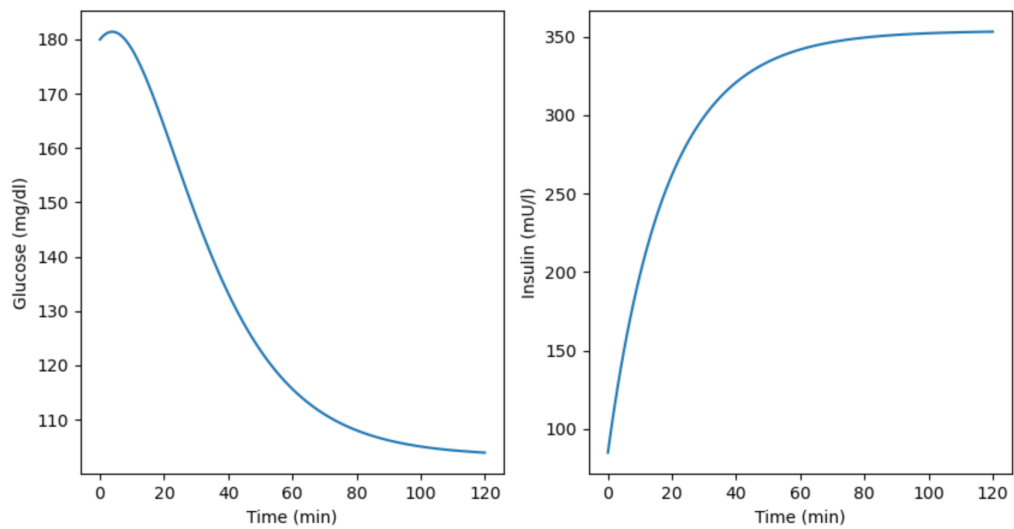


Figure 23: Generated graphs of glycemic oscillation and insulin concentration for 120 min. of exercise.

to measure the insulin resistance.

The second result was the development of the Tesseract model, based on agents, more specifically with the Spade (SPADE, 2019) library with BDI plugin (SPADE-BDI, 2021). The supervised learning (ALFIAN et al., 2020) algorithm was delegated to the ML agent, and reinforcement learning governs the entire model (Q-LEARNING, 2019). The mathematical agent, based on differential equations, is one of the agents in the model. With the test environment created, the evaluation metrics were defined and applied to the dataset: MAE, MAPE, TIR and Parkes Error Grid (PEG) considering zones A+B.

9.1 Applying Tesseract to data from Brazilian Volunteers

The data of the seven Brazilian volunteers, characterized in the subsection 8.1, were used to verify the evaluation metrics, and the individual's activity periods were personalized, as follows:

- **R-BRA01:** daytime (08am–10:40pm) and nighttime (10:41pm–07:59am);
- **R-BRA02:** daytime (06am–10pm) and nighttime (10:01pm–05:59am);
- **R-BRA03:** daytime (08am–10pm) and nighttime (10:01pm–07:59am);
- **R-BRA04:** daytime (09am–9:15pm) and nighttime (9:16pm–08:59am);

- **R-BRA05:** daytime (07:35am–11:58pm) and nighttime (11:59pm–07:34am);
- **R-BRA06:** daytime (05:30am–9:50pm) and nighttime (9:51pm–05:29am);
- **R-BRA07:** daytime (06am–8:50pm) and nighttime (8:51pm–05:59am).

In relation to Parkes Error Grid (PEG) for Brazilian volunteers, Table 18 details each prediction horizon (PH), in the daytime, in addition to the general average of Tesseractus model, and Figure 24 represents a total of 3126 predictions, and on average 95.1% fell in zones A and B. The bar between 0 and 4, on the right side of the PEG, represents the degree of accuracy between the measured and predicted values, with the lightest (0.0) being the best state, and the darkest (4.0) being the worst. Dark green dots are in the zone A, light green dots in the zone B, yellow dots in the zone C, red dots in the zone D and black dots in the zone E.

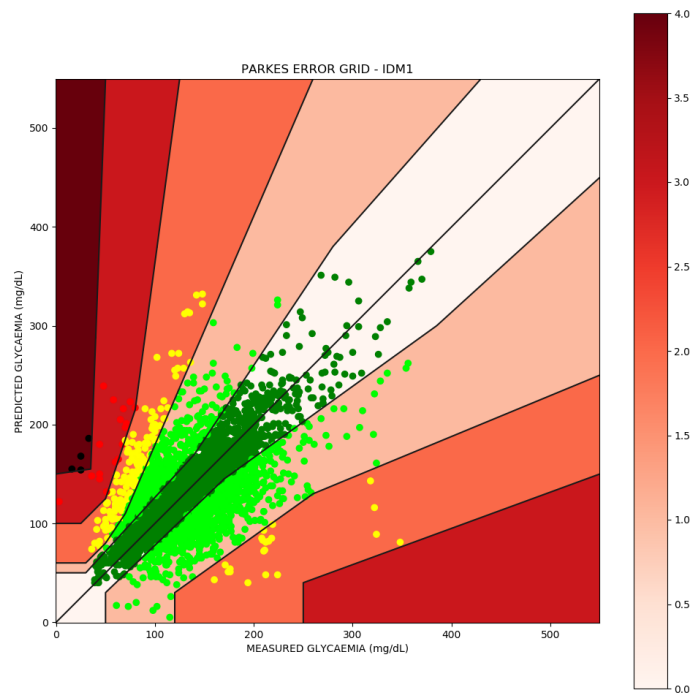


Figure 24: Parkes Error Grid linked with 7 Brazilian volunteers (daytime).

Table 19 details the PEG of each prediction horizon, in the night period, in addition to the Tesseractus model itself and, Figure 25 represents a total of 1400 predictions, and on average 93.7% fell in zones A and B.

PH	A	B	C	D	E	A+B	# of predictions
Average	62.3%	32.8%	4.4%	0.5%	0%	95.1%	3126
15 min	93%	6.8%	0.2%	0%	0%	99.8%	644
30 min	76.9%	22.2%	0.8%	0%	0%	99.1%	589
60 min	56.4%	41.5%	2%	0.1%	0%	97.9%	509
90 min	50.1%	44.9%	4.7%	0.3%	0%	95%	443
120 min	50.3%	41.8%	7.4%	0.5%	0%	92.1%	392
180 min	46%	44%	8.9%	0.9%	0.2%	90%	305
240 min	49.6%	40.4%	9.7%	0.3%	0%	90%	244

Table 18: Results of Parkes Error Grid for Tesseractus (zones) - daytime (Brazil).

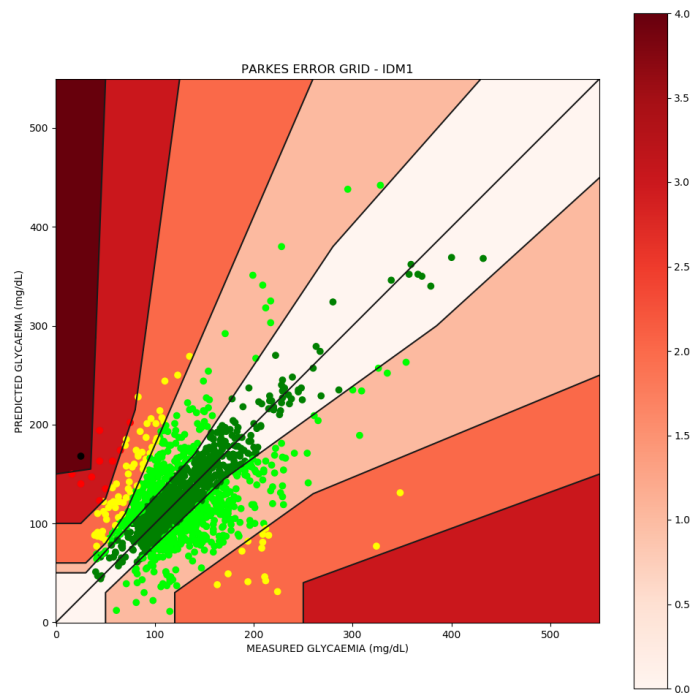


Figure 25: Parkes Error Grid linked with 7 Brazilian volunteers (night time).

The daytime mean absolute error (MAE) is represented in Table 20 and nighttime MAE in Table 21. The daytime mean absolute percentual error (MAPE) is represented in Table 22 and nighttime MAPE in Table 23.

PH	A	B	C	D	E	A+B	# of predictions
Average	55.8%	37.9%	5.6%	0.7%	0%	93.7%	1400
15 min	86%	12.4%	1.7%	0%	0%	98.4%	163
30 min	72.2%	26.9%	0.9%	0%	0%	99.1%	159
60 min	57.1%	41.8%	1.1%	0%	0%	98.9%	154
90 min	50%	44.4%	5.6%	0%	0%	94.4%	151
120 min	47.7%	46.7%	5.6%	0%	0%	94.4%	139
180 min	45.3%	44.7%	8.6%	0.7%	0.6%	90%	121
240 min	48.8%	42.2%	8.4%	0.6%	0%	91%	110
300 min	46.2%	44.8%	8%	1.2%	0%	91%	107
360 min	54.2%	37.8%	6.5%	1.5%	0%	92%	108
420 min	52.3%	39.7%	6.7%	1.3%	0%	92%	98
480 min	62%	33%	4.5%	0.5%	0%	95%	90

Table 19: Results of Parkes Error Grid for Tesseractus (zones) - nighttime (Brazil).

PH	Average
Tesseractus	24.56
15 min	9.18
30 min	16.97
60 min	26.41
90 min	30.24
120 min	30.54
180 min	33.61
240 min	25.01

Table 20: MAE (mg/dL) - daytime (Brazil).

PH	Average
Tesseractus	27.77
15 min	9.27
30 min	16.09
60 min	26.26
90 min	28.09
120 min	28.3
180 min	32.68
240 min	34.49
300 min	35.16
360 min	34.97
420 min	33.96
480 min	26.37

Table 21: MAE (mg/dL) - nighttime (Brazil).

PH	Average
Tesseractus	24
15 min	8
30 min	13.32
60 min	20.52
90 min	24.98
120 min	30.79
180 min	33.26
240 min	37.82

Table 22: MAPE (%) - daytime (Brazil).

PH	Average
Tesseractus	24.72
15 min	8.8
30 min	15.46
60 min	23.53
90 min	27.74
120 min	24.56
180 min	29.16
240 min	29.31
300 min	23.84
360 min	34.89
420 min	30.24
480 min	24.42

Table 23: MAPE (%) - nighttime (Brazil).

9.2 Applying Tesseractus to data from Ohio University

The data of eight volunteers from University of Ohio, characterized in the subsection 8.1, were used to verify the evaluation metrics, and the individual's activity periods were personalized, as follows:

- **OHIO544:** daytime (07:50am–10:15pm) and nighttime (10:16pm–07:49am);
- **OHIO552:** daytime (05:15am–11:30pm) and nighttime (11:31pm–05:14am);
- **OHIO563:** daytime (05am–9:55pm) and nighttime (9:56pm–04:59am);
- **OHIO570:** daytime (06am–9:10pm) and nighttime (9:11pm–05:59am);
- **OHIO584:** daytime (05am–9:15pm) and nighttime (9:16pm–04:59am);

- **OHIO588**: daytime (06:35am–10:55pm) and nighttime (10:56pm–06:34am);
- **OHIO591**: daytime (06am–11:10pm) and nighttime (11:11pm–05:59am);
- **OHIO596**: daytime (06:50am–10:15pm) and nighttime (10:16pm–06:49am).

In relation to PEG of volunteers from Ohio, Table 24 details each PH, in the daytime, in addition to the general average of Tesseractus model, and Figure 26 represents a total of 8934 predictions, and on average 94.3% fell in zones A and B.

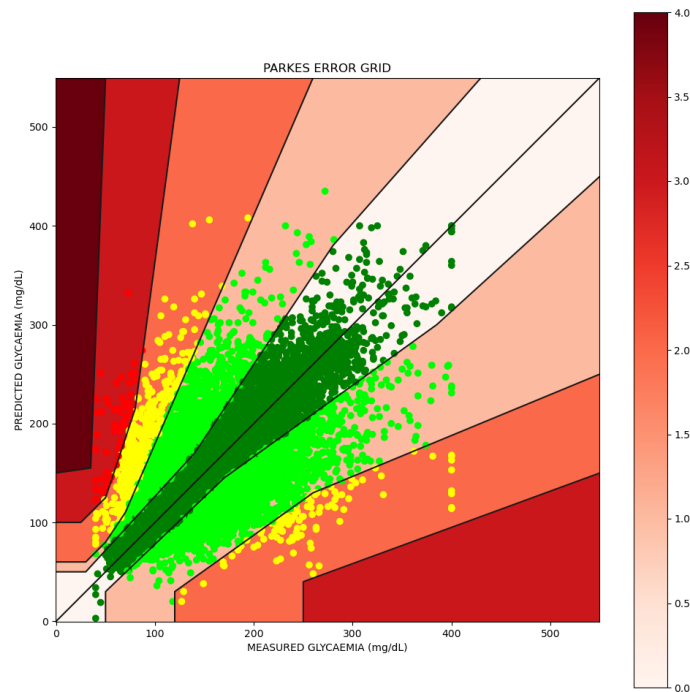


Figure 26: Parkes Error Grid linked with 8 volunteers from OHIO (day time).

Table 25 details the PEG of each PH, in the night period, in addition to the Tesseractus model itself and, Figure 27 represents a total of 3283 predictions, and on average 91.9% fell in zones A and B.

The daytime MAE is represented in Table 26 and nighttime MAE in Table 27.

The daytime MAPE is represented in Table 28 and nighttime MAPE in Table 29.

PH	A	B	C	D	E	A+B	# of predictions
Average	57%	37.3%	5.1%	0.6%	0%	94.3%	8934
15 min	88.3%	11.5%	0.2%	0%	0%	99.8%	1874
30 min	73.5%	25.5%	0.9%	0.1%	0%	99%	1731
60 min	53.7%	42.6%	3.2%	0.5%	0%	96.3%	1480
90 min	48.8%	44.7%	5.5%	1%	0%	93.5%	1214
120 min	44.9%	48.1%	6%	1%	0%	93%	1073
180 min	41.2%	48.6%	9.1%	0.8%	0%	89.8%	854
240 min	38.6%	49.3%	11%	1.1%	0%	87.9%	708

Table 24: Results of Parkes Error Grid for Tesseractus (zones) - daytime (Ohio).

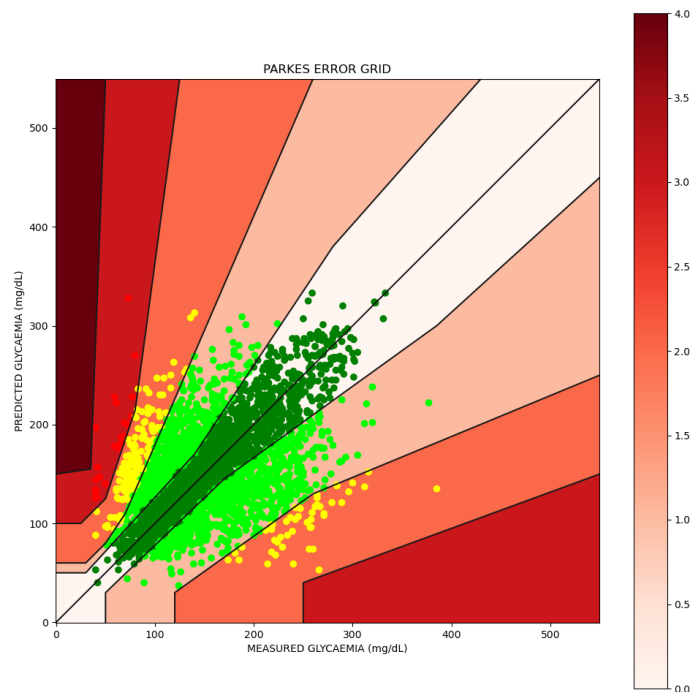


Figure 27: Parkes Error Grid linked with 8 volunteers from OHIO (night time).

9.3 Applying Tesseractus to data from virtual individuals

Data of nine virtual individuals, characterized in the subsection 8.1, were used to verify the evaluation metrics, and the individual's activity periods were defined, as follows: daytime (07am–6:50pm) and nighttime (6:51pm–06:59am). Based on this, they were created with these IDs: **Adult#001 - 003**, **Adolescent#001 - 003** and **Child#001**

PH	A	B	C	D	E	A+B	# of predictions
Average	49.1%	42.8%	7.1%	1%	0%	91.9%	3283
15 min	93.1%	5.7%	1.2%	0%	0%	98.8%	452
30 min	80.2%	19.2%	0.6%	0%	0%	99.4%	444
60 min	61.8%	36%	1.1%	1.1%	0%	97.8%	417
90 min	52.6%	40.8%	5.2%	1.4%	0%	93.4%	405
120 min	52.5%	42.1%	4.6%	0.7%	0%	94.6%	361
180 min	43%	49.4%	6.4%	1.2%	0%	92.4%	280
240 min	40.1%	48.6%	9.7%	1.6%	0%	88.7%	213
300 min	39.8%	49.3%	10%	0.9%	0%	89.1%	211
360 min	41.7%	46.3%	10.6%	1.4%	0%	88%	178
420 min	42.7%	47.9%	8.9%	0.6%	0%	90.6%	162
480 min	49.3%	43.1%	7.1%	0.5%	0%	92.4%	160

Table 25: Results of Parkes Error Grid for Tesseractus (zones) - nighttime (Ohio).

PH	Average
Tesseractus	35.09
15 min	12.07
30 min	21.55
60 min	34.44
90 min	40.53
120 min	44.84
180 min	45.93
240 min	42.14

Table 26: MAE (mg/dL) - daytime (Ohio).

PH	Average
Tesseractus	33.19
15 min	12.48
30 min	19.5
60 min	27.37
90 min	32.34
120 min	33.66
180 min	39.21
240 min	42.66
300 min	42.62
360 min	41
420 min	42
480 min	38

Table 27: MAE (mg/dL) - nighttime (Ohio).

PH	Average
Tesseractus	21
15 min	10
30 min	12
60 min	19
90 min	24
120 min	27
180 min	30
240 min	29

Table 28: MAPE (%) - daytime (Ohio).

PH	Average
Tesseractus	22
15 min	6
30 min	11
60 min	17
90 min	23
120 min	24
180 min	28
240 min	29
300 min	30
360 min	29
420 min	28
480 min	23

Table 29: MAPE (%) - nighttime (Ohio).

- 003.

In relation to PEG, Table 30 details each PH, in the daytime, in addition to the general average of Tesseractus model and, Figure 28 represents a total of 1824 predictions, and on average 97.2% fell in zones A and B.

PH	A	B	C	D	E	A+B	# of predictions
Average	68.3%	28.9%	2.2%	0.6%	0%	97.2%	1824
15 min	88.3%	10.9%	0.8%	0%	0%	99.2%	384
30 min	79.7%	20.3%	0%	0%	0%	100%	384
60 min	60.7%	37.5%	1.8%	0%	0%	98.2%	336
90 min	51.1%	45.8%	2.1%	1%	0%	96.9%	288
120 min	62.5%	37.5%	0%	0%	0%	100%	240
180 min	62.5%	32.5%	5%	0%	0%	95%	120
240 min	45.8%	41.7%	8.3%	4.2%	0%	87.5%	72

Table 30: Results of Parkes Error Grid for Tesseractus (zones) - daytime (Virtual).

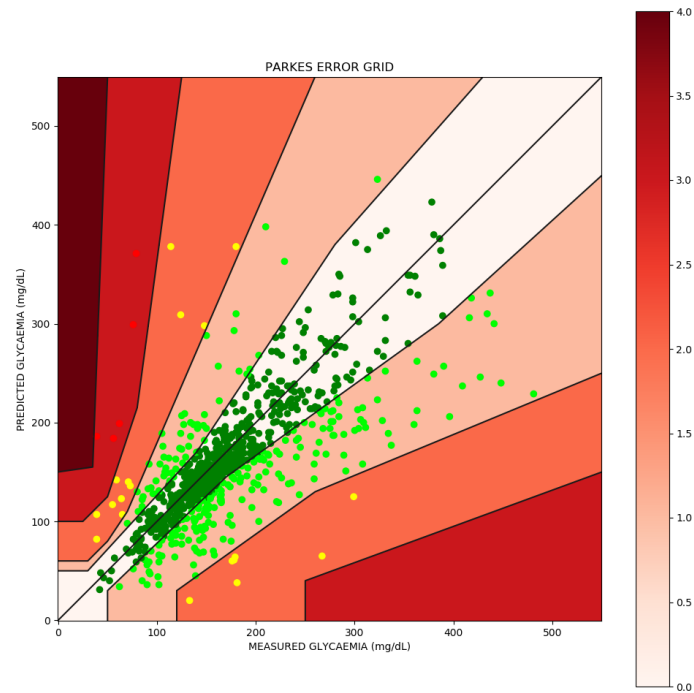


Figure 28: Parkes Error Grid linked with nine virtual individuals (day time).

Table 31 details the PEG of each PH, in the night period, in addition to the Tesseractus model itself and, Figure 29 represents a total of 936 predictions, and on average 99.7% fell in zones A and B.

PH	A	B	C	D	E	A+B	# of predictions
Average	72.1%	27.6%	0.3%	0%	0%	99.7%	936
15 min	93.8%	6.2%	0%	0%	0%	100%	216
30 min	79.2%	20.8%	0%	0%	0%	100%	192
60 min	56.2%	43.8%	0%	0%	0%	100%	168
90 min	50%	50%	0%	0%	0%	100%	96
120 min	37.5%	62.5%	0%	0%	0%	100%	72
180 min	37.5%	62.5%	0%	0%	0%	100%	48
240 min	12.5%	87.5%	0%	0%	0%	100%	48
300 min	37.5%	50%	12.5%	0%	0%	87.5%	24
360 min	75%	25%	0%	0%	0%	100%	24
420 min	71.9%	28.1%	0%	0%	0%	100%	24
480 min	84.7%	15.3%	0%	0%	0%	100%	24

Table 31: Results of Parkes Error Grid for Tesseractus (zones) - nighttime (Virtual).

The daytime MAE is represented in Table 32 and nighttime MAE in Table 33. The

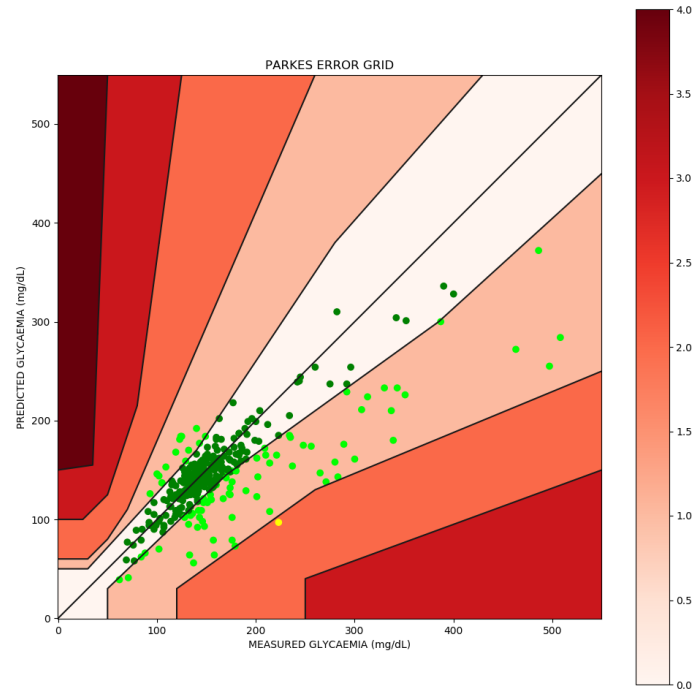


Figure 29: Parkes Error Grid linked with nine virtual individuals (night time).

daytime MAPE is represented in Table 34 and nighttime MAPE in Table 35.

PH	Average
Tesseractus	20.61
15 min	8.49
30 min	13.78
60 min	24.9
90 min	30.72
120 min	25.24
180 min	19.65
240 min	21.52

Table 32: MAE (mg/dL) - daytime (Virtual).

9.4 Using Tesseractus as a Recommender to one Brazilian Volunteer

In this test, the personalized recommendations of the Tesseractus model were applied to the individual R-BRA05, with authorization from the Ethics Council (see ap-

PH	Average
Tesseractus	20.54
15 min	8.76
30 min	11.24
60 min	19.14
90 min	26.04
120 min	30.56
180 min	26.74
240 min	25.45
300 min	25.48
360 min	22.69
420 min	19.81
480 min	10.09

Table 33: MAE (mg/dL) - nighttime (Virtual).

PH	Average
Tesseractus	13.24
15 min	6.21
30 min	9.97
60 min	14.7
90 min	18.81
120 min	14.63
180 min	13.19
240 min	15.21

Table 34: MAPE (%) - daytime (Virtual).

PH	Average
Tesseractus	16.16
15 min	5.16
30 min	5.8
60 min	12.4
90 min	16.08
120 min	22.28
180 min	19.31
240 min	24.11
300 min	26.39
360 min	20.85
420 min	17.47
480 min	7.98

Table 35: MAPE (%) - nighttime (Virtual).

pendix B). Thus, the **Recommender** agent has in its knowledge base (KB) some pre-defined rules/actions between the endocrinologist and the individual, and that are verified for each stimulus from the environment (individual):

1. Practice at least 60 minutes of physical exercise, from medium to high intensity, daily or at least 3 times a week;
2. Does not practice physical exercises during the day;
3. Glycemic target by R-BRA05: between 100–140 mg/dL (personalized), with the ideal being between 80–120 mg/dL;
4. If the glycemic value, coming from the sensor, is above 300 mg/dL or below 80 mg/dL, request a capillary measurement for double verification;
5. Glycemic level correction factor, if the level is above 180 mg/dL: 1U of rapid-acting insulin (aspart) to 50 mg/dL;
6. Daily amount of basal effect insulin: 28U;
7. In the morning, the rapid insulin:carbohydrate ratio should be 1:10, with 1U of insulin aspart for 10g of carbohydrates;
8. In the afternoon, the rapid insulin:carbohydrate ratio should be 1:12, with 1U of insulin aspart for 12g of carbohydrates;
9. At night, the rapid insulin:carbohydrate ratio should be 1:15, with 1U of insulin aspart for 15g of carbohydrates.

If the prediction values are not in the personalized glycemic range (100–140 mg/dL), after 2 hours of receiving a new data, new prediction calculations with $\pm 20\%$ of the input values are requested (amount of macronutrients, insulin dose and exercise time) for the **ML** and **Math** agents, based on the predictor agent. Thus, the following recommendations were modified after the first 7 days of learning:

1. **Recommendation: practice at least 90 minutes of medium to high intensity physical exercise, daily or at least 3 times a week;**
2. **Recommendation: practice physical exercises in the afternoon;**
3. Non-altered glycemic target for R-BRA05: between 100-140 mg/dL;

4. If the glycemic value, coming from the sensor, is above 300 mg/dL or below 80 mg/dL, request a capillary measurement for double verification;
5. Glycemic level correction factor remained the same (1:50);
6. Daily amount of basal effect insulin remained the same: 28U;
7. In the morning, the insulin:carbohydrate ratio should remain 1:10;
8. **Recommendation: in the afternoon, the carbohydrate ratio should be 1:12**, as the individual daily had routine hyperglycemic indexes between lunch and dinner;
9. **Recommendation: at night, the carbohydrate rate should be 1:16**, as the individual daily had routine hypoglycemic indexes after dinner.

Thus, after the recommendations, the TIR (Time in Range) values underwent positive changes, compared to the 14 days of historical data collected:

- TIR at day period: from 70% of (229 hours) to 72% after 7 days of personalized recommendations;
- TIR at night period: from 65% of (106 hours) to 66% after 7 days of personalized recommendations.

Regarding the MAE, MAPE and Parkes Error Grid (PEG) evaluation metrics, Tables 36 and 37 show the results improvement, after 7 days of learning and recommendations, as the daytime and the night period MAE decreased by 2.13% and 1.81%, respectively, and the amount of predictions within PEG A+B zones increased by 3.31% in the daytime period and 2.77% in the night period. The individual R-BRA05 did not have 4-hour predictions in the daytime period, because the period between activation triggers of the Tesseract model, with new data, was less than four hours. The Count column in Table 36 represents the number of predictions.

The graph in Figure 30 represents the telemetry of the glycemic oscillation of the R-BRA05, coming from the FreeStyle Libre[®] sensor, and shows the effect of the personalized recommendations after 5 o'clock afternoon of a specific day.

The results showed improvement of the Tesseract model with the inclusion of more data and continuous learning, considering 7 more days of learning, and it is discussed in the section 9.5.

R-BRA05	MAPE (before)	MAPE (after)	MAE (before)	MAE (after)	PEG A+B before	PEG A+B after	Count
Tesseractus (average)	24.26%	23.75%	22.49	22.02	86.05%	88.9%	232
15 min	12.48%	12.22%	11.28	11.04	100%	100%	74
30 min	22%	21.54%	22.4	21.93	95.1%	98.43%	61
60 min	29.11%	28.5%	31.32	30.66	90%	93.15%	40
90 min	34.47%	33.74%	33.15	32.45	81.2%	84.04%	32
120 min	28.9%	28.29%	25.5	24.96	90%	93.15%	20
180 min	42.91%	42.01%	33.8	33.09	60%	62.1%	5

Table 36: Results through metrics after recommendations at daytime (R-BRA05).

R-BRA05	MAPE (before)	MAPE (after)	MAE (before)	MAE (after)	PEG A+B before	PEG A+B after	Count
Tesseractus (average)	31%	30.45%	29.79	29.26	80.6%	82.84%	119
15 min	7.86%	7.72%	5.72	5.62	100%	100%	13
30 min	17.4%	17.09%	14	13.75	100%	100%	12
60 min	23.09%	22.68%	22.9	22.49	100%	100%	12
90 min	29.4%	28.88%	26.08	25.62	83.3%	85.61%	12
120 min	40.6%	39.88%	32.5	31.92	75%	77.08%	12
180 min	50.4%	49.5%	32.69	32.11	69.3%	71.23%	11
240 min	44.47%	43.68%	38.5	37.82	75%	77.08%	11
300 min	41.2%	40.1%	38	37.32	75%	77.08%	11
360 min	39.37%	38.67%	39.09	38.39	72.8%	74.82%	11
420 min	50.4%	49.5%	40.54	39.82	63.7%	65.47%	10
480 min	38.05%	37.37%	37.75	37.08	75%	77.08%	4

Table 37: Results through metrics after recommendations at nighttime(R-BRA05).

9.5 Discussion

If we consider an overall average between the three datasets in the circadian cycle, two *in vivo* and one *in silico*, Tesseractus model has pioneering results for long-term glycemic predictions (from four to eight hours): **MAE (26.96 mg/dL)**, **MAPE (20.18%)** and **PEG in zones A+B (95.31%)**, out of a total of **19503** requested predictions.

This work achieved mean absolute errors (MAE) of **less than 30 mg/dL** for long-term prediction horizons (PH). For short-term PHs (up to 2h), the Tesseractus model achieved even better results: **MAE (23.3 mg/dL)**, **MAPE (16.55%)** and **PEG in zones A+B (97.63%)**. At this point, it is important to emphasize the importance of

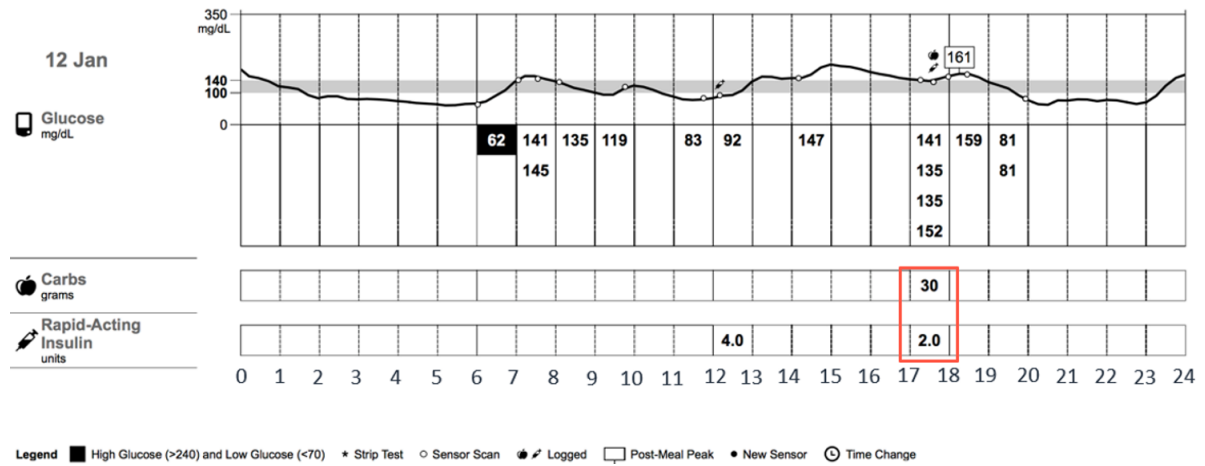


Figure 30: FreeStyle Libre[®] sensor graph related to 24 hours with recommendations (5pm).

long-term prediction in the night periods, in order to mitigate the risks of nocturnal hypoglycemia, and short-term to cover the total time of carbohydrate to glucose conversion, in the human body.

Even considering only a single individual for the prediction analysis based on personalized recommendations, there were improvements in terms of time within the ideal and personalized glycemic level, **being four hours during the day and one hour at night**. However, this improvement projection can be expanded with more days of data collection, being exponential with more individuals in the database.

Comparing the results of the Tesseract model (PEG 95.31% and 97.63%) with the current accuracy requirements of the Health Organizations or Federations, for blood glucose meters in real time, that is, PH equal to zero, as ISO1597 of 2015 (KATZ, 2020) or FDA (KATZ et al., 2020): (1) 95% of values in the range ± 15 mg/dL to < 100 mg/dL - ISO15197 (Europe); (2) 95% of all values must be in the range $\pm 15\%$; - FDA (USA), it is necessary to have a new taxonomy for evaluating success with longer PHs (180, 240, 300, 360, 420 and 480 min.), according to medicine of precision. This new requirement comes from the need for predictability of glycemic oscillation, not only in real time or short-term to avoid irreversible risks, but in the long term reducing the possibility of the appearance of comorbidities derived from poor control of the glycemic level.

However, it is worth remembering that the model still needs to be validated with more individuals, as it is still in a proof-of-concept phase. The model also requires a high degree of commitment from the individual, due to the numerous measurements and data capture. In addition, the model was tested only with individuals who use insulin pumps, CGMs, and users of rapid insulin analogues (lispro and aspart) and long-acting analogues

(degludec and glargine), however the model can be expanded to users of FIASP (FIASP, 2020), NPH and perhaps even regular insulin.

In summary, the Tesseractus model is valid from the point of view of clinical applicability, besides the perspective of a medical and individual decision support system, through personalized recommendations. The result of this work demonstrated the feasibility of the Tesseractus model to be applied to an open artificial pancreas (OPENAPS, 2021), artificial pancreas (closed-loop) (FDA, 2019), insulin pumps (MINIMED-640G, 2020) or (CONTROL-IQ, 2022), applications of endocrinologists and/or nutritionists, for example, via telemedicine. In this way, it can facilitate and improve the T1D's lifestyle, as well as avoid mental fatigue due to numerous extra decisions.

10 CONCLUSION AND FUTURE WORK

This Chapter is to discuss the main contributions of the Tesseractus model, future work and publications.

10.1 Final remarks

Providing a model that efficiently and effectively meets the personalized and dynamic needs of each individual with T1D is, however, challenging. Even with advances in technology with continuous glucose monitors (FREESTYLE-LIBRE, 2020) and artificial pancreas (FDA-CONTROLIQ, 2019), there is no PH compatible with the busy lifestyle of today's individuals with T1D. Another reason that makes glucose prediction complicated is the development of ML models and mathematical models that mimic glucose-insulin regulatory system of individuals with T1D.

Succinctly, the main needs are: (1) create treatment approaches that bring better results in terms of short-term glycemic control and reduction of the risks of developing long-term complications; (2) improve the accuracy of prediction models for individuals with T1D (IT1D), especially in high-risk populations, to enable effective and safe interventions that avoid hypoglycemic or hyperglycemic conditions; (3) there are no models or software that have long PHs ($>$ six hours), in order to avoid, for example, nocturnal hypoglycemia; (4) the most therapies are based on generalist values, according to scientific societies (IDF, 2022); (5) there is no accurate mechanism for prior personalized recommendation; (6) the PH of pharmaceutical devices already available on the market, such as insulin pumps, does not exceed 30 minutes (BROWN et al., 2019b) and (MINIMED-670G, 2020), and consequently does not have a desirable predictability, for example postprandial ($>$ two hours). Thus, this work directly addresses challenge (1) and indirectly addresses challenges (2)–(6).

In this context, the present work presented a hybrid model called Tesseractus, based on a Multi-agent System (MAS), to predict the glycemic oscillation, in a horizon of four

to eight hours. Moreover, it recommends the amount of exogenous, fast-acting and basal insulin, in addition to the amount of macronutrients to be ingested, time and intensity of exercise. The main objective is to keep glucose within the ideal range for as long as possible through these personalized recommendations. A continuous learning system is used with three Artificial Intelligence techniques: (1) supervised learning; (2) reinforcement learning; (3) active learning with knowledge transfer.

The proposed model becomes a gray-box hybrid (DUUN-HENRIKSEN et al., 2013) as it uses physiological models to mimic the glucose-insulin regulatory system of the individuals with T1D, together with the continuous collection of data from each individual. Active learning takes advantage of ODE for the glucose compartment, and polynomial approximation functions for insulin pharmacokinetics, to mimic the individualized behavior of glucose-insulin regulatory system of each individual with T1D.

One of the great advantages of Tesseractus model is the use of different models, which can mitigate errors between the predicted and continuously measured values, in addition to the ODE's own input parameters. In phase one of learning and labeling, the combination of techniques is advantageous, as it consists of models with complementary functions, resulting in a cohesive, well-adjusted model capable of generalization. In the second phase of learning and prediction, the model takes advantage of the best prediction technique, either based on ODE, approximation by polynomials and supervised learning algorithm, being governed by continuous reinforcement learning with the receipt of punishments or rewards.

From a theoretical point of view, it is worth mentioning that during the bibliographic survey, no other work was identified that combined the advantages of a MAS with the hybrid techniques of the gray-box model, that is, prediction of glucose in individuals with T1D, with physiological and data-based models. And the use of agents was crucial to bring flexibility to the model to include new prediction models, in order to have positive competition, in addition to continuous and dynamic error correction.

Another characteristic that makes the results of the Tesseractus model pioneer are the overall average between the prediction horizons (15 min to eight hours): (1) **MAE (26.96 mg/dL)**; (2) **MAPE (20.18%)**; (3) **PEG in zones A+B (95.31%)**. This work also achieved MAE **less than 30 mg/dL** for long-term prediction horizons (PH). For short-term PHs (up to 2h), the Tesseractus model achieved even better results: **MAE (23.3 mg/dL)**, **MAPE (16.55%)** and **PEG in zones A+B (97.63%)**.

In summary, the idea is to empirically show, with virtual and real data from individ-

uals with T1D, that the hybrid model named Tesseractus is able to predict glucose oscillation with an accuracy lower than 30 mg/dL (1.7 mmol/L). The idea is to continuously improve the performance of the Tesseractus model and consequently reduce the error of the predicted value, while removing some specific restrictions related in the literature: (a) fixed values of parameters for prediction calculations, in mathematical models; (b) agent's support for continuous learning and correction of the values of each input parameter of the ODEs; (c) not having barriers to combine different prediction models, using Active Learning, reusing, combining and adapting knowledge from different agents (KHOLGHI et al., 2015).

10.1.1 Main contributions of Tesseractus Model

The main contributions of this thesis is defining a model that:

1. **combines different techniques** in the same model working in an **orchestrated way**, from mathematics to ML (supervised and reinforced learning), represented by agents;
2. adopts **continuous learning** for applicability in **real individuals** with T1D;
3. uses a **Multi-Agent System** to delegate the task of **continuous self-correcting** process about prediction errors;
4. it is possible to consider real and virtual individuals, so it is **independent of sex, age or ethnicity**;
5. was **tested with 15 real individuals**, in addition to the nine virtual ones;
6. it has direct applicability in **technology-based healthcare**;
7. provides **prediction of glycemic oscillation of up to 8 hours**, depending on the individual's lifestyle, with acceptable absolute error;
8. **built a new dataset** with data from 24 T1D individuals, in order to share with the academic core;
9. **can be the research base for a new taxonomy of long-term prediction softwares/apps**, for individuals with T1D, for example, for ANVISA from Brazil (National Health Surveillance Agency) to validate software as a medical device (ANVISA, 2022);

10. it can support the **automation of the 180 extra health-related decisions daily** that individuals with T1D have compared to individuals without DM, in an **attempt to reduce mental fatigue** related to these individuals with T1D;
11. it provides **hyper-personalized recommendations** about on macronutrients, insulin and physical exercise, based on models, not just fixed rules;
12. is flexible for using different types of insulin.

However, some limitations need to be defined, which can be addressed in future work:

1. Tesseratus is not tested with pregnant women and individuals with type 2 diabetes mellitus;
2. For now it only supports four types of insulin analogues: aspart, lispro, glargine and degludec;
3. The dataset is still small and performed with historical data from only 24 individuals between real and virtual;
4. Tesseratus was testes with only 1 individual for future predictions;
5. Only a few insulin sensors or pumps were tested during the research;
6. Add new test variables: stress, hormonal effects, blood oxygen, heart rate.

10.2 Future Work

Tesseratus model could be coupled to mobile devices through an app, with voice commands and volumetric recognition of food (ZHU et al., 2010), in order to facilitate the lifestyle of individuals with T1D with visual impairments and to evaluate the user experience when entering data. In addition, it could be integrated into *homecare* systems to provide early warning to other actors, in the remote control system about the current state of the individual. Even the prototype based on the Tesseratus is in the development phase (HMP, 2023).

Additionally, work with other data could be considered to improve the accuracy and precision of the model, for example: (1) stress level; (2) hormonal effects; (3) blood oxygenation; (4) heartbeats and associate with the levels of exercise intensity: light, moderate and intense; (5) test with alcohol consumption. In addition, the idea is to

expand to tests with hundreds of individuals, and consider feedback, after Tesseractus recommendation, from an endocrinologist or nutritionist directly in the app.

The same framework could be adapted to support individuals with type 2 and gestational DM (IDF, 2022), and to extend more tests with an anomaly detection system (ANOMALY, 2022). In addition to adapting the supervised algorithm for time series analysis, other algorithms such as SARIMAX (MONTASER; DíEZ; BONDIA, 2017) could also compete for the best prediction result of glycemic oscillation. Other techniques within the field of Artificial Intelligence could be applied, such as Algorithms with Predictions (AZR; PANIGRAHI; TOUITOU, 2022) and Deep-Learning (ZHU et al., 2021), to check improvements in MAE (≤ 15 mg/dL), MAPE and PEG (zones A+B $\geq 98\%$).

Another interesting topic that could be addressed is the direct integration with open artificial pancreas OpenAPS (OPENAPS, 2021). Such integration would allow verifying if the Tesseractus model can contribute to improve the OpenAPS management system, increase the PH and decrease the absolute error between the measured and predicted values.

10.3 Publications

As mentioned in the Chapter 2, the research project of this thesis was discussed in a *Doctoral Consortium*, at the *31st International Symposium IEEE CBMS* (Computer Based Medical Systems) (CBMS, 2018). As reported in activity 3, the dissemination of preliminary results has already been carried out (PEREIRA et al., 2019), in an academic conference on *Intelligent Systems* (INTELLISYS, 2019). Final results about seven Brazilian volunteers were compiled and published in the journal *Applied Sciences* (PEREIRA et al., 2022). The next step is to submit another paper to the journal *Engineering Applications of Artificial Intelligence* (EAAI, 2022), when we compare the results of the application of Tesseractus in the Ohio individuals (OHIO-UNIV-T1D, 2020) versus the nine subjects generated by the simulator of the University of Virginia (UNIV-VIRGINIA, 2020).

The work was awarded with the title of *Honorable Mention* for its e-poster: "A Hybrid Model to Predict Glucose Oscillation for Patients with Type 1 Diabetes and Suggest Customized Recommendations", in the category related to Goal 3 - Health and Well-Being of the United Nations (UN) (ONU-SGD, 2022) at the *Second Graduate Meeting of the Universidade de São Paulo: "A society in transformation"*, from 10/19/2021 to

10/20/2021.

The software based on Tesseractus was registered in the Brazilian National Institute of Intellectual Property (INPI) in 2022, under the process BR5112022000522-0 (INPI, 2022).

REFERENCES

- ABE, S. et al. Two-way crossover comparison of insulin glargine and insulin detemir in basal-bolus therapy using continuous glucose monitoring. *Diabetes, Metabolic Syndrome and Obesity: Targets and Therapy*, Dove Press, v. 4, p. 283, 2011.
- ACCU-CHECK. 2020. Available in: <<https://www.accu-check.com.br/monitores-de-glicemia/active>> [Accessed: 2020-11-11].
- ACKERMAN, E.; ROSEVEAR, J. W.; MCGUCKIN, W. F. A mathematical model of the glucose-tolerance test. *Physics in medicine & Biology*, IOP Publishing, v. 9, n. 2, p. 203, 1964.
- ADA. 2023. Available in: <<https://ada.com/conditions/diabetes/>> [Accessed: 2023-01-05].
- AL-HUSSEIN, A.-B. A.; TAHIR, F. R. A New Model For Endocrine Glucose-Insulin Regulatory System. *Iraqi Journal for Electrical and Electronic Engineering*, 03 2020.
- ALFIAN, G. et al. Blood glucose prediction model for type 1 diabetes based on extreme gradient boosting. *IOP Conference Series: Materials Science and Engineering*, IOP Publishing, v. 803, p. 012012, may 2020. <<https://doi.org/10.1088/1757-899x/803/1/012012>> [Accessed: 2020-08-25].
- AMIGONI, F. et al. Anthropic agency: a multiagent system for physiological processes. *Artificial Intelligence in Medicine*, ScienceDirect, v. 27, p. 305–334, 2003. <<https://www.sciencedirect.com/science/article/pii/S09333365703000083>>.
- ANOMALY. 2022. Available in: <<https://azure.microsoft.com/en-us/services/cognitive-services/anomaly-detector/#features>> [Accessed: 2022-01-31].
- ANVISA. 2022. Available in: <<https://www.in.gov.br/en/web/dou/-/resolucao-de-diretoria-colegiada-rdc-n-340-de-6-de-marco-de-2020-247280742>> [Accessed: 2022-02-18].
- AZR, Y.; PANIGRAHI, D.; TOUITOU, N. Online graph algorithms with predictions. In: _____. *Proceedings of the 2022 Annual ACM-SIAM Symposium on Discrete Algorithms (SODA)*. [S.l.: s.n.], 2022. p. 35–66. <<https://epubs.siam.org/doi/abs/10.1137/1.9781611977073.3>> [Accessed: 2022-04-22].
- AZURE. 2022. Available in: <<https://azure.microsoft.com/en-us/overview/what-is-azure/>> [Accessed: 2020-05-15].
- AZURE-MESH. 2022. Available in: <<https://docs.microsoft.com/en-us/azure/cloud-adoption-framework/scenarios/cloud-scale-analytics/architectures/what-is-data-mesh>> [Accessed: 2020-04-25].

BARNETT, A. H. Insulin glargine in the treatment of type 1 and type 2 diabetes. *Vascular health and risk management*, Dove Press, v. 2, n. 1, p. 59, 2006.

BELL, K. J. et al. Impact of fat, protein, and glycemic index on postprandial glucose control in type 1 diabetes: Implications for intensive diabetes management in the continuous glucose monitoring era. *Diabetes Care*, American Diabetes Association, v. 38, n. 6, p. 1008–1015, 2015. ISSN 0149-5992. Disponível em: <<https://care.diabetesjournals.org/content/38/6/1008>>.

BERGMAN, R. N.; COBELLIT, C.; TOFFOLO, G. Minimal models of glucose/insulin dynamics in the intact organism: A novel approach for evaluation of factors controlling glucose tolerance. *Transactions of the Institute of Measurement and Control*, Sage Publications Sage CA: Thousand Oaks, CA, v. 3, n. 4, p. 207–216, 1981.

BERTACHI, A. et al. Prediction of blood glucose levels and nocturnal hypoglycemia using physiological models and artificial neural networks. In: *KHD@ IJCAI*. [S.l.: s.n.], 2018. p. 85–90.

BORDINI, R. H.; HÜBNER, J.; WOOLDRIDGE, M. *Programming multi-agent systems in agent-speak using Jason*. [S.l.]: Wiley, 2007. ISBN 978-0-470-02900-8.

BRATUSCH-MARRAIN, P.; KOMJATI, M.; WALDHÄUSL, W. Efficacy of pulsatile versus continuous insulin administration on hepatic glucose production and glucose utilization in type i diabetic humans. *Diabetes*, Am Diabetes Assoc, v. 35, n. 8, p. 922–926, 1986.

BROWN, S. A. et al. Six-month randomized, multicenter trial of closed-loop control in type 1 diabetes. *New England Journal of Medicine*, v. 381, n. 18, p. 1707–1717, 2019. Disponível em: <<https://doi.org/10.1056/NEJMoa1907863>>.

BROWN, S. A. et al. Six-month randomized, multicenter trial of closed-loop control in type 1 diabetes. *New England Journal of Medicine*, v. 381, n. 18, p. 1707–1717, 2019. <<https://doi.org/10.1056/NEJMoa1907863>> [Accessed: 2020-09-25].

BROWNLEE, M. et al. Complications of diabetes mellitus. p. 1417–1501, 01 2011.

BUNESCU, R. et al. Blood glucose level prediction using physiological models and support vector regression. In: IEEE. *2013 12th International Conference on Machine Learning and Applications*. [S.l.], 2013. v. 1, p. 135–140.

BUTCHER, J. C. *Numerical Methods for Ordinary Differential Equations*. 3. ed. [S.l.]: Wiley, 2016. ISBN 1119121507,9781119121503,9781119121510.

CAMPBELL, S. A.; NCUBE, I. Stability in a scalar differential equation with multiple, distributed time delays. *Journal of Mathematical Analysis and Applications*, Elsevier, v. 450, p. 1104–1122, 2017. ISSN 0022-247X. <<https://www.sciencedirect.com/science/article/pii/S0022247X17300938>> [Accessed: 2019-03-08].

CAO, J. Michaelis-menten equation and detailed balance in enzymatic networks. *J Phys Chem B.*, p. 5493–8, 05 2011.

CARTA, S. M. et al. Explainable machine learning exploiting news and domain-specific lexicon for stock market forecasting. *IEEE Access*, v. 9, p. 30193–30205, 2021.

CBMS. 2018. Available in: <<https://site.ieee.org/sweden/event/31st-ieee-cbms-international-symposium-on-computer-based-medical-systems/>>.

CESCON, M.; JOHANSSON, R.; RENARD, E. Subspace-based linear multi-step predictors in type 1 diabetes mellitus. *Biomedical Signal Processing and Control*, Elsevier, v. 22, p. 99–110, 2015.

CHAKI, J. et al. Machine learning and artificial intelligence based diabetes mellitus detection and self-management: A systematic review. *Journal of King Saud University - Computer and Information Sciences*, p. 511, 07 2020. Disponível em: <<https://www.sciencedirect.com/science/article/pii/S1319157820304134>>.

CILFONE, N.; KIRSCHNER, D.; LINDERMAN, J. Strategies for efficient numerical implementation of hybrid multi-scale agent-based models to describe biological systems. *Cellular and Molecular Bioengineering*, v. 8, p. 119–136, 03 2014.

CLARKE, W. L. et al. Evaluating clinical accuracy of systems for self-monitoring of blood glucose. *Diabetes care*, Am Diabetes Assoc, v. 10, n. 5, p. 622–628, 1987.

CNOGA. 2020. Available in: <<https://cnoga.com.br/produtos/combo-glucometer-tensortip-cog/#1575260758002-27498f7c-2204>> [Accessed: 2020-07-20].

COBELLI, C.; RENARD, E.; KOVATCHEV, B. . Artificial pancreas: past, present, future. *American Diabetes Association*, v. 60(11), p. 2672–2682, 2011. Available in: <<https://www.ncbi.nlm.nih.gov/pmc/articles/PMC3198099/>>.

CONTRERAS, I. et al. Using grammatical evolution to generate short-term blood glucose prediction models. In: *KHD@IJCAI*. [S.l.: s.n.], 2018. p. 91–96.

CONTRERAS, S. et al. A novel synthetic model of the glucose-insulin system for patient-wise inference of physiological parameters from small-size ogtt data. *Frontiers in Bioengineering and Biotechnology*, v. 8, 2020. ISSN 2296-4185. Available in: <<https://www.frontiersin.org/article/10.3389/fbioe.2020.00195>>.

CONTROL-IQ. 2020. Available in: <<https://www.tandemdiabetes.com/providers/products/control-iq>> [Accessed: 2021-12-02].

CONTROL-IQ. 2022. Available in: <<https://cnoga.com.br/produtos/combo-glucometer-tensortip-cog/#1575260758002-27498f7c-2204>> [Accessed: 2022-08-18].

DANEMAN, D. Type 1 diabetes. *The Lancet*, v. 367, n. 9513, p. 847–858, 2006. ISSN 0140-6736. Available in: <<http://www.sciencedirect.com/science/article/pii/S0140673606683414>> [Accessed: 2019-02-27].

DAVIES, K. J. A. Adaptive homeostasis. *Molecular aspects of medicine*, v. 49, p. 1–7, 06 2016. Available in: <<https://www.ncbi.nlm.nih.gov/pmc/articles/PMC4868097/>>.

DDE23. 2019. Available in: <<https://www.radford.edu/~thompson/webddes/tutorial.pdf>> [Accessed: 2019-01-28].

DEXCOM-G6. 2020. Available in: <<https://www.dexcom.com/pt-PT>> [Accessed: 2020-08-25].

DU, S. et al. Clinical diagnosis for dusk phenomenon of diabetes. *Medicine*, v. 97, 2018.

DUUN-HENRIKSEN, A. K. et al. Model identification using stochastic differential equation grey-box models in diabetes. *Journal of diabetes science and technology*, SAGE Publications, v. 7, n. 2, p. 431–440, 2013.

EAAI. 2022. Available in: <<https://www.journals.elsevier.com/engineering-applications-of-artificial-intelligence>>.

ELEMENTO, O. The future of precision medicine: towards a more predictive personalized medicine. *Emerging Topics in Life Sciences*, v. 4, n. 2, p. 175–177, 08 2020. ISSN 2397-8554. Disponible em: <<https://doi.org/10.1042/ETLS20190197>>.

EPSHTEYN, A.; VOGEL, A.; DEJONG, G. Active reinforcement learning. In: *Proceedings of the 25th international conference on Machine learning*. [S.l.: s.n.], 2008. p. 296–303.

EPSTEIN, E. J. et al. Use of the estimated glucose disposal rate as a measure of insulin resistance in an urban multiethnic population with type 1 diabetes. *Diabetes Care*, American Diabetes Association, v. 36, n. 8, p. 2280–2285, 2013. ISSN 0149-5992. Available in: <<https://care.diabetesjournals.org/content/36/8/2280>>.

EULER, L. *Fundamentals of Differential Equations*. I. [S.l.]: Springer, 1988. ISBN 978-1-4612-1021-4.

FANG, S. et al. An end-to-end image-based automatic food energy estimation technique based on learned energy distribution images: Protocol and methodology. *Nutrients*, Multidisciplinary Digital Publishing Institute, v. 11, n. 4, p. 877, 2019.

FDA. 2016. Available in: <<http://wayback.archive-it.org/7993/20170111141252/http://www.fda.gov/MedicalDevices/ProductsandMedicalProcedures/DeviceApprovalsandClearances/Recently-ApprovedDevices/ucm522764.html>> [Accessed: 2017-12-12].

FDA. 2019. Available in: <<https://www.fda.gov/news-events/press-announcements>> [Accessed: 2022-08-01].

FDA. 2020. Available in: <https://www.accessdata.fda.gov/drugsatfda_docs/label/2012/020986s057lbl.pdf> [Accessed: 2020-04-05].

FDA. 2021. Available in: <https://www.accessdata.fda.gov/cdrh_docs/pdf17/DEN170088.pdf> [Accessed: 2021-09-10].

FDA-ASPART. 2022. Available in: <https://www.accessdata.fda.gov/drugsatfda_docs/label/2012/020986s057lbl.pdf> [Accessed: 2021-09-10].

FDA-CONTROLIQ. 2019. Available in: <<https://www.fda.gov/news-events/press-announcements>> [Accessed: 2019-10-20].

FDA-DEGLUDEC. 2022. Available in: <https://www.accessdata.fda.gov/drugsatfda_docs/label/2015/203314lbl.pdf> [Accessed: 2021-09-10].

- FDA-GLARGINE. 2022. Available in: <https://www.accessdata.fda.gov/drugsatfda_docs/label/2007/021081s024lbl.pdf> [Accessed: 2021-09-10].
- FDA-LISPRO. 2022. Available in: <https://www.accessdata.fda.gov/drugsatfda_docs/label/2003/20563scm044_humalog_lbl.pdf> [Accessed: 2018-05-28].
- FDA-PA. 2020. Available in: <<https://www.fda.gov/medical-devices/artificial-pancreas-device-system/what-pancreas-what-artificial-pancreas-device-system>> [Accessed: 2020-08-29].
- FIASP. 2020. Available in: <https://www.novonordisk.com.br/content/dam/brazil/affiliate/www-novonordisk-br/Bulas/2019-12-19/Bula\%20paciente_Fiasp_Vial.pdf> [Accessed: 2020-07-18].
- FOSS-FREITAS, M. C. et al. *930-P: Blood Glucose Levels Prediction Accuracy for T1DM Patients Using Neural Networks to Combine Insulin Doses, Food Nutrients, and Heart Rate. Diabetes*, v. 68, 2019. ISSN 0012-1797.
- FOSS-FREITAS, M. C. et al. *Accuracy Analysis of an Autonomous System to Personalize Blood Glucose Prediction for T1DM Patients with Real World Data*. In: . [S.l.: s.n.], 2020.
- FREESTYLE. 2020. Available in: <<https://www.freestylelibre.com.br/>> [Accessed: 2020-08-18].
- FREESTYLE-LIBRE. 2020. Available in: <<https://provider.myfreestyle.com/accuracy.html>> [Accessed: 2020-09-10].
- FRIEDMAN, J. H. Greedy function approximation: A gradient boosting machine. *Annals of Statistics*, v. 29, p. 1189–1232, 2001.
- FURUTANI, E. Closed-loop blood glucose control for type 1 diabetes. *Electronics and Communications in Japan*, v. 102, n. 7, p. 22–26, 2019. Available in: <<https://onlinelibrary.wiley.com/doi/abs/10.1002/ecj.12179>> [Accessed: 2018-11-11].
- GARDNER, D.; SHOBACK, D. *Greenspan's Basic Clinical Endocrinology*. 10. ed. [S.l.]: Mc Graw Hill, 2018. ISBN 978-1-25-958929-4.
- GEORGA, E. I. et al. Multivariate prediction of subcutaneous glucose concentration in type 1 diabetes patients based on support vector regression. *IEEE journal of biomedical and health informatics*, IEEE, v. 17, n. 1, p. 71–81, 2013.
- GINSBERG, B. H. Factors affecting blood glucose monitoring: sources of errors in measurement. *Journal of diabetes science and technology*, SAGE Publications, v. 3, n. 4, p. 903–913, 2009.
- GLIC. 2022. Available in: <<http://gliconline.net/quem-somos/>> [Accessed: 2022-01-17].
- GLUCOMETER. 2020. Available in: <<https://www.diabetes.org.br/publico/colunas/32-dr-carlos-negrato>> [Accessed: 2021-12-03].

- GROSSI, S. A. A. et al. Home blood glucose monitoring in type 1 diabetes mellitus. *Revista Latino-Americana de Enfermagem*, scielo, v. 17, p. 194 – 200, 04 2009. ISSN 0104-1169. Available in: <http://www.scielo.br/scielo.php?script=sci_arttext&pid=S0104-11692009000200009&nrm=iso> [Accessed: 2019-10-25].
- GUPTA, L.; LAL, P. R.; KHANDELWAL, D. Optimizing macronutrients in people with diabetes. *Journal of Social Health and Diabetes* 2018, v. 06(02), p. 65–1, 2018. Available in: <<https://www.thieme-connect.com/products/ejournals/html/10.1055/s-0038-1675684#N67502>> [Accessed: 2018-09-07].
- GYLFE, E.; GILON, P. Glucose regulation of glucagon secretion. *Diabetes Research and Clinical Practice*, v. 103, p. 1–10, 01 2014.
- HAJIZADEH, I. et al. Incorporating unannounced meals and exercise in adaptive learning of personalized models for multivariable artificial pancreas systems. *Journal of diabetes science and technology*, SAGE Publications Sage CA: Los Angeles, CA, v. 12, n. 5, p. 953–966, 2018.
- HASAN, M. K. et al. Diabetes prediction using ensembling of different machine learning classifiers. *IEEE Access*, v. 8, p. 76516–76531, 2020.
- HEISE, T. et al. Faster-acting insulin aspart: earlier onset of appearance and greater early pharmacokinetic and pharmacodynamic effects than insulin aspart. *Diabetes, Obesity and Metabolism*, Wiley Online Library, v. 17, n. 7, p. 682–688, 2015.
- HEISE, T. et al. Faster-acting insulin aspart: earlier onset of appearance and greater early pharmacokinetic and pharmacodynamic effects than insulin aspart. *Diabetes, Obesity and Metabolism*, Wiley Online Library, v. 17, n. 7, p. 682–688, 2015.
- HEISE, T. et al. Pharmacokinetic and pharmacodynamic properties of faster-acting insulin aspart versus insulin aspart across a clinically relevant dose range in subjects with type 1 diabetes mellitus. *Clinical pharmacokinetics*, Springer, v. 56, n. 6, p. 649–660, 2017.
- HMP. 2023. Available in: <<https://hmp.health/en/>> [Accessed: 2023-01-22].
- HOBBS, N. et al. Improving glucose prediction accuracy in physically active adolescents with type 1 diabetes. *Journal of Diabetes Science and Technology*, v. 13, n. 4, p. 718–727, 2019. Available in: <<https://doi.org/10.1177/1932296818820550>> [Accessed: 2022-03-04].
- HOVORKA, R. et al. Nonlinear model predictive control of glucose concentration in subjects with type 1 diabetes. *Physiological measurement*, IOP Publishing, v. 25, n. 4, p. 905, 2004.
- IDF. 2022. Available in: <<https://www.diabetesatlas.org/en/>> [Accessed: 2022-03-02].
- IDF-ATLAS. 2021. Available in: <https://diabetesatlas.org/idfawp/resource-files/2021/07/IDF_Atlas_10th_Edition_2021.pdf> [Accessed: 2023-01-10].
- IG-CG. 2016. Available in: <<https://www.diabetes.org.br/publico/colunistas/96-dra-gisele-rossi-goveia/1267-indice-glicemico-ig-e-carga-glicemica-cg>> [Accessed: 2019-05-28].

- INPI. 2022. Available in: <<http://revistas.inpi.gov.br/rpi/>>.
- INTELLISYS. 2019. Available in: <<https://saiconference.com/Conferences/IntelliSys2019>>.
- ISFAHANI, M. K. et al. A hybrid dynamic wavelet-based modeling method for blood glucose concentration prediction in type 1 diabetes. *Journal of Medical Signals and Sensors*, v. 10, n. 3, p. 174–184, 2020.
- ISTEPANIAN, R. S. H.; AL-ANZI, T. M. m-health interventions for diabetes remote monitoring and self management: clinical and compliance issues. *mHealth*, v. 4.4, 02 2018. Available in: <<https://www.ncbi.nlm.nih.gov/pmc/articles/PMC5847844/>> [Accessed: 2019-12-12].
- JAVAD, M. O. M. et al. A reinforcement learning-based method for management of type 1 diabetes: Exploratory study. *JMIR diabetes*, JMIR Publications Inc., Toronto, Canada, v. 4, n. 3, p. e12905, 2019.
- JENDRIKE, N. et al. Iso 15197: 2013 evaluation of a blood glucose monitoring system's measurement accuracy. *J Diabetes Sci Technol.*, v. 11, n. 6, p. 1275–1276, 2017.
- KAKU, K. et al. Pharmacokinetics and pharmacodynamics of insulin aspart, a rapid-acting analog of human insulin, in healthy japanese volunteers. *Diabetes research and clinical practice*, Elsevier, v. 49, n. 2-3, p. 119–126, 2000.
- KARAMANOU, M. et al. Milestones in the history of diabetes mellitus: The main contributors. *World Journal of Diabetes*, p. 1–7, 01 2016.
- KARINKA, S. A. et al. *910-P: Improved Accuracy of 14-Day Factory-Calibrated FreeStyle Libre System with New Glucose Algorithm*. [S.l.]: Am Diabetes Assoc, 2019.
- KATSAROU, A. et al. Type 1 diabetes mellitus. *Nature Rev Dis Primers*, v. 3, 03 2017. Available in: <<https://www.nature.com/articles/nrdp201716>> [Accessed: 2018-12-05].
- KATZ, L. et al. Meeting the new fda standard for accuracy of self-monitoring blood glucose test systems intended for home use by lay users. *J Diabetes Sci Technol.*, v. 14, n. 5, p. 912–916, 2020.
- KATZ, L. B. e. a. Meeting the new fda standard for accuracy of self-monitoring blood glucose test systems intended for home use by lay users. *Journal of diabetes science and technology*, v. 14, n. 5, p. 912–916, 2020.
- KAWAMORI, D.; KULKARNI, R. N. Insulin modulation of glucagon secretion: The role of insulin and other factors in the regulation of glucagon secretions. *Islets*, v. 1:3, p. 276–279, 08 2009. Available in: <<https://doi.org/10.4161/isl.1.3.9967>> [Accessed: 2019-09-13].
- KEEN, H.; BARNES, D. The diagnosis and classification of diabetes mellitus and impaired glucose tolerance. *Textbook of diabetes*. UK: Blackwell science, p. 2–1, 1997.
- KEUM, D. H. et al. Wireless smart contact lens for diabetic diagnosis and therapy. *Science Advances*, American Association for the Advancement of Science, v. 6, n. 17, 2020. Available in: <<https://advances.sciencemag.org/content/6/17/eaba3252>> [Accessed: 2021-08-14].

- KHOLGHI, M. et al. Active learning: a step towards automating medical concept extraction. *Journal of the American Medical Informatics Association*, v. 23, n. 2, p. 289–296, 08 2015. ISSN 1067-5027. Available in: <<https://doi.org/10.1093/jamia/ocv069>> [Accessed: 2018-11-15].
- KISSLER, S. et al. Determination of personalized diabetes treatment plans using a two-delay model. *Journal of Theoretical Biology*, v. 359, p. 101–111, 10 2014.
- LAYMAN, E. Research and policy model for health informatics and information management. *Perspectives in health information management*, v. 6, 2009.
- LEHMANN, E.; DEUTSCH, T. A physiological model of glucose-insulin interaction in type 1 diabetes mellitus. *Journal of biomedical engineering*, Elsevier, v. 14, n. 3, p. 235–242, 1992.
- LGPD. 2023. Disponível em: <<https://www.gov.br/cidadania/pt-br/aceso-a-informacao/lgpd>>.
- LI, J.; KUANG, Y.; MASON, C. Modeling the glucose–insulin regulatory system and ultradian insulin secretory oscillations with two explicit time delays. *Journal of Theoretical Biology*, v. 242, p. 722–735, 10 2006.
- LIM, M. H. et al. A blood glucose control framework based on reinforcement learning with safety and interpretability: In silico validation. *IEEE Access*, v. 9, p. 105756–105775, 2021.
- LINDHOLM, A.; JACOBSEN, L. V. Clinical pharmacokinetics and pharmacodynamics of insulin aspart. *Clinical pharmacokinetics*, Springer, v. 40, n. 9, p. 641–659, 2001.
- LINNEBJERG, H. et al. Comparison of the pharmacokinetics and pharmacodynamics of ly2963016 insulin glargine and eu-and us-approved versions of lantus insulin glargine in healthy subjects: three randomized euglycemic clamp studies. *Diabetes Care*, Am Diabetes Assoc, v. 38, n. 12, p. 2226–2233, 2015.
- LIU, C. et al. Long-term glucose forecasting using a physiological model and deconvolution of the continuous glucose monitoring signal. *Sensors*, Multidisciplinary Digital Publishing Institute, v. 19, n. 19, p. 4338, 2019.
- LIU, C. et al. Enhancing blood glucose prediction with meal absorption and physical exercise information. *arXiv preprint arXiv:1901.07467*, 2018.
- LIU, C. et al. *Long-Term Glucose Forecasting Using a Physiological Model and Deconvolution of the Continuous Glucose Monitoring Signal*. *Sensors (Basel)*, v. 19, n. 19, p. 4338, 2019. Available in: <<https://doi.10.3390/s19194338>> [Accessed: 2021-07-29].
- MAKROGLOU, A.; LI, J.; KUANG, Y. Mathematical models and software tools for the glucose-insulin regulatory system and diabetes: An overview. *Applied Numerical Mathematics*, v. 56, p. 559–573, 03 2006.
- MAN, C. D. et al. Minimal model estimation of glucose absorption and insulin sensitivity from oral test: validation with a tracer method. *American Journal of Physiology-Endocrinology and Metabolism*, American Physiological Society, v. 287, n. 4, p. E637–E643, 2004.

MANUAL-CC. 2020. Available in: <<https://www.diabetes.org.br/publico/images/manual-de-contagem-de-carboidrato2016.pdf>> [Accessed: 2020-08-21].

MANUAL1-CC. 2020. Available in: <<https://cdbh.com.br/wp-content/uploads/2019/05/Manual-de-contagem-de-carboidrato-CDBH.pdf>> [Accessed: 2020-08-21].

MEHMOOD, S. et al. Artificial pancreas control strategies used for type 1 diabetes control and treatment: A comprehensive analysis. *Applied System Innovation*, MDPI AG, v. 3, n. 3, p. 31, Jul 2020. ISSN 2571-5577. Available in: <<http://dx.doi.org/10.3390/asi3030031>> [Accessed: 2021-11-01].

MINIMED-640G. 2020. Available in: <<https://www.medtronicdiabeteslatino.com/br/wp-content/uploads/2018/12/Sistema-Minimed-640G.pdf>> [Accessed: 2020-12-03].

MINIMED-670G. 2020. Available in: <<https://www.medtronicdiabetes.com/products/minimed-670g-insulin-pump-system>> [Accessed: 2022-03-28].

MINIMED-754. 2020. Available in: <<https://www.medtronicdiabeteslatino.com/br/wp-content/uploads/2018/12/Veo-754.pdf>> [Accessed: 2020-07-14].

MIRSHEKARIAN, S. et al. Using lstms to learn physiological models of blood glucose behavior. In: IEEE. *2017 39th Annual International Conference of the IEEE Engineering in Medicine and Biology Society (EMBC)*. [S.l.], 2017. p. 2887–2891.

MONGODB. 2022. Available in: <<https://aws.amazon.com/quickstart/architecture/mongodb/>> [Accessed: 2022-08-25].

MONTANARI, V. A. *Comparação entre três calculadoras de bolus de insulina para aumento do tempo no alvo glicêmico, em adultos com diabetes mellitus tipo 1, com controle glicêmico insatisfatório em um país em desenvolvimento*. Escola Paulista de Medicina, Universidade Federal de São Paulo, 2022. Disponível em: <<https://repositorio.unifesp.br/xmlui/handle/11600/63988>>.

MONTASER, E.; DíEZ, J.; BONDIA, J. Stochastic seasonal models for glucose prediction in the artificial pancreas. *J Diabetes Sci Technol*, v. 11(6), p. 1124–1131, 10 2017.

MOSER, O.; YARDLEY, J. E.; BRACKEN, R. M. Interstitial glucose and physical exercise in type 1 diabetes: Integrative physiology, technology, and the gap in-between. *Nutrients*, v. 10(1), January 2018. Available in: <<https://www.ncbi.nlm.nih.gov/pmc/articles/PMC5793321/>> [Accessed: 2019-06-30].

MUNOZ-ORGANERO, M. Deep physiological model for blood glucose prediction in t1dm patients. *Sensors*, p. 3896, 07 2020.

NAGLE, R. K. N.; SAFF, E. B. S.; SNIDER, A. D. *Introduction to Analysis of the Infinite*. 9. ed. [S.l.]: Pearson, 2017. ISBN 0321977068,9780321977069.

NATH, A. et al. Physiological models and control for type 1 diabetes mellitus: A brief review. *IFAC-PapersOnLine*, v. 51, n. 1, p. 289–294, 2018. ISSN 2405-8963. Available in: <<https://www.sciencedirect.com/science/article/pii/S2405896318302416>> [Accessed: 2019-01-06].

NELSON, R. K. et al. Daily physical activity predicts degree of insulin resistance: a cross-sectional observational study using the 2003–2004 national health and nutrition examination survey. *International Journal of Behavioral Nutrition and Physical Activity*, BMC, v. 10(1), 01 2013. ISSN 0104-1169. Available in: <<https://ijbnpa.biomedcentral.com/articles/10.1186/1479-5868-10-10>> [Accessed: 2018-12-12].

NIGHTSCOUT. 2020. Available in: <<https://github.com/nightscout/cgm-remote-monitor>> [Accessed: 2020-12-04].

NOLAN, J. J. et al. ADA/EASD Precision Medicine in Diabetes Initiative: An International Perspective and Future Vision for Precision Medicine in Diabetes. *Diabetes Care*, v. 45, n. 2, p. 261–266, 01 2022. ISSN 0149-5992. Disponível em: <<https://doi.org/10.2337/dc21-2216>>.

OHIO-UNIV-T1D. 2020. Available in: <<http://smarthealth.cs.ohio.edu/OhioT1DM-dataset.html>> [Accessed: 2020-06-28].

OMANA, J.; MOORTHI, M. Predictive analysis and prognostic approach of diabetes prediction with machine learning techniques. *Wireless Personal Communications*, v. 127, p. 465–478, 11 2022.

ONU-SGD. 2022. Available in: <<https://sdgs.un.org/goals>> [Accessed: 2022-10-05].

OPENAPS. 2021. Available in: <<https://openaps.org/>> [Accessed: 2021-02-26].

ØSTERBERG, O. et al. Pharmacokinetic and pharmacodynamic properties of insulin aspart and human insulin. *Journal of pharmacokinetics and pharmacodynamics*, Springer, v. 30, n. 3, p. 221–235, 2003.

OVIEDO, S. et al. A review of personalized blood glucose prediction strategies for t1dm patients. *International journal for numerical methods in biomedical engineering*, Wiley Online Library, v. 33, n. 6, p. e2833, 2017.

OWENS, D. R. et al. Clinical relevance of pharmacokinetic and pharmacodynamic profiles of insulin degludec (100, 200 u/ml) and insulin glargine (100, 300 u/ml)—a review of evidence and clinical interpretation. *Diabetes & Metabolism*, Elsevier, v. 45, n. 4, p. 330–340, 2019.

PANKOWSKA, E.; BLAZIK, M.; GROELE, L. Does the fat-protein meal increase postprandial glucose level in type 1 diabetes patients on insulin pump: the conclusion of a randomized study. *Diabetes Technol Ther.*, v. 14.1, p. 16–22, 2011. Disponível em: <<https://pubmed.ncbi.nlm.nih.gov/22013887>>.

PANUNZI, S. et al. A revised sorenson model: Simulating glycemic and insulinemic response to oral and intra-venous glucose load. *PLOS ONE*, v. 15, p. e0237215, 08 2020.

PARADIGM-715. 2020. Available in: <<https://www.medtronicdiabeteslatino.com/br/wp-content/uploads/2018/12/Paradigm-715.pdf>> [Accessed: 2021-06-27].

PARKES, J. L. et al. A new consensus error grid to evaluate the clinical significance of inaccuracies in the measurement of blood glucose. *Diabetes Care*, American Diabetes Association, v. 23, n. 8, p. 1143–1148, 2000.

- PEFFERS, K. et al. A design science research methodology for information systems research. *Journal of Management Information Systems*, Routledge, v. 24, n. 3, p. 45–77, 2007. Available in: <<https://doi.org/10.2753/MIS0742-1222240302>> [Accessed: 2020-01-26].
- PEREIRA, J. P. A. et al. A hybrid model to predict glucose oscillation for patients with type 1 diabetes and suggest customized recommendations. In: *Intelligent Systems and Applications*. Cham: Springer International Publishing, 2019. v. 38, p. 790–801. ISBN 978-3-030-29513-4.
- PEREIRA, J. P. A. et al. A multi-agent approach used to predict long-term glucose oscillation in individuals with type 1 diabetes. *Applied Sciences*, v. 12, n. 19, 2022. ISSN 2076-3417. Available in: <<https://www.mdpi.com/2076-3417/12/19/9641>>.
- PETERS, A. L.; DAVIDSON, M. B. Protein and fat effects on glucose responses and insulin requirements in subjects with insulin-dependent diabetes mellitus. *Am J Clin Nutr*, v. 58, p. 555–560, 10 1993. Disponível em: <<https://pubmed.ncbi.nlm.nih.gov/8379513/>>.
- PFÜTZNER, A. et al. Technical aspects of the parkes error grid. *Journal of Diabetes Science and Technology*, SAGE Publications Sage CA: Los Angeles, CA, v. 7, n. 5, p. 1275–1281, 2013.
- PLANK, J. et al. A direct comparison of insulin aspart and insulin lispro in patients with type 1 diabetes. *Diabetes care*, Am Diabetes Assoc, v. 25, n. 11, p. 2053–2057, 2002.
- PORCELLATI, F. et al. Pharmacokinetics and pharmacodynamics of the long-acting insulin analog glargine after 1 week of use compared with its first administration in subjects with type 1 diabetes. *Diabetes care*, Am Diabetes Assoc, v. 30, n. 5, p. 1261–1263, 2007.
- PØRKSEN, N. et al. Pulsatile insulin secretion: Detection, regulation, and role in diabetes. *Diabetes*, American Diabetes Association, v. 51, n. suppl 1, p. S245–S254, 2002. ISSN 0012-1797. Available in: <https://diabetes.diabetesjournals.org/content/51/suppl_1/S245> [Accessed: 2018-11-30].
- PRIYA, G.; KALRA, S. A review of insulin resistance in type 1 diabetes: is there a place for adjunctive metformin? *Diabetes Therapy*, Springer, v. 9, n. 1, p. 349–361, 2018.
- Q-LEARNING. 2019. Available in: <<https://github.com/ankonzoid/LearningX>> [Accessed: 2019-01-14].
- RABASA-LHORET, R. et al. Guidelines for premeal insulin dose reduction for postprandial exercise of different intensities and durations in type 1 diabetic subjects treated intensively with a basal-bolus insulin regimen (ultralente-lispro). *Diabetes Care*, American Diabetes Association, v. 24, n. 4, p. 625–630, 2001. ISSN 0149-5992. Available in: <<https://care.diabetesjournals.org/content/24/4/625>> [Accessed: 2019-09-27].
- RAMÍREZ, F. A. A.; PÉREZ-AGUILA, R. A method for obtaining the tesseract by unraveling the 4d hypercube. In: *WSCG*. [S.l.: s.n.], 2002.

ROACH, P.; WOODWORTH, J. R. Clinical pharmacokinetics and pharmacodynamics of insulin lispro mixtures. *Clinical pharmacokinetics*, Springer, v. 41, n. 13, p. 1043–1057, 2002.

RODRÍGUEZ, I. R. Gestión de la diabetes mellitus tipo 1 con dispositivos internet de las cosas y técnicas de aprendizaje automático. *Proyecto de investigación*, 02 2020. Available in: <<http://hdl.handle.net/10201/87361>> [Accessed: 2021-12-18].

RODRÍGUEZ-RODRÍGUEZ, I. et al. Feature selection for blood glucose level prediction in type 1 diabetes mellitus by using the sequential input selection algorithm (sisal). *Symmetry*, v. 11, p. 1164, 09 2019.

RODRÍGUEZ-RODRÍGUEZ, I.; ZAMORA-IZQUIERDO, M.-; RODRÍGUEZ, J.-V. Towards an ict-based platform for type 1 diabetes mellitus management. *Applied Sciences*, MDPI AG, v. 8, n. 4, p. 511, Mar 2018. ISSN 2076-3417. Available in: <<http://dx.doi.org/10.3390/app8040511>> [Accessed: 2019-08-01].

ROEP, B. O. β -cells, autoimmunity, and the innate immune system: “un ménage á trois”? *Diabetes*, American Diabetes Association, v. 62, n. 6, p. 1821–1822, 2013. ISSN 0012-1797. Available in: <<https://diabetes.diabetesjournals.org/content/62/6/1821>> [Accessed: 2022-01-30].

RUSSELL, S. J.; NORVIG, P. *Artificial Intelligence: A Modern Approach*. 3. ed. [S.l.]: Pearson Education, 2016. ISBN 9781292153964.

SAITI, K. et al. Ensemble methods in combination with compartment models for blood glucose level prediction in type 1 diabetes mellitus. *Computer Methods and Programs in Biomedicine*, Elsevier, v. 196, p. 105628, 2020.

SANOFI. 2020. Available in: <<http://products.sanofi.ca/en/lantus.pdf>> [Accessed: 2020-05-24].

SBD. 2019. Available in: <<https://www.diabetes.org.br/profissionais/images/pdf/Nota-Tecnica-Dep.-Nutrio-SBD.pdf>> [Accessed: 2019-12-11].

SBD. 2020. Available in: <[\\$> \[Accessed: 2020-05-29\].](https://www.diabetes.org.br/publico/diabetes/tipos-de-diabetes?gclid=EAIaIQobChMI79OQ8Zv06gIVi4iRCh3vpgM5EAAAYASAAEgL9JPD_BwE\)

SBD. 2021. Available in: <https://www.diabetes.org.br/publico/images/Posicionamento_Oficial_Sbd_N012020v6_brLC.PDF?fbclid=IwAR0SsEnS6znmOt7bb5UvjSdSZkc9EFSVMPXUV8vRIjKFI5kkxi4cB-m3XcU> [Accessed: 2021-05-12].

SBD. 2022. Available in: <<https://diretriz.diabetes.org.br/>> [Accessed: 2022-05-05].

SBD. 2022. Available in: <<https://diretriz.diabetes.org.br/metas-no-tratamento-do-diabetes/>> [Accessed: 2023-05-01].

SBD. 2022. Available in: <<https://diabetes.org.br/atividade-fisica/>> [Accessed: 2022-05-16].

SCHINDELBOECK, D.; PRAUS, F.; GALL, W. A diabetes self-management prototype in an aal-environment to detect remarkable health states. v. 223, p. 273–280, 2016. Available in: <<https://pubmed.ncbi.nlm.nih.gov/27139414/>> [Accessed: 2019-12-14].

SEAQUIST, E. R. et al. Hypoglycemia and diabetes: a report of a workgroup of the american diabetes association and the endocrine society. *Diabetes Care*, American Diabetes Association, v. 36, n. 5, p. 1384–95, 2013.

SETTLES, B. *Active learning literature survey*. [S.l.], 2009.

SHI. 2020. Available in: <<https://www.sciencehistory.org/historical-profile/frederick-banting-charles-best-james-collip-and-john-macleod#:~:text=In%20the%20early%201920s%20Frederick,for%20their%20work%20in%201923.>> [Accessed: 2020-04-18].

SHLOMO, M. et al. *Williams Textbook of Endocrinology*. 14. ed. [S.l.]: Elsevier, 2019. ISBN 9780323555968.

SIDDIQUI, S. A. et al. Pain-free blood glucose monitoring using wearable sensors: Recent advancements and future prospects. *IEEE Reviews in Biomedical Engineering*, v. 11, p. 21–35, 2018.

SILVA, F. L. da. Methods and algorithms for knowledge reuse in multiagent reinforcement learning. In: . [S.l.: s.n.], 2020.

SLATTERY, D.; AMIEL, S.; CHOUDHARY, P. Optimal prandial timing of bolus insulin in diabetes management: a review. *Diabetic Medicine*, Wiley Online Library, v. 35, n. 3, p. 306–316, 2018.

SMART, C. E. et al. Both dietary protein and fat increase postprandial glucose excursions in children with type 1 diabetes, and the effect is additive. *Diabetes Care*, American Diabetes Association, v. 36, n. 12, p. 3897–3902, 2013. ISSN 0149-5992. Disponível em: <<https://care.diabetesjournals.org/content/36/12/3897>>.

SMITH, H. *An Introduction to Delay Differential Equations with Applications to the Life Sciences*. 1. ed. [S.l.]: Springer-Verlag New York, 2011. (Texts in Applied Mathematics 57). ISBN 1441976450,9781441976451,9781441976468.

SPADE. 2019. Available in: <<https://pypi.org/project/spade/>> [Accessed: 2019-11-01].

SPADE-BDI. 2021. Available in: <<https://spade-bdi.readthedocs.io/en/latest/>> [Accessed: 2021-04-28].

STURIS, J. et al. Computer model for mechanisms underlying ultradian oscillations of insulin and glucose. *Am. J. Physiol.*, v. 260, n. 5, p. 1–10, 05 1991. Available in: <<https://pubmed.ncbi.nlm.nih.gov/2035636/>> [Accessed: 2019-02-15].

TACK, C. J. et al. Glucose control, disease burden, and educational gaps in people with type 1 diabetes: Exploratory study of an integrated mobile diabetes app. *JMIR Diabetes*, v. 3, n. 4, 2018.

THORVE, S. et al. An active learning method for the comparison of agent-based models. In: *Proceedings of the 19th International Conference on Autonomous Agents and MultiAgent Systems*. [S.l.: s.n.], 2020. p. 1377–1385.

TOLIĆ, I. M.; MOSEKILDE, E.; STURIS, J. Modeling the insulin–glucose feedback system: the significance of pulsatile insulin secretion. *Journal of theoretical biology*, Elsevier, v. 207, n. 3, p. 361–375, 2000.

UNIV-VIRGINIA. 2020. Available in: <<https://med.virginia.edu/diabetes-technology/>> [Accessed: 2020-05-13].

VEHÍ, J. et al. Prediction and prevention of hypoglycaemic events in type-1 diabetic patients using machine learning. *Health Informatics Journal*, SAGE Publications Sage UK: London, England, v. 26, n. 1, p. 703–718, 2020.

VERSTRAETEN, T. et al. Multi-agent thompson sampling for bandit applications with sparse neighbourhood structures. In: NATURE. *Scientific Reports*. [S.l.], 2020. v. 10, p. 2045–2322.

VISENTIN, R. et al. The uva/padova type 1 diabetes simulator goes from single meal to single day. *Journal of diabetes science and technology*, SAGE Publications Sage CA: Los Angeles, CA, v. 12, n. 2, p. 273–281, 2018.

VOICE-AZURE. 2022. Available in: <<https://azure.microsoft.com/en-us/services/cognitive-services/speech-services/#overview>> [Accessed: 2022-06-14].

WADGHIRI, M. et al. Ensemble blood glucose prediction in diabetes mellitus: A review. *Computers in Biology and Medicine*, v. 147, p. 105674, 2022. ISSN 0010-4825. Available in: <<https://www.sciencedirect.com/science/article/pii/S0010482522004620>> [Accessed: 2022-07-22].

WANG, W. et al. A glucose-insulin mixture model and application to short-term hypoglycemia prediction in the night time. *IEEE Transactions on Biomedical Engineering*, IEEE, 2020.

WATKINS, C. J. C. H.; DAYAN, P. Q-learning. *Machine Learning*, v. 8, n. 5, p. 279–292, 1992. Disponível em: <<https://doi.org/10.1007/BF00992698>>.

WHO. 2022. Available in: <<https://www.who.int/news-room/photo-story/photo-story-detail/the-many-faces-of-diabetes>> [Accessed: 2022-02-02].

WOLDAREGAY, A. Z. et al. Data-driven modeling and prediction of blood glucose dynamics: Machine learning applications in type 1 diabetes. *Artificial intelligence in medicine*, Elsevier, v. 98, p. 109–134, 2019.

WOOLDRIDGE, M. *An Introduction to Multiagent Systems*. 2. ed. Chichester, UK: Wiley, 2009. ISBN 978-0-470-51946-2.

XGBOOST. 2019. Available in: <<https://xgboost.readthedocs.io/en/stable/>> [Accessed: 2019-01-05].

ZARKOGIANNI, K. et al. Personalized glucose-insulin metabolism model based on self-organizing maps for patients with type 1 diabetes mellitus. In: IEEE. *13th IEEE International Conference on BioInformatics and BioEngineering*. [S.l.], 2013. p. 1–4.

ZECCHIN, C. et al. Jump neural network for online short-time prediction of blood glucose from continuous monitoring sensors and meal information. *Computer methods and programs in biomedicine*, Elsevier, v. 113, n. 1, p. 144–152, 2014.

ZHU, F. et al. The use of mobile devices in aiding dietary assessment and evaluation. *IEEE J Sel Top Signal Proces*, v. 4(4), p. 756–766, 08 2010. Available in: <<https://pubmed.ncbi.nlm.nih.gov/20862266/>> [Accessed: 2020-11-30].

ZHU, T. et al. Blood glucose prediction in type 1 diabetes using deep learning on the edge. In: *2021 IEEE International Symposium on Circuits and Systems (ISCAS)*. [S.l.: s.n.], 2021. p. 1–5.

ZHU, T. et al. An insulin bolus advisor for type 1 diabetes using deep reinforcement learning. *Sensors*, Multidisciplinary Digital Publishing Institute, v. 20, n. 18, p. 5058, 2020.

APPENDIX A – ETHICS COMMITTEE







	USP - HOSPITAL UNIVERSITÁRIO DA UNIVERSIDADE DE SÃO PAULO - HU/USP	
PARECER CONSUBSTANCIADO DO CEP		
DADOS DO PROJETO DE PESQUISA		
Título da Pesquisa: Um modelo híbrido para prever a oscilação da glicose em pacientes com diabetes tipo 1 e sugerir recomendações personalizadas.		
Pesquisador: JOAO PAULO ARAGAO PEREIRA		
Área Temática:		
Versão: 1		
CAAE: 31140920.7.0000.0076		
Instituição Proponente: UNIVERSIDADE DE SAO PAULO		
Patrocinador Principal: Financiamento Próprio		
DADOS DO PARECER		
Número do Parecer: 4.037.757		

Figure 31: Embodied Opinion of the Ethics Committee.

LISTA DE APRECIÇÕES DO PROJETO							
Apreciação	Pesquisador Responsável	Versão	Submissão	Modificação	Situação	Exclusiva do Centro Coord.	Ações
PO	JOAO PAULO ARAGAO PEREIRA	1	13/03/2020	20/05/2020	Aprovado	Não	   

HISTÓRICO DE TRÂMITES							
Apreciação	Data/Hora	Tipo Trâmite	Versão	Perfil	Origem	Destino	Informações
PO	20/05/2020 10:36:18	Parecer liberado	1	Coordenador	USP - Hospital Universitário da Universidade de São Paulo - HU/USP	PESQUISADOR	
PO	20/05/2020 10:35:37	Parecer do colegiado emitido	1	Coordenador	USP - Hospital Universitário da Universidade de São Paulo - HU/USP	USP - Hospital Universitário da Universidade de São Paulo - HU/USP	
PO	20/05/2020 10:34:07	Parecer do relator emitido	1	Coordenador	USP - Hospital Universitário da Universidade de São Paulo - HU/USP	USP - Hospital Universitário da Universidade de São Paulo - HU/USP	
PO	20/05/2020 10:18:02	Aceitação de Elaboração de Relatoria	1	Coordenador	USP - Hospital Universitário da Universidade de São Paulo - HU/USP	USP - Hospital Universitário da Universidade de São Paulo - HU/USP	
PO	20/05/2020 10:13:21	Confirmação de Indicação de Relatoria	1	Coordenador	USP - Hospital Universitário da Universidade de São Paulo - HU/USP	USP - Hospital Universitário da Universidade de São Paulo - HU/USP	
PO	29/04/2020 11:51:29	Indicação de Relatoria	1	Secretária	USP - Hospital Universitário da Universidade de São Paulo - HU/USP	USP - Hospital Universitário da Universidade de São Paulo - HU/USP	
PO	29/04/2020 11:50:10	Aceitação do PP	1	Secretária	USP - Hospital Universitário da Universidade de São Paulo - HU/USP	USP - Hospital Universitário da Universidade de São Paulo - HU/USP	
PO	15/03/2020 20:55:19	Submetido pela CONEP para avaliação do CEP	1	Administrador	CONEP	USP - Hospital Universitário da Universidade de São Paulo - HU/USP	
PO	13/03/2020 00:04:58	Submetido para avaliação do CEP	1	Pesquisador Principal	PESQUISADOR	CONEP	


Figure 32: Proof of approval on 05/20/2020.

APPENDIX B – AUTHORIZATION FROM THE ETHICS COMMITTEE OF THE UNIVERSITY HOSPITAL OF USP

DETALHAR PROJETO DE PESQUISA

DADOS DA VERSÃO DO PROJETO DE PESQUISA

Título da Pesquisa: Um modelo híbrido para prever a oscilação da glicose em pacientes com diabetes tipo 1 e sugerir recomendações personalizadas.
 Pesquisador Responsável: JOAO PAULO ARAGAO PEREIRA
 Área Temática:
 Versão: 2
 CAAE: 31140920.7.0000.0076
 Submetido em: 01/09/2021
 Instituição Proponente: UNIVERSIDADE DE SAO PAULO
 Situação da Versão do Projeto: Aprovado
 Localização atual da Versão do Projeto: Pesquisador Responsável
 Patrocinador Principal: Financiamento Próprio

Comprovante de Recepção:  PB_COMPROVANTE_RECEPCAO_1819188

DOCUMENTOS DO PROJETO DE PESQUISA

Versão Atual Aprovada (E1) - Versão 2

- Emenda (E1) - Versão 2
 - Documentos do Projeto
 - Comprovante de Recepção - Submissão
 - Folha de Rosto - Submissão 1
 - Informações Básicas do Projeto - Subm
 - Outros - Submissão 1
 - Projeto Detalhado / Brochura Investiga
 - TCLE / Termos de Assentimento / Justif
 - Apreciação 1 - USP - Hospital Universitário
 - Projeto Completo

Tipo de Documento	Situação	Arquivo	Postagem	Ações

LISTA DE APRECIÇÕES DO PROJETO






Apreciação	Pesquisador Responsável	Versão	Submissão	Modificação	Situação	Exclusiva do Centro Coord.	Ações
E1	JOAO PAULO ARAGAO PEREIRA	2	01/09/2021	24/09/2021	Aprovado	Não	   
PO	JOAO PAULO ARAGAO PEREIRA	1	13/03/2020	20/05/2020	Aprovado	Não	

Figure 33: Proof of authorization for recommendation with one individual.

APPENDIX C – FLOWCHART OF ACTIONS

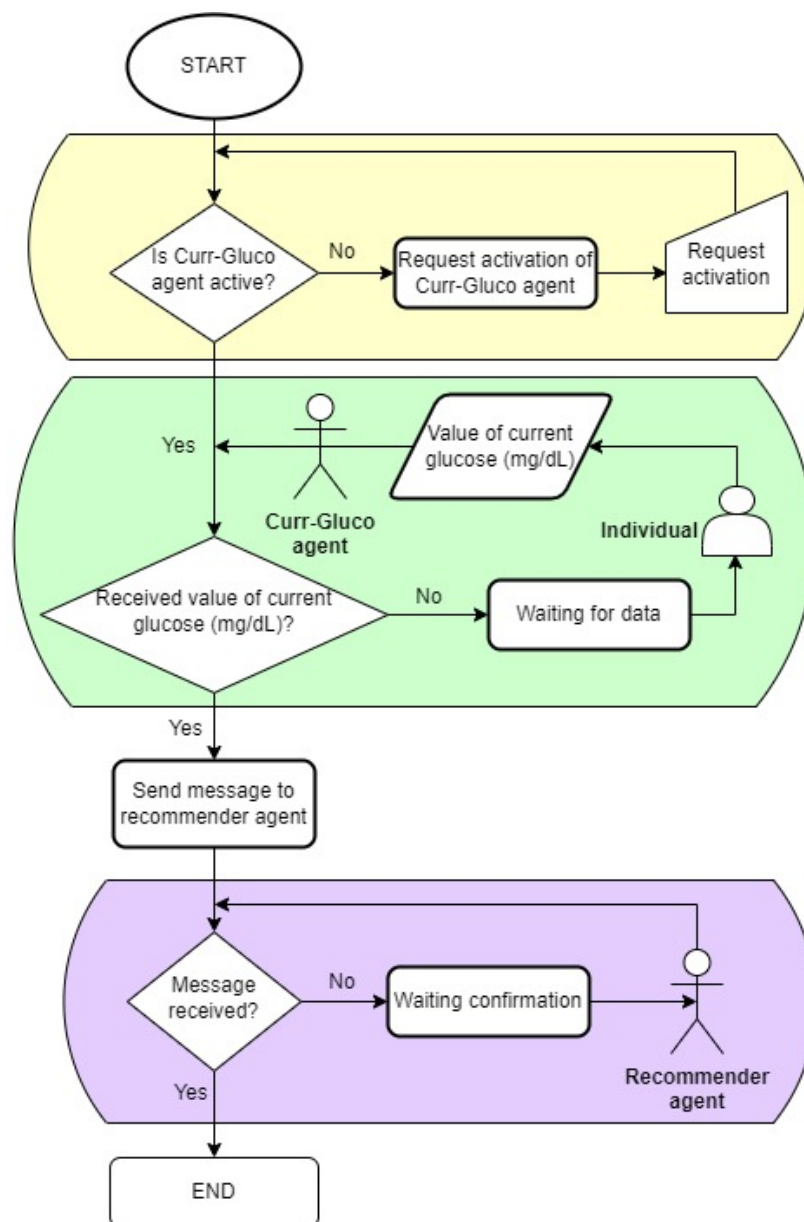


Figure 34: Curr-Gluco agent action flowchart.

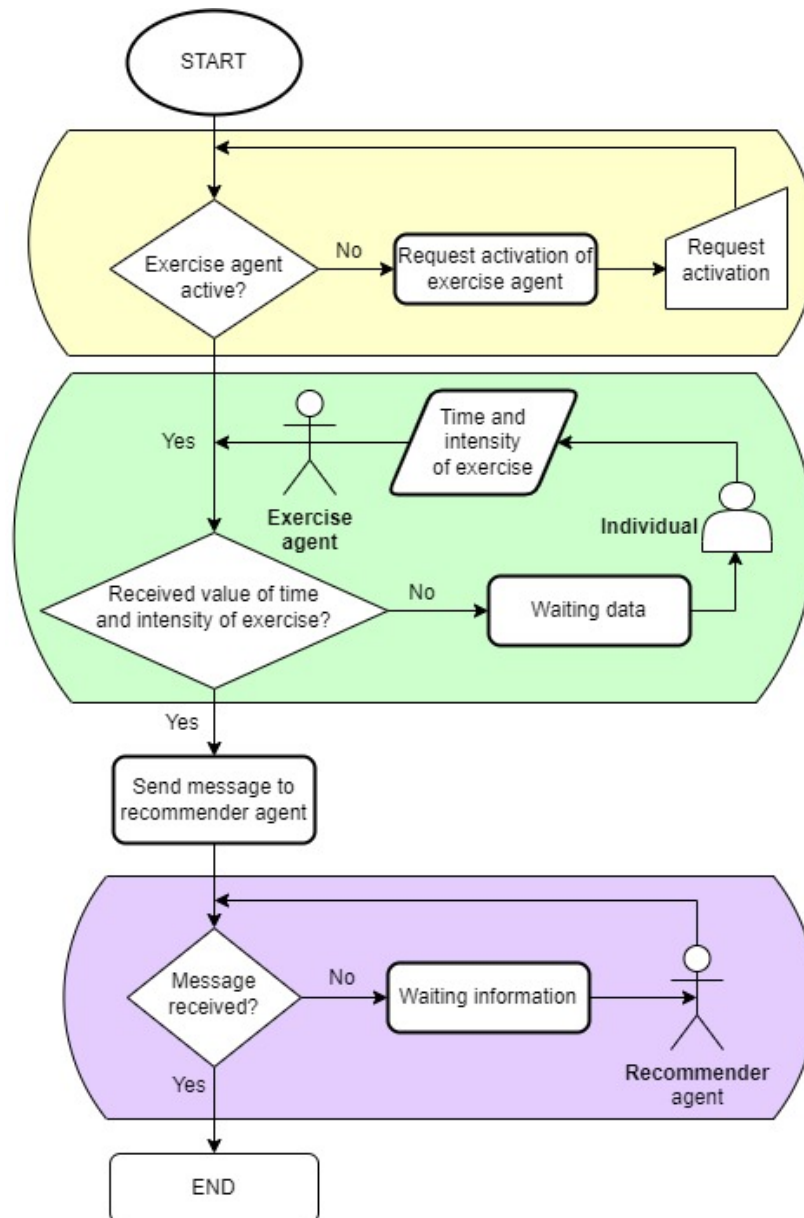


Figure 35: Exercise agent action flowchart.

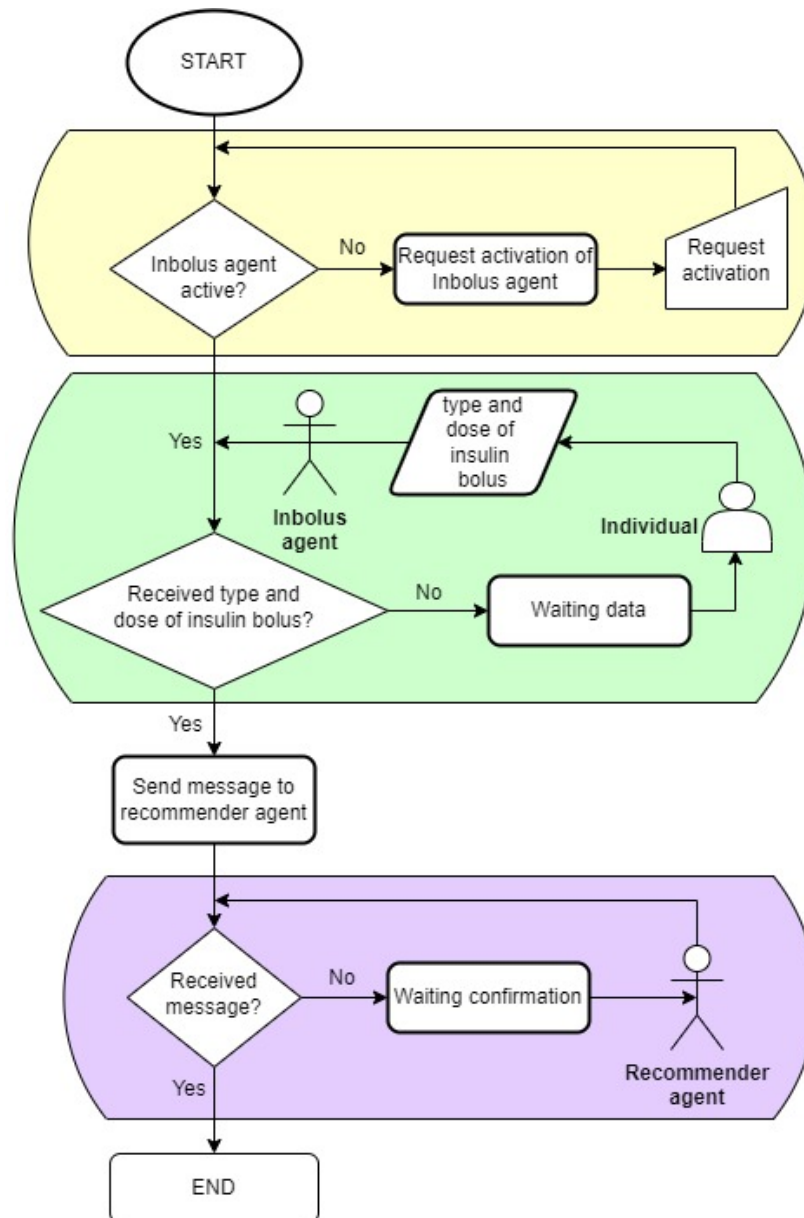


Figure 36: Inbolus agent action flowchart.

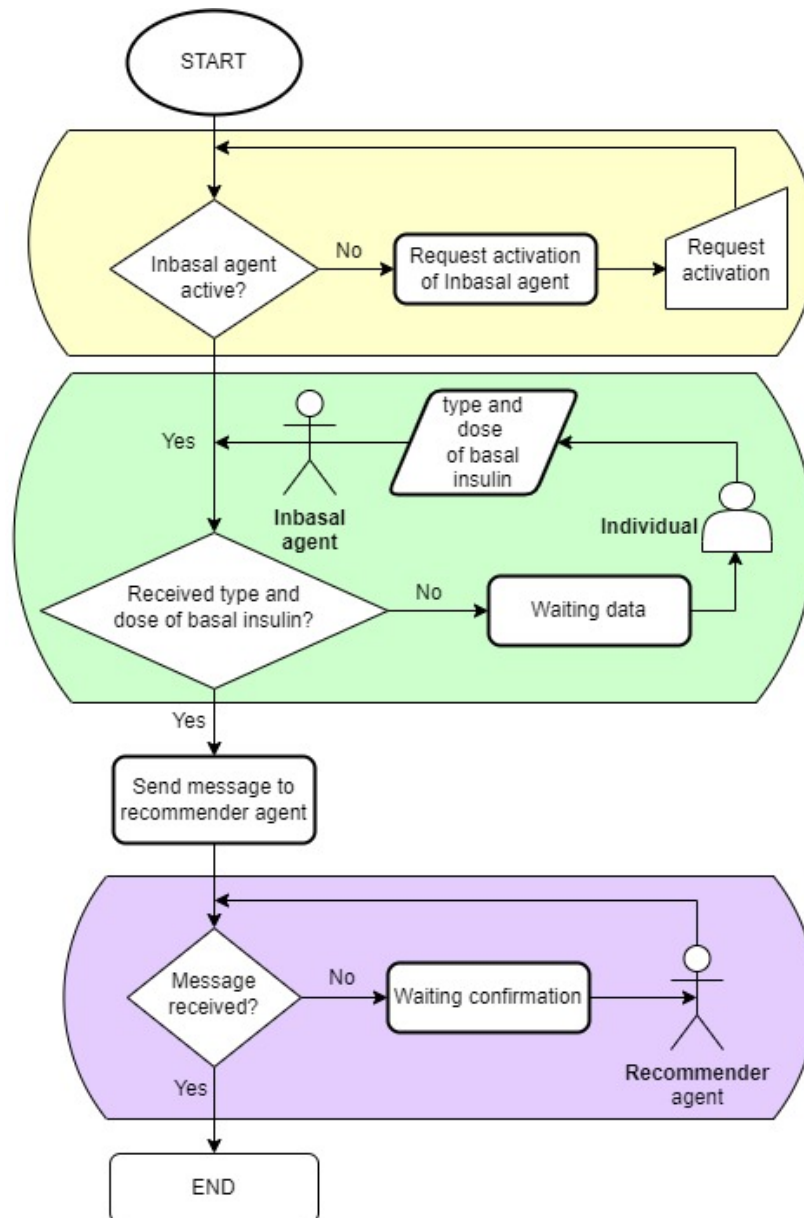


Figure 37: Inbasal agent action flowchart.

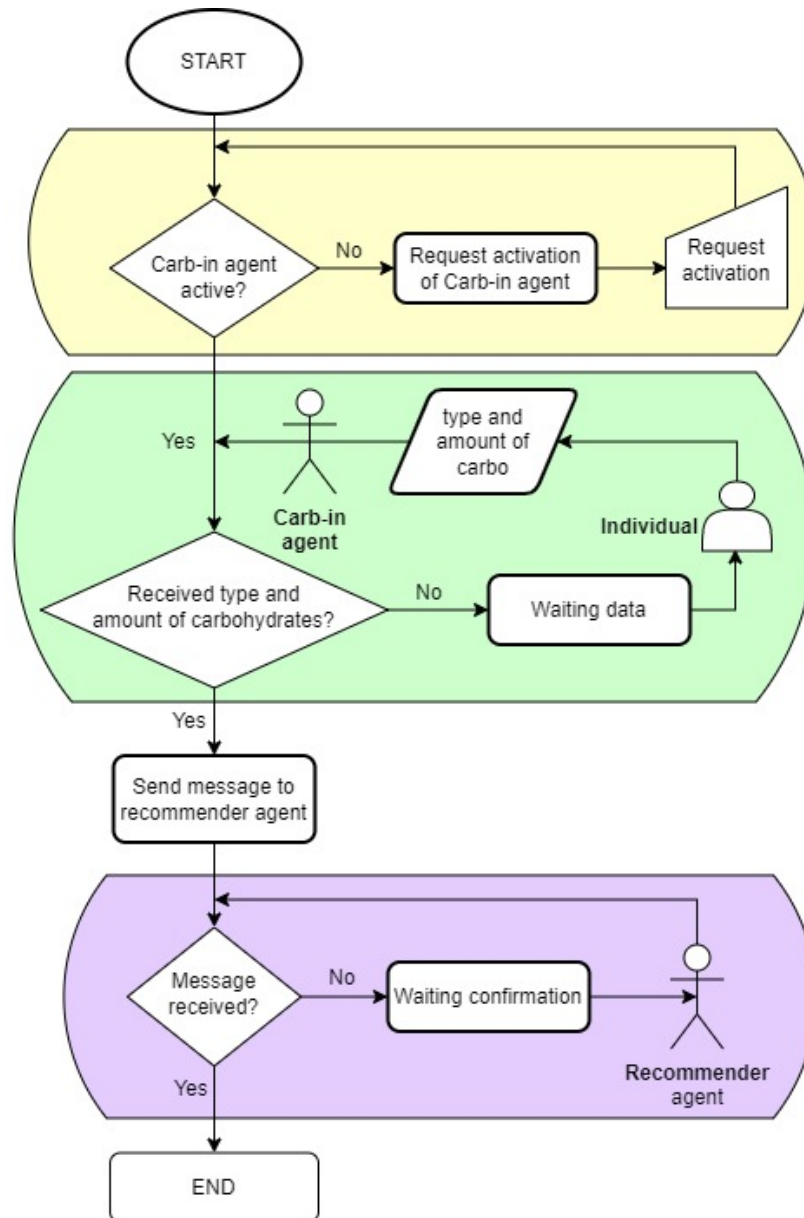


Figure 38: Carb-in agent action flowchart.

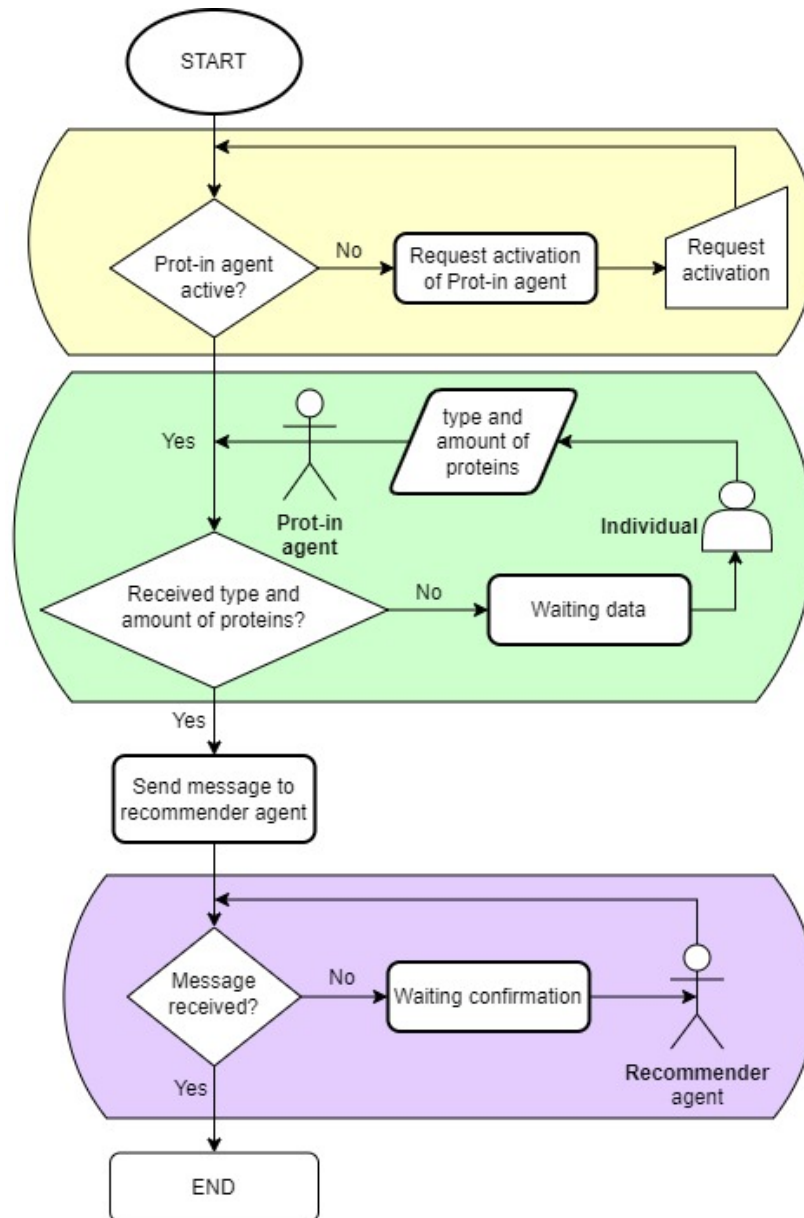


Figure 39: Prot-in agent action flowchart.

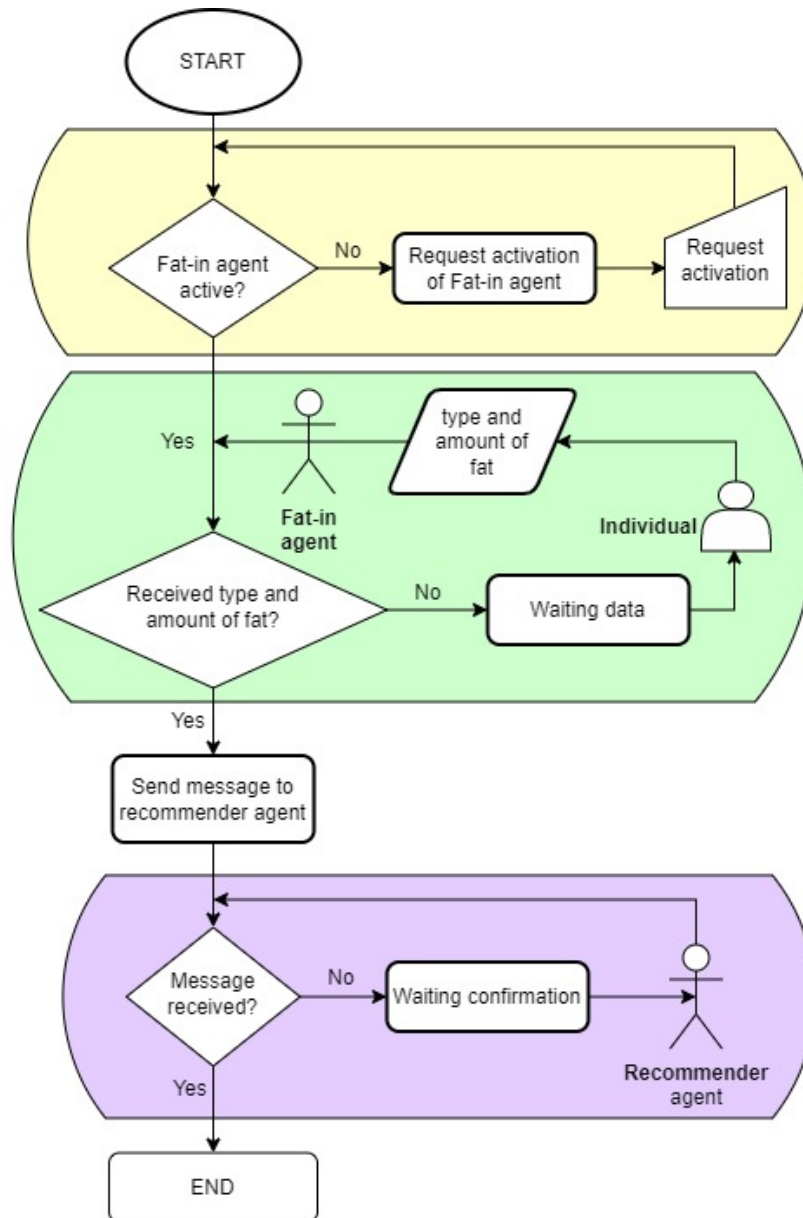


Figure 40: Fat-in agent action flowchart.

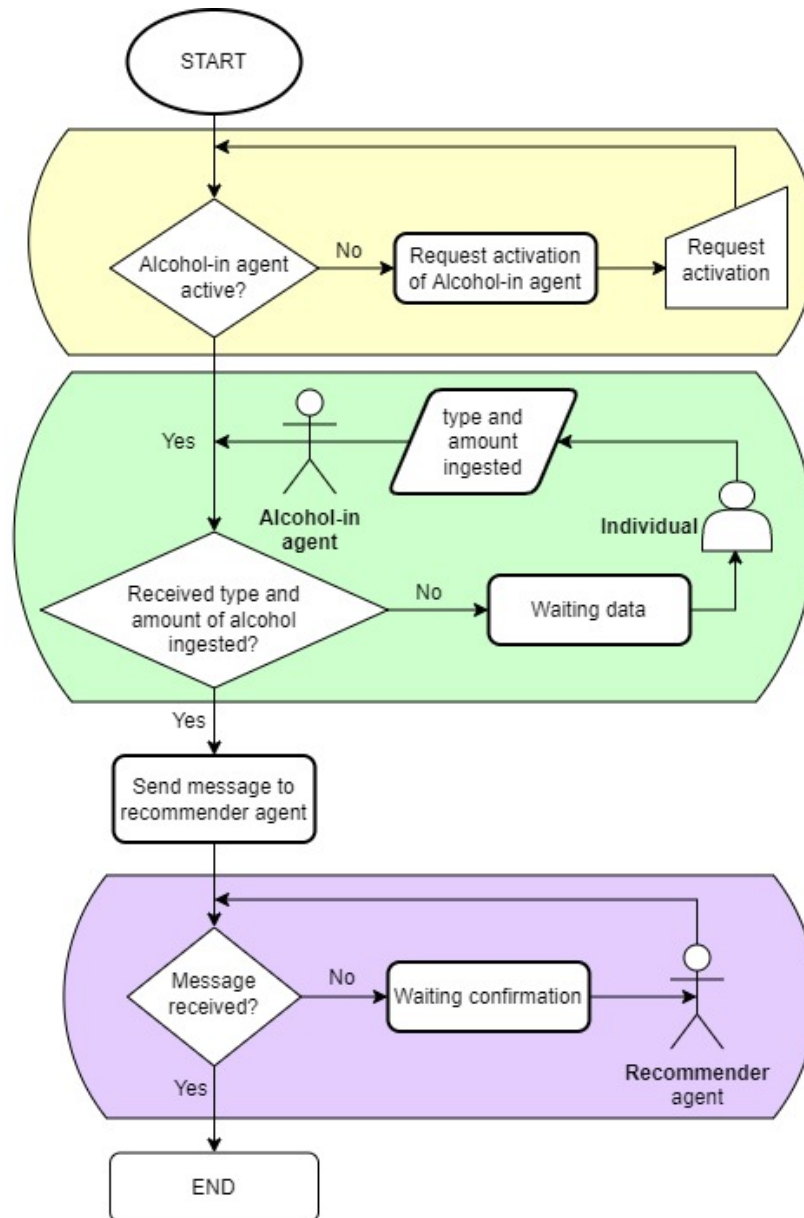


Figure 41: Alcohol-in agent action flowchart.

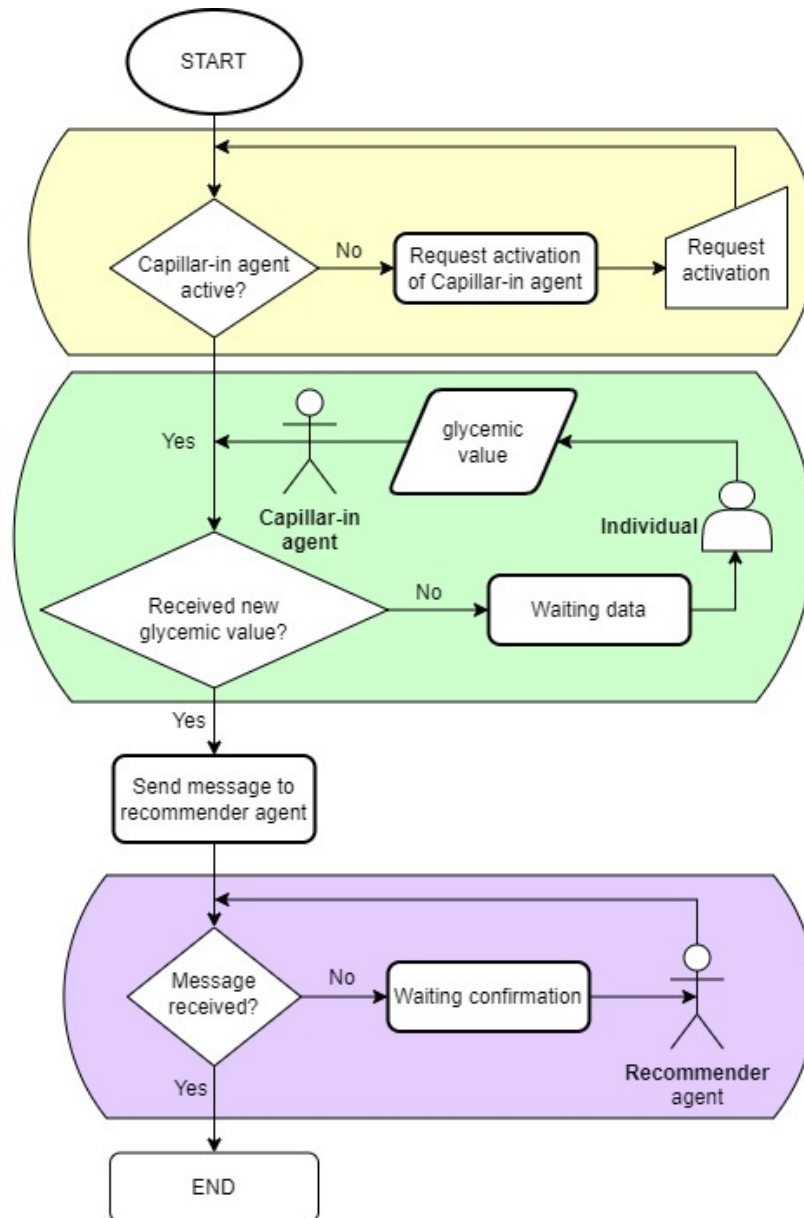


Figure 42: Capillar-in agent action flowchart.

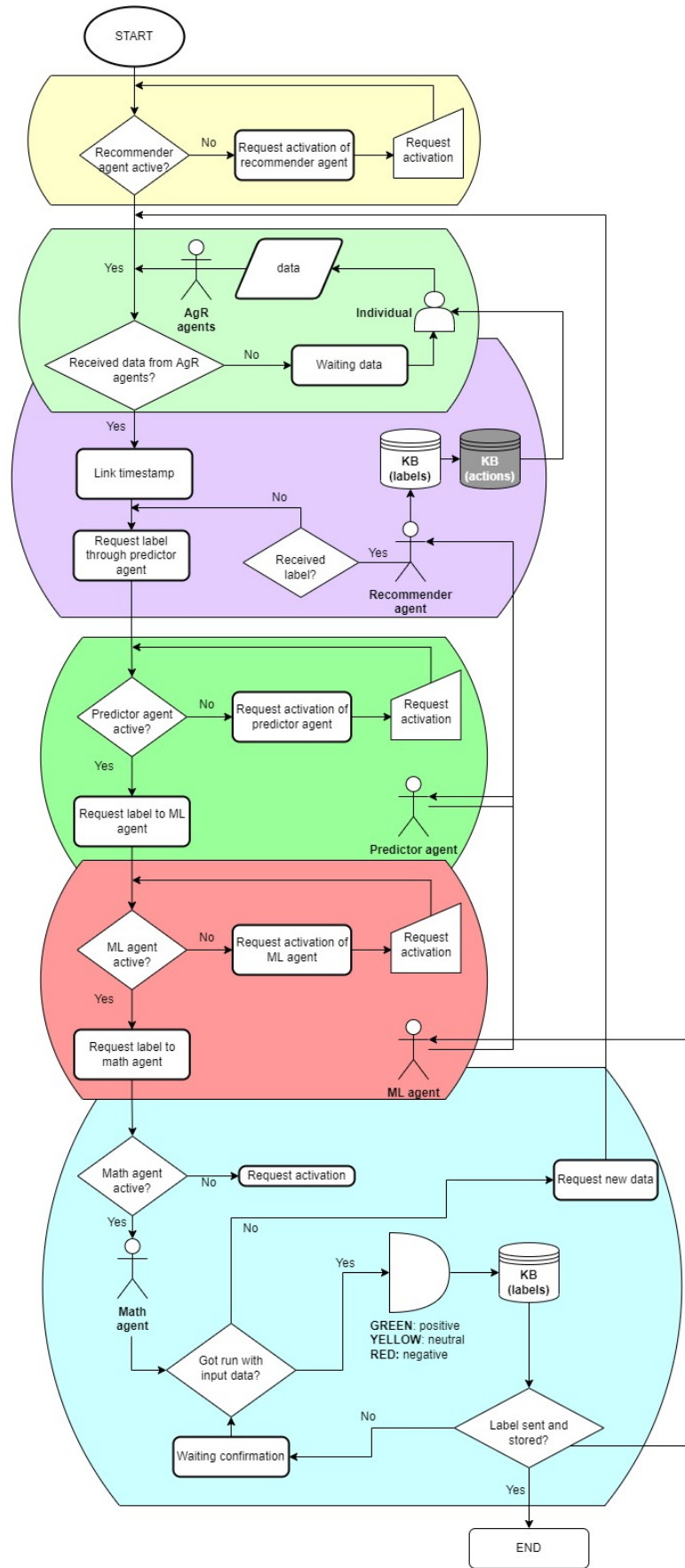


Figure 43: Tesseract model: phase 1 of learning.

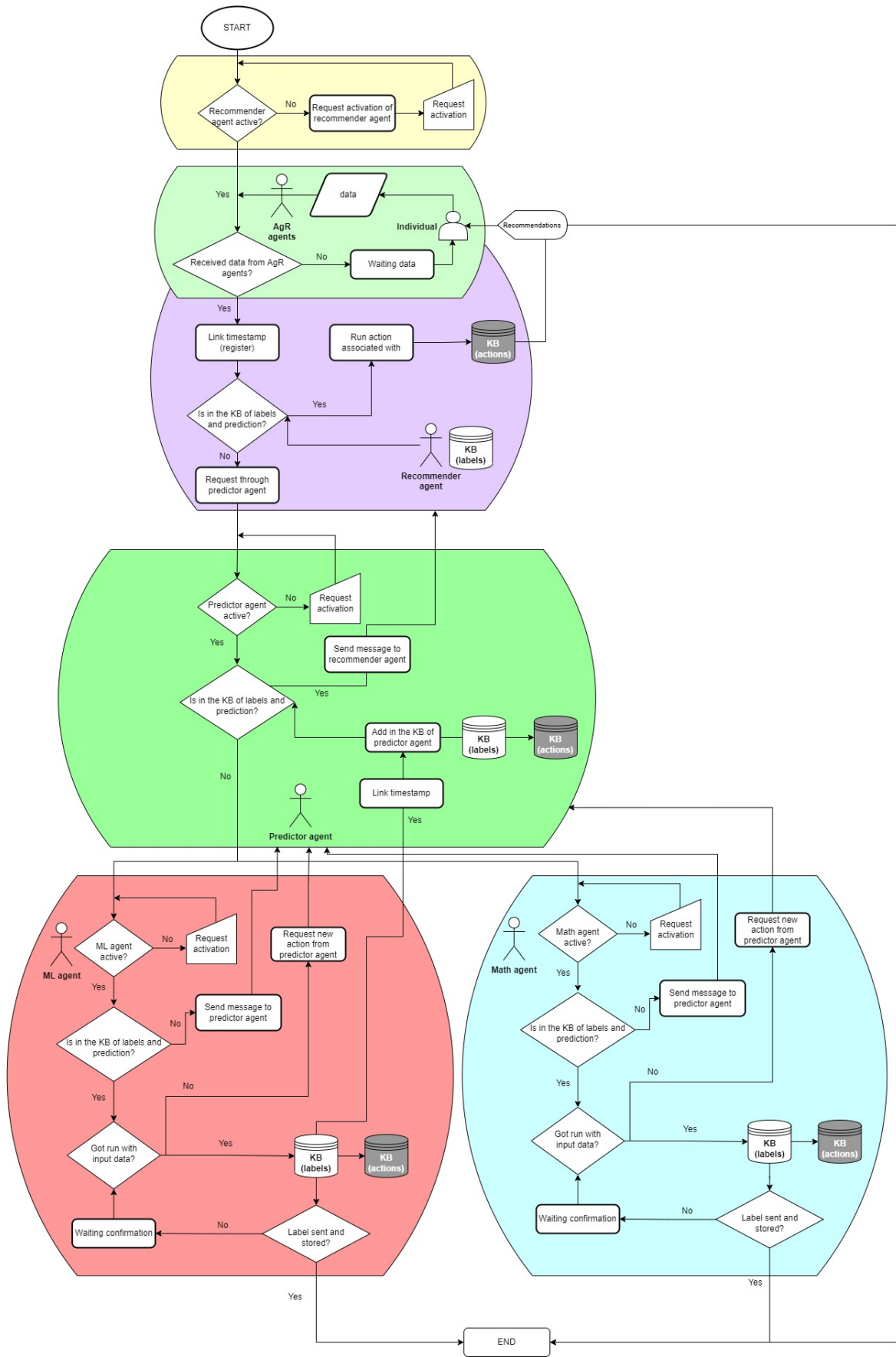


Figure 44: Tesseractus model: phase 2 of learning.

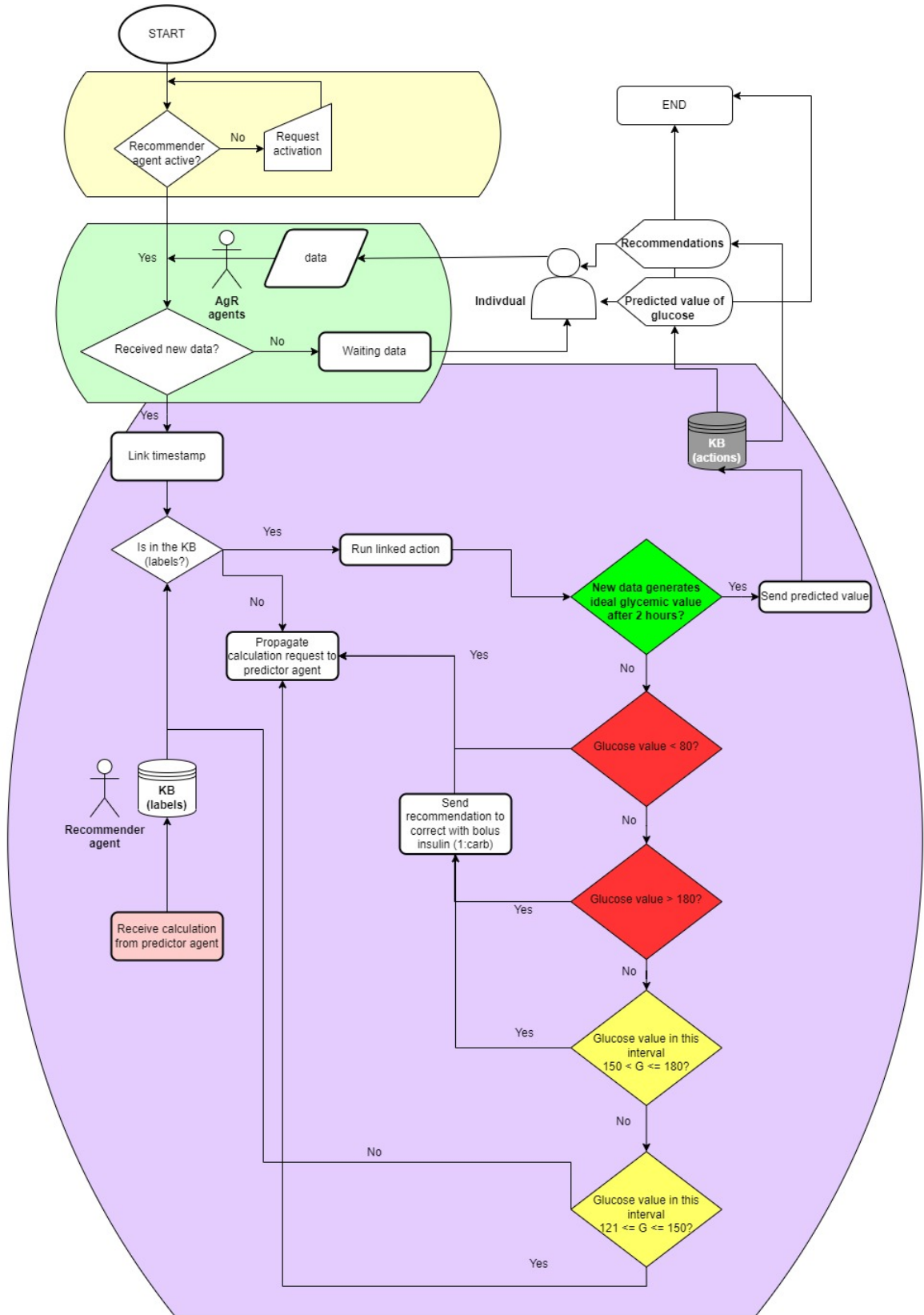


Figure 45: Recommender agent action flowchart.

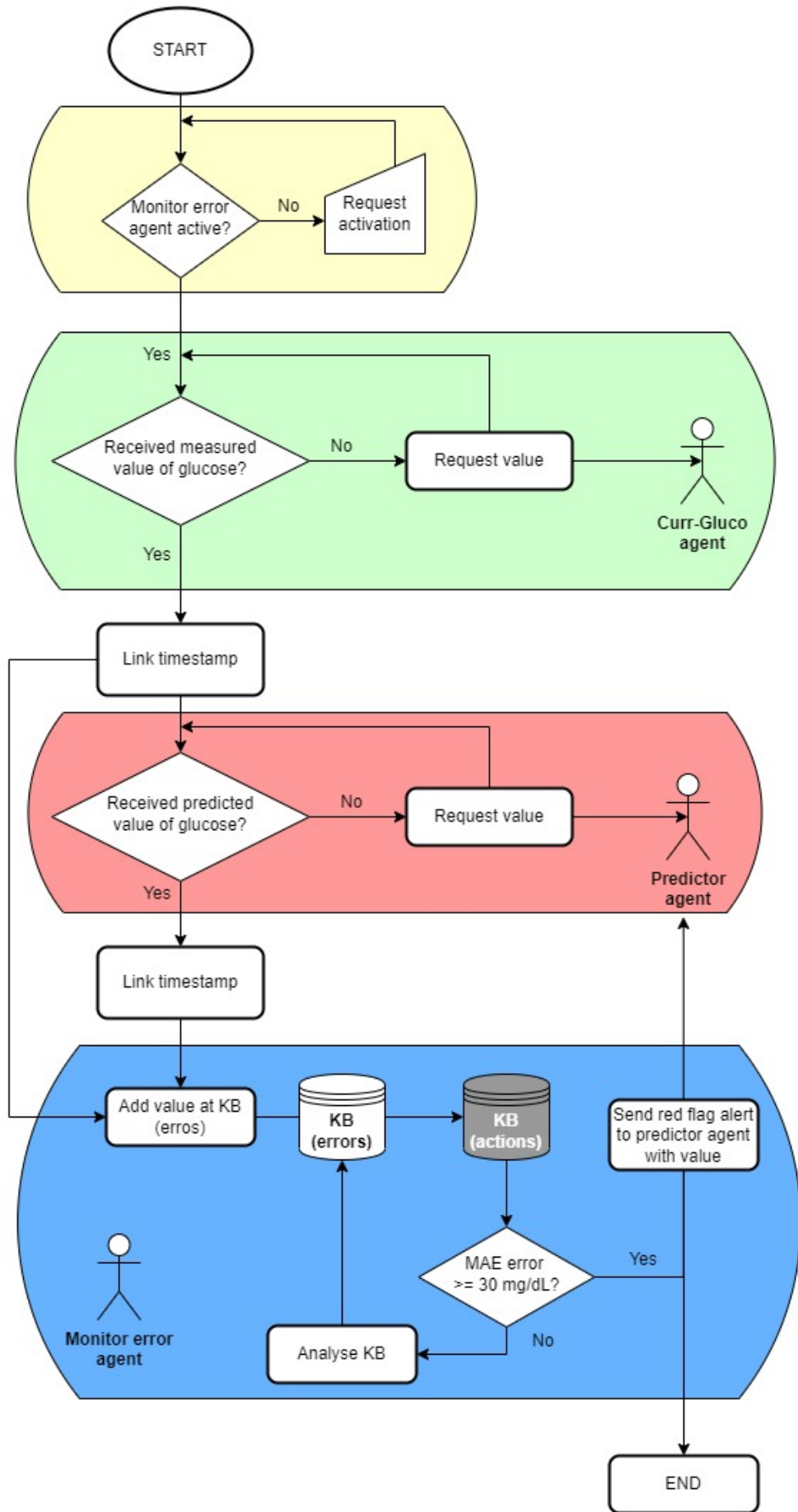


Figure 46: Monitor error agent action flowchart.

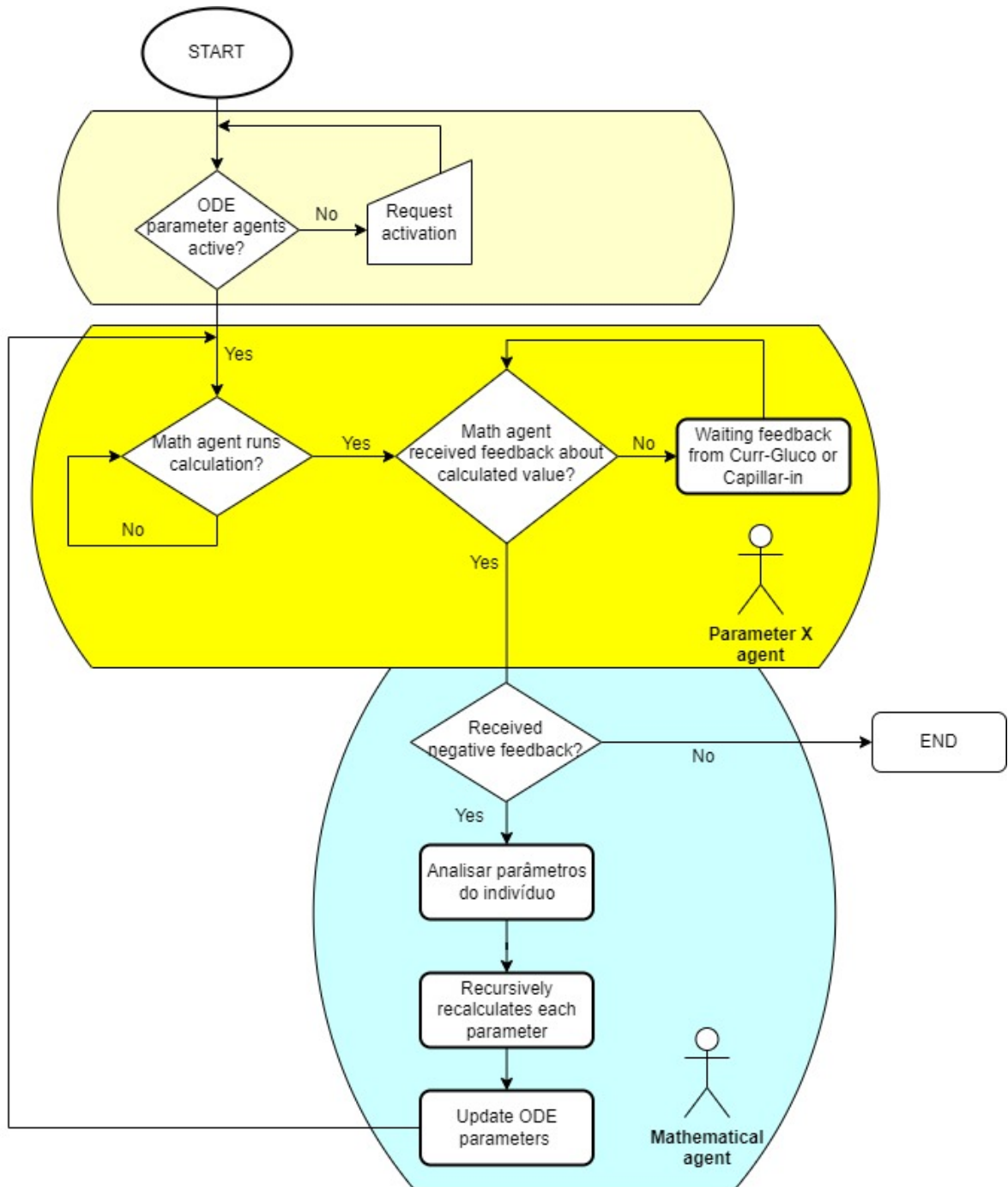


Figure 47: ODE parameters actions flowchart.

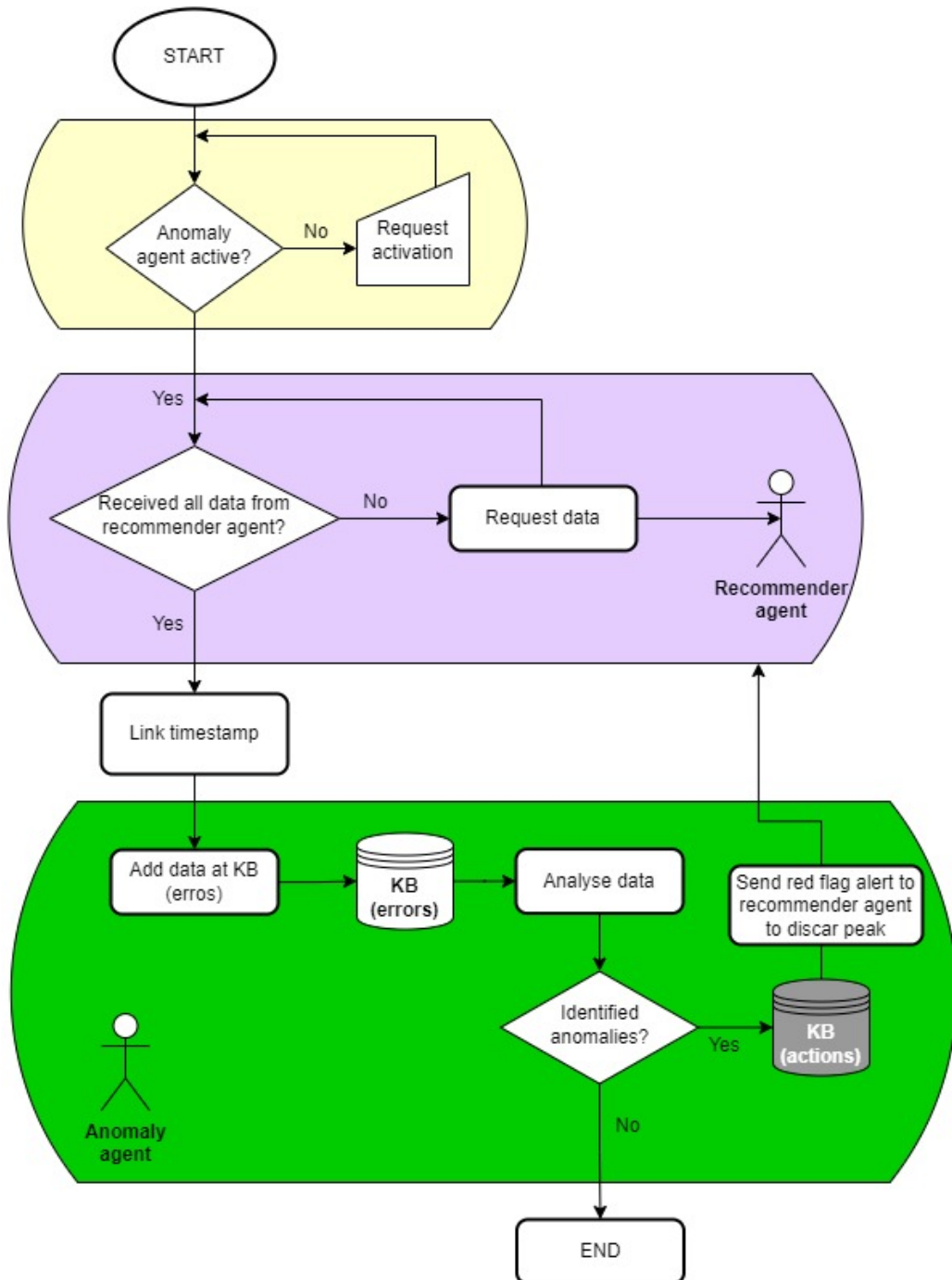


Figure 48: Anomaly detector action flowchart.

**APPENDIX D – TABLES OF AGENT
ACTIONS AND
CONDITIONS**

State	Rule/condition (customizable)	Action (messages)
Curr-Gluco and Capillar-in agents		
Received current blood glucose value	Previously entered	Send to recommender agent
Exercise agent		
Received exercise duration and intensity value: 1- moderate, 2- intense	Previously entered	Send to recommender agent
Inbolus Agent		
Received dose of insulin aspart	Previously entered	Send to recommender agent
Received dose of insulin lispro	Previously entered	Send to recommender agent
Inbasal agent		
Insulin glargine dose received	Previously inserted	Send to recommender agent
Received dose of insulin degludec	Previously inserted	Send to recommender agent
Carb-in agent		
Received food information (grams)	Previously entered	Check food to carbohydrate conversion table
Food converted to carb. (grams)	Previously entered	Send to recommender agent
Received amount of carb. (grams)	Previously entered	Send to recommender agent
Prot-in agent		
Received amount of protein (grams)	Previously entered	Checks with carb-in agent if carbohydrates were ingested
Received amount of protein (grams)	Previously entered	Checks if the amount is greater than 75g alone or combined with carb.
If $\geq 75g$	Previously inserted	Send to recommender agent with high protein alert and delayed glycemic increase (100min)
If $> 30g$ and associated with carbohydrates	Previously entered	Sends alerts about protein associated with carbs to the recommender agent, and delay in glycemic increase of 47 mg/dL (300 min.)
Fat-in agent		
Received amount of fat (grams)	Previously entered	Checks if the amount is equal to or greater than 35g
If $\geq 35g$	Previously inserted	Send to recommender agent with high fat alert and delayed glycemic increase (120–180 min.)

Table 38: Actions and conditions of reactive agents (AgR).

State	Rule/Condition (Customizable)	Action
Parameter agents		
Parameter values already entered	Previously entered	Wait for message from predictor agent
Received message from predictor agent	Previously inserted	Change parameter with the value in the message

Table 39: ODE Parameter agents actions and conditions (AgR).

Status	Rule/condition (customizable)	Action
Monitor Error agent		
Received the current measured blood glucose value from the Curr-Gluco agent	Previously entered	Stores information in your KB
Received the current measured blood glucose value from the Capillar-in agent	Previously entered	Stores information in your KB
Received predicted blood glucose value from predictor agent	Previously entered	Stores information in your KB
Received both measures from KB	Previously entered	Calculate absolute error between measured x predicted
Error \geq 30 mg/dL	Previously entered	Associate timestamp and send alert message to predictor agent
Error message (alert) sent	Previously entered	Wait recalculation to correct value of predicted value from predictor agent
Error $<$ 30 mg/dL	Previously entered	Associate timestamp and do not send message until threshold value of MAE error (30 mg/dL)
Error value decreased to one mg/dL	Automated	Check each five minutes if error increases

Table 40: Actions and conditions of Monitor Error agent.

Status	Rule/condition (customizable)	Action
Anomaly Detector agent		
Received all data from recommender agent	Automated	Stores information in your KB
Analyze KB to correlate them	Automated	Find sudden changes in data patterns
If find changes or peaks ± 50 mg/dL	Automated	Check all historical data in the same period of the day (interval of \pm two hours) and request measure from Capillar-in agent
If peak suspicion is real	Automated	Review the correction process with recommender agent
If peak suspicion is not real	Automated	Ignore peak and stores information

Table 41: Actions and conditions of Anomaly Detector agent.

Status	Rule/condition (customizable)	Action
Recommender agent		
Received the blood glucose value from the current glycemic agent	Previously entered	Stores information in your KB, associates it with a time frame and asks if there is more data
Received the value about exercises from the Exercise agent	Previously entered	Stores information in your KB, associates it with a time frame and asks if there is more data
Received the value of insulins from Inbolus and Inbasal agents	Previously entered	Stores information in your KB, associates it with a time frame and asks if there is more data
Received value on carb., protein and fat from Carb-in, Prot-in and Fat-in agents	Previously entered	Stores information in your KB, associates it with a time frame and asks if there is more data
If you received all values at that moment	Previously inserted	Stores information in your KB with the tuple data:time
If received all values at that time	Previously inserted	Checks if there is an action associated with the tuple data:time
If action exists and glycemic value is between 80–120 mg/dL	Previously inserted	Send predicted curve to the environment, without recommendations
If action exists and glycemic value is < 80 mg/dL	Automated	Retrieve information on the carb:glycemia ratio at different times of the day, and analyze other actions that can increase the glycemic value
If action exists and glycemic value is > 180 mg/dL	Automated	Retrieve information on the glycemic:insulin ratio at different times of the day, and analyze other actions that can decrease the glycemic value
If action exists and glycemic value is 150 < G <= 180	Automated	Check corrective actions, e.g. inject 1U bolus insulin, increase exercise intensity
If action exists and glycemic value is 121 <= G <= 150	Automated	Check if corrective actions are needed
If action does not exist	Previously inserted	Request label for tuple <data:time> for predictor agent

Table 42: Actions and conditions of the smart Recommender agent.

Status	Rule/condition (customizable)	Action
Predictor agent		
Received a prediction request from the recommender agent	Previously inserted	Analyzes if tuple data:time is in your KB
If tuple already exists and value is in (80–120 mg/dL)	Previously inserted	Send to recommender agent
If tuple already exists, value is not in (80–120 mg/dL)	Previously inserted	Send calculation request to ML and mathematical agents
If tuple does not exist in your KB	Previously inserted	Send calculation request to ML and mathematical agents
Received predicted value from ML and mathematical agents	Previously inserted	Analyzes if value is in (80–120 mg/dL)
If value is not in (80–120 mg/dL)	Automated	Prompts recalculation with $\pm 20\%$ of tuple data values
Received a new label from ML and mathematical agents	Automated	Stores all tuples in your KB, but sends to the recommender agent only those with values that generate the ideal value (80–120 mg/dL)
Receives message of mathematical agent input parameters settings	Automated	Sends request to each of the ODE parameters agents
Received confirmation of settings	Automated	Send confirmation to mathematical agent
Received request from Monitor Error agent about predicted glycemic value	Automated	Send message to mathematical agent and also recommender
Received predicted glycemic value from the mathematical agent	Automated	Send message to Monitor Error agent
Received predicted glycemic value from the recommender agent	Automated	Sends message to Monitor Error agent

Table 43: Actions and conditions of the smart Predictor agent.

Status	Rule/condition (customizable)	Action
Mathematical agent		
Received a prediction request from the predictor agent	Previously inserted	Analyzes if tuple data:time is in your KB
If tuple already exists in your KB	Previously inserted	Send label to predictor agent
If tuple does not already exist in your KB	Previously inserted	Calculates the ODE of blood glucose and uses polynomial insulin functions
Calculated value	Previously inserted	Sends label (+, neutral or -) to the predictor agent, based on glycemic values
If you receive a recalculation request from the predictor agent	Automated	Recalculates the blood glucose ODE and uses insulin polynomial functions, based on the new range of values
After recalculation	Automated	Store all generated tuples in your KB (labels)
Calculated value	Automated	Evaluates new labels, based on glycemic values, for example, every five mg/dL and expands the traffic light in the figures ?? and ??
Calculates glycemic values and fixes them	Automated	Analyzes all parameters recursively to evaluate hypothetical adjustments for each individual
If new calculated parameter values	Automated	Send message to predictor agent

Table 44: Actions and conditions of the smart Mathematical agent.

Status	Rule/condition (customizable)	Action
Machine Learning (ML) agent		
Received a prediction request from the predictor agent	Previously inserted	Analyzes if tuple data:time is in your KB
If tuple already exists in your KB	Previously inserted	Send label/results to predictor agent
If tuple does not already exist in your KB	Previously inserted	Calculates glycemic oscillation (supervised algorithm)
If receives a recalculation request from the predictor agent	Automated	Recalculates the glycemic oscillation (supervised algorithm), based on the new range of values
After recalculation	Automated	Store all generated tuples in your KB (labels)
If receives new measured values from the predictor agent	Automated	Check the predicted value in your KB and check the semaphore to reward or punish
In reward or punishment process	Automated	Increase the check counter
In reward or punishment process	Automated	Increase the counter of Tesseractus model

Table 45: Actions and conditions of the smart ML agent.

APPENDIX E – BIBLIOGRAPHIC RESEARCH METHODOLOGY

The directed study was defined in four stages. In the first step, in order to understand the state of the art, a search was carried out for related works between the years 2012 to 2021, using the following terms to define the search STRING:(a) glucose prediction or blood glucose prediction models; (b) individuals with T1D.

The keywords agent, multi-agent system and agent-based model were not used together with (a) and (b), because even though they are important in the proposed study, there were no relevant results in the researched literature. Only one article (ZHU et al., 2020) relevant, but based only on data, was found using Reinforcement Learning combined with agents. However, there were tests with only 20 virtual individuals, and the prediction horizon of blood glucose was not declared.

The literature offers a large number of articles that relate the terms (a) and (b), and the literature review was carried out considering seven databases: (1) Google Scholar; (2) PubMed; (3) JDST (Journal of Diabetes Science and Technology); (4) Science Direct; (5) IEEE (Institute of Electrical and Electronic Engineers); (6) DBLP (Digital Bibliography & Library Project); (7) DTT (Diabetes Technology & Therapeutics). Search terms were explored and combined, resulting in **1319 registers**.

The seven databases were validated as reliable tools for retrieving information about medical research, mathematics and machine learning, in addition to their respective combinations. A criterion for inclusion in this research is that the article should develop, test and discuss the proposed model, in addition to explaining the prediction horizon of blood glucose.

Still in the first stage, the articles were explored to find content relevant to the main focus of this study. In addition, a first exclusion criterion was established with the key-

words: (c) Type 2 Diabetes Mellitus; (d) Gestational Diabetes Mellitus, as well as repeated articles among the seven databases. After screening, **263** articles were included in the next stage, as described in the table 46.

Repository	#
Google Scholar	106
IEEE	69
Science Direct	29
PubMed	24
JDST	23
DTT	7
DBLP Computer Science	5
Total	263

Table 46: Results after first filter.

The 263 records were categorized by type of predictive model: (1) physiological models that mimic the oscillatory behavior of the glucose-insulin system; (2) models based on machine learning related data; (3) hybrid models that combine (1) and (2). According to (DUUN-HENRIKSEN et al., 2013), each predictive model can also be classified as white-box models: (1) physiological models, (2) black-box: based on data and (3) gray-box models: hybrids.

In this work, only works related to hybrid models were analyzed, and thus **54** articles with these characteristics were considered. In this consolidated database, three more criteria were applied to keep the articles in the evaluation base: (e) prediction horizon (PH) greater than or equal to 30 minutes; (f) the article should explain the error value either in the format of standard deviation (SD), least squares error (LSE) or by the Clarke Error Grid (CEG) (CLARKE et al., 1987) or Parkes Error Grid (PEG) (PARKES et al., 2000); (g) the dataset must have individuals *in vivo*, not only *in silico*.

After the last filter, **16** articles remained, according to the table 47, which serve as a basis for comparison for our work. The PH column of the table 47, contains only the largest values, and is in ascending order in terms of the smallest squared error, with individuals with T1D. The figure 49 represents the flowchart of the methodology used in this work to select and filter them.

After the first step of the thorough review, the second step consisted of analyzing the functionalities of the ODEs (NAGLE; SAFF; SNIDER, 2017), and which would be the best to mathematically represent the physiological processes and the dynamics of blood glucose, in addition to the approximation functions of insulins. In the third stage, the

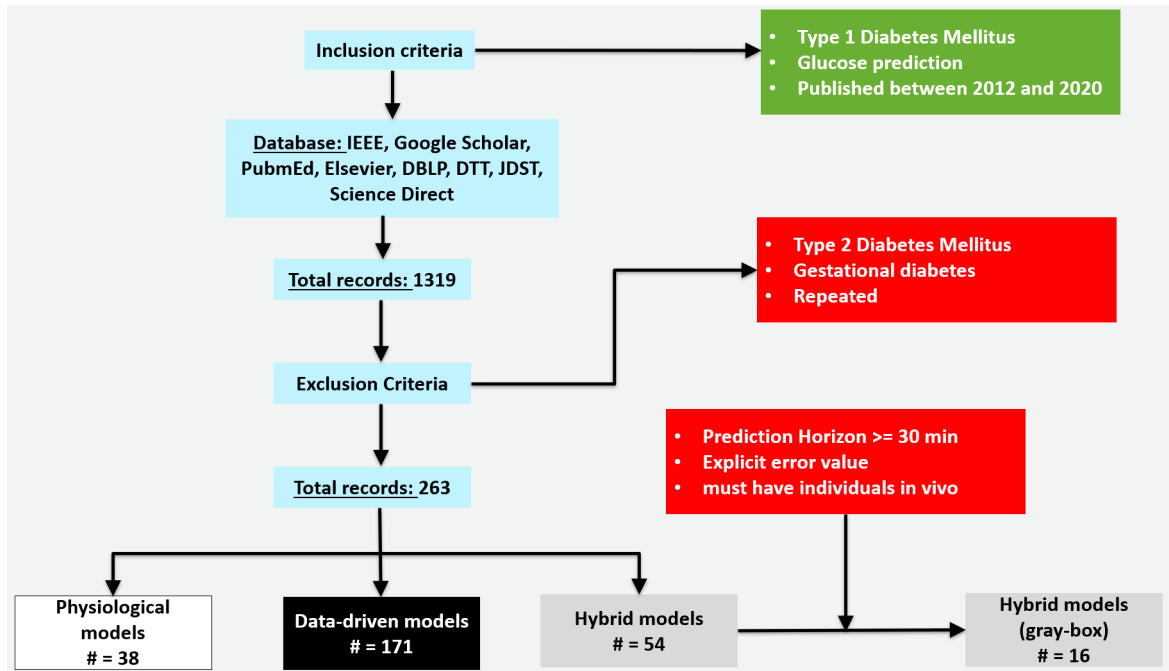


Figure 49: Flowchart of the bibliographic research methodology.

analysis of several functionalities of a MAS (RUSSELL; NORVIG, 2016) was carried out, to understand the possible advantages of its use in the regulation of physiological processes (KISSLER et al., 2014), and calibration of the values parameters of compartmental mathematical models and functions. In the last step, the possibility of using supervised and/or active reinforcement learning (KHOLGHI et al., 2015) among the agents of the model was analyzed, in order to have the correct discernment for long-term prediction (four to eight hours), in addition to accelerating the MAS learning.

Article	PH (max)	LSE - glucose (mg/dL)	CEG % zones (A+B)	Individual: Virtual (V) or Real (R)	Method - Physiological Models +
(GEORGA et al., 2013)	120	7.62	—	27R	Support Vector Machine (SVM)
(LIU et al., 2019)	120	34.74 (V) and 40.46 (R)	95.27 (R) and 93.86 (V)	10V and 10R	Latent Variable and Exogenous Autoregressive
(CESCON; JOHANSSON; RENARD, 2015)	120	58.06	—	14R	Autoregressive and Kalman Filter
(CONTRERAS et al., 2018)	90	36.26	96	200R	Grammatical Evolution
(MUNOZ-ORGANERO, 2020)	60	4.72 (V) and 11.35 (R)	87.22 (R) and 99.32 (V)	40V and 9R	Neural networks
(ZARKOGIANNI et al., 2013)	60	23.19	—	12R	Self-Organization
(SAITI et al., 2020)	60	27.41	—	6R	Autoregressive, SVM
(BUNESCU et al., 2013)	60	30.9	—	5R	SVM
(BERTACHI et al., 2018)	60	31.72	—	6R	Neural networks
(LIU et al., 2018)	60	35.96 (R and V)	—	10V and 10R	Latent Variable
(MIRSHEKARIAN et al., 2017)	60	38	—	10R	Neural networks
(VEHÍ et al., 2020)	60	—	96.8 (R) and 97.7 (V)	100V and 16R	Machine Learning
(WANG et al., 2020)	30	9.5	—	12R	Bayesian inference
(ISFAHANI et al., 2020)	30	10.79 (R) and 11.15 (V)	—	33V and 12R	Fuzzy Logic and Neural Networks
(ZECCHIN et al., 2014)	30	16.6	—	10R	Neural networks
(HAJIZADEH et al., 2018)	30	25.5	98.87	10R	Autoregressive and Kalman Filter

Table 47: Articles related to hybrid models.